Mechanism of *Clostridium difficile* Toxin A Entry into Host Cells

By

Ramyavardhanee Chandrasekaran

Dissertation

Submitted to the Faculty of the

Graduate School of Vanderbilt University

in partial fulfillment of the requirements

for the degree of

DOCTOR OF PHILOSOPHY

in

Microbiology and Immunology

December 16, 2017

Nashville, Tennessee

Approved:

Eric P. Skaar, Ph.D.

Anne K. Kenworthy, Ph.D.

Matthew J. Tyska, Ph.D.

Christopher R. Aiken, Ph.D.

D. Borden Lacy, Ph.D.

To my family

ACKNOWLEDGMENTS

I would like to thank Borden for her unwavering support, guidance, and friendship. Her positive attitude, patience, and encouragement have been critical for my research success and for my growth as an independent scientist. She allowed me the freedom to be creative and pursue my ideas, even if it took us to unfamiliar paths. Her constructive feedbacks have also helped me improve my written and oral communication skills. Finally, I want to thank Borden for always treating me as her colleague instead of her trainee. It gave me the confidence to dream big and be bold, and I will forever be grateful for that.

I would also like to thank all the members of the Lacy lab for their advice, technical help, and scientific discussions. They have been a great support system for these past 5+ years. I want to thank Stacey Seeback for being my best friend, my work buddy, and my western guru. I have benefitted so much from her kindness, friendship, and willingness to always lend a helping hand whenever I needed. I want to thank Heather Kroh for being a fantastic co-worker and a collaborator. She was so easy to work with and was always willing to listen and give me advice on both personal and professional matters. She was always willing to step up and take charge of lab organization and instrument maintenance. Her behind-the-scenes work ensured smooth running of the lab and I am grateful for that. I want to thank Paige Spencer for helping me practice my mentoring skills, and for her efforts in pursuing some of my grand, technically-challenging ideas. I want to thank Mitch LaFrance for getting me started on cell work, Dave Anderson for inspiring me to think outside the box, and Jaime Jenson for sharing candy and cat videos. Finally, I want to thank J Shupe, Ryan Craven, Joe Alvin, Kevin Childress, and Mike Sheedlo for their friendship and many fun conversations. I also want to thank Ben Spiller for his insightful questions and comments during lab meetings. The Spiller lab has been my second home these past few years and I want to thank Stacey Riccardi and Caleb Sutton for their help.

I want to thank my thesis committee: Eric Skaar, Anne Kenworthy, Matt Tyska, Terry Dermody, and Chris Aiken. They were supportive of my research and my career goals and were always ready to help me when I needed. So many of my ideas were borne out of my committee meeting discussions and very soon I started looking forward to my committee meetings. I also

received constructive feedbacks on my presentation skills, which helped me become a better speaker. I want to thank Anne for her extensive help with my entry project and for being a great collaborator. Her endocytosis expertise and attention to detail helped strengthen my project. I want to thank the staff, students, and postdocs who worked in the Skaar, Kenworthy, Tyska and Dermody labs. I want to thank Nichole Lobdell and William Burns from Skaar lab for their technical assistance with Cytation 5. I want to thank Courtney Copeland and Krishnan Ragunathan from the Kenworthy lab for providing me antibodies and for the many scientific discussions about my project. I want to thank Nathan Grega-Larson and Scott Crawley from the Tyska lab for providing me shRNA and plasmid constructs and for always taking the time to give me technical advice. I want to thank Bernardo Mainou, Alison Ashbrook and Jonathan Knowlton from Dermody lab for their technical advice.

I want to thank Dave Aronoff for giving me the opportunity to be a part of ANAEROBE 2016 planning. This was such a great learning experience for me. I also want to thank the BRET Career Office for giving me the opportunity to work with their team and plan career symposiums. I want to thank Dr. Jay Jerome for inviting me to give a talk at the Microscopy and Microanalyses meeting, where I also got to meet many great scientists and learn about cutting edge microscopy tools. I want to thank the PMI administrative personnel, Helen Chomicki, Lorie Franklin, Tracy Bradford, Pradeep Srivastava, and Eve Stephens. Their behind-the-scenes work made my work-life so much easier.

I want to Kathy Gould for giving me the opportunity to be a part of a one of a kind international program called the Vanderbilt International Scholar Program (VISP). Kathy has been a mentor and a role model to me, and I am so fortunate to have her in my corner. VISP has been my family here at Vanderbilt and has made my experience here a positive one. VISP also provided funding for the first and second year of my graduate study, which made me an attractive candidate for many labs. I want to also thank my other funding sources- American Heart Association, Vanderbilt Institute for Clinical and Translational Research, and National Institutes of Health. Finally, I want to thank my family and friends for sharing my victories and failures, for always being there when I needed them, and for helping me through tough times.

TABLE OF CONTENTS

LIST OF TABLES

LIST OF FIGURES

LIST OF ABBREVIATIONS

CDI	*C. difficile* infection
TcdA	*C. difficile* toxin A
TcdB	*C. difficile* toxin B
CDT	*C. difficile* transferase
PMC	Pseudomembranous colitis
REA	Restriction endonuclease analysis
MLST	Multi-locus sequence typing
PFGE	Pulsed field gel electrophoresis
PCR	Polymerase chain reaction
NCBI	National Center for Biotechnology Information
LCT	Large clostridial toxins
TcsL	*C. sordellii* lethal toxin
TcsH	*C. sordellii* hemorrhagic toxin
Tcnα	*C. novyi* alpha toxin
TpeL	*C. perfringens* large cytotoxin
PaLoc	Pathogenicity locus
SNPs	Single nucleotide polymorphisms
TcdR	*C. difficile* sigma factor
TcdC	*C. difficile* anti-sigma factor

TcdE	*C. difficile* holin-like protein
CcpA	Carbon catabolite control protein A
GTD	Glucosyltransferase domain
APD	Autoprocessing domain
CROPS	Combined repetitive oligopeptides
GP96	Glycoprotein 96
TLRs	Toll-like receptors
CSPG4	Chondroitin sulfate proteoglycan 4
PVRL3	Poliovirus receptor-like 3
TNS	2-(p-toluidinyl) naphthalene-6-sulfonic acid, sodium salt
$InsP_6$	Inositol hexakisphosphate
GEF	Guanine nucleotide exchange factor
GAP	GTPase activating protein
GDI	Guanine nucleotide dissociation inhibitor
UDP	Uridine diphosphate
MLD	Membrane localization domain
Cdk	Cyclin-dependent kinase
MOMP	Mitochondrial outer membrane permeabilization
ATP	Adenosine triphosphate
ADP	Adenosine diphosphate
GTP	Guanosine triphosphate

GDP	Guanosine diphosphate
ROS	Reactive oxygen species
NADPH	Nicotinamide adenine dinucleotide phosphate
NOX	NADPH oxidase
EGFR	Epidermal growth factor receptor
MT	Microtubule
VSV	Vesicular stomatitis virus
HIV-1	Human immunodeficiency virus-1
SV40	Simian virus 40
IL-2	Interleukin-2
AAV2	Adeno-associated virus 2
MHC I	Major histocompatibility complex
HSV-1	Herpes simplex virus type 1
CME	Clathrin-mediated endocytosis
RNA	Ribonucleic acid
siRNA	Small interfering RNA
shRNA	Short hairpin RNA
CHC	Clathrin heavy chain
CIE	Clathrin-independent endocytosis
FEME	Fast endophilin-mediated endocytosis
Cav1	Caveolin1

PACSIN2	Protein kinase C and casein kinase substrate in neurons 2
MEF	Mouse embryonic fibroblast
Caco-2	Human colorectal adenocarcinoma cells
EEA1	Early endosomal antigen 1
CLIC	Clathrin-independent carriers
PTRF	Polymerase I transcript release factor
N-WASP	Neuronal Wiskott-Aldrich Syndrome Protein
CTxB	Cholera toxin B
BSA	Bovine serum albumin
PBS	Phosphate buffered saline
MDCK	Madin-Darby Canine Kidney
FHL2	Four and a half LIM domains protein 2
NAV2	Neuron navigator 2
VMP1	Vacuole membrane protein 1
ADNP	Activity-dependent neuroprotector homeobox
TAB1	TGF-beta activated kinase 1 (MAP3K7) binding protein 1
PHAX	Phosphorylated adaptor for RNA export
BCAT1	Branched chain amino-acid transaminase 1, cytosolic
FAK	Focal adhesion kinase
sdAbs	Single-domain antibodies

CHAPTER I

INTRODUCTION

Clostridium difficile is a bacterial pathogen that is the leading cause of nosocomial antibiotic-associated diarrhea and pseudomembranous colitis worldwide. The incidence, severity, mortality, and healthcare costs associated with *C. difficile* infection (CDI) are rising, making *C. difficile* a major threat to public health. Traditional treatments for CDI involve use of antibiotics such as metronidazole and vancomycin, but disease recurrence occurs in about 30% of patients, highlighting the need for new therapies. The pathogenesis of *C. difficile* is primarily mediated by the actions of two large clostridial glucosylating toxins, toxin A (TcdA) and toxin B (TcdB). These toxins act on the colonic epithelium and immune cells and induce a complex cascade of cellular events that result in fluid secretion, inflammation, and tissue damage, hallmark features of the disease. In Chapter 1, I will summarize the structures, molecular mechanisms, and cellular responses to TcdA and TcdB. The content within the introductory chapter has been published in FEMS Microbiology Reviews.

Clostridium difficile

Clostridium difficile is an anaerobic, spore-forming, Gram-positive bacterium that was first described in 1935 by Ivan Hall and Elizabeth O'Toole (1). While the bacterium (originally named *Bacillus difficile*) was identified as part of the normal intestinal flora of heathy new-born infants, Hall and O'Toole noted that the organism was capable of causing disease in animals, likely through the production of soluble exotoxin(s). *C. difficile* gained recognition as an

important human pathogen when it was identified as the etiologic agent of antibiotic-associated pseudomembranous colitis (PMC) (2, 3). PMC is a severe inflammatory disease of the colon, characterized by the formation of pseudomembranes that are composed of necrotic epithelial cells, fibrin, mucous, and leukocytes. Since that discovery, it has become clear that *C. difficile* can cause a spectrum of clinical conditions in humans, collectively known as *C. difficile* infections (CDI), which range from mild and possibly recurrent diarrhea to life-threatening complications such as pseudomembranous colitis, toxic megacolon, and colonic perforation (4). *C. difficile* has become a major healthcare problem in the United States with an estimated half a million infections and 29,000 deaths each year (5).

Several molecular typing methods, including PCR ribotyping, restriction endonuclease analysis (REA), multi-locus sequence typing (MLST), and pulsed field gel electrophoresis (PFGE), have been developed for *C. difficile* classification and epidemiological analyses (6). Owing to the initial lack of a globally standardized typing method for this genetically heterogeneous species, *C. difficile* isolates were often referred to by multiple typing designations. For example, PCR ribotype 027 strains that have been associated with outbreaks in many countries are often indicated as REA group BI/PFGE type NAP1/PCR ribotype 027 (BI/NAP1/027) (7). While PCR ribotyping has gained widespread acceptance for typing *C. difficile* and an internationally-standardized, high-resolution ribotyping protocol has been recently validated (8), more and more whole genome sequences are becoming available as the cost of this technology gets less expensive. Recently, Lawson and colleagues proposed that *Clostridium difficile* should be reclassified as *Clostridioides difficile* based on phenotypic, chemotaxonomic, and phylogenetic analyses (9). This nomenclature has been adopted by the National Center for Biotechnology Information (NCBI).

C. difficile transmission occurs via the fecal-oral route, primarily in the form of spores. The spores traverse the acidic pH of the stomach and germinate in the small intestine in

response to certain primary bile acids (10, 11). The metabolically active vegetative cells colonize and infect the colon following antibiotic-induced dysbiosis of the gut microbiota (6, 12). While antibiotic exposure, hospitalization, advanced age, and immunocompromise increase the risk for disease, reports of community-acquired infections in otherwise healthy young adults who were not exposed to prior antibiotics are not uncommon (13). Although several virulence factors contribute to *C. difficile* adherence and colonization, the symptoms of CDI correlate with the production of two exotoxins, toxin A (TcdA) and toxin B (TcdB) (14). TcdA and TcdB are 308 and 270 kDa proteins, respectively. The toxins belong to the family of large clostridial toxins (LCTs), which are a group of homologous, high molecular weight proteins that further include the lethal and hemorrhagic toxins from *C. sordellii* (TcsL and TcsH, respectively), α-toxin from *C. novyi* (Tcnα), and a cytotoxin from *C. perfringens* (TpeL) (Table 1-1). The LCTs are glycosyltransferases that inactivate specific Rho and Ras GTPases, leading to the disruption of host cell function. Some *C. difficile* strains, including the epidemic PCR ribotypes 027 and 078, produce a third toxin named *C. difficile* transferase (CDT; or binary toxin). CDT is an actin-specific ADP-ribosyltransferase that is homologous to iota toxin from *C. perfringens* (15) and is thought to enhance *C. difficile* virulence and disease severity.

Overview of toxin genetics, expression, and secretion

The genes encoding TcdA (*tcdA*) and TcdB (*tcdB*) are located within a 19.6 kb chromosomal region termed the pathogenicity locus (PaLoc) (Figure 1-1) (16, 17). In non-toxigenic strains, the PaLoc is replaced by a 75-115 nucleotide non-coding sequence or a 7.2 kb sequence of unknown function (16, 18-20).

Table 1-1. Sequence comparisons of the large glucosylating toxins

		TcdA	TcdB	TcsH	TcsL	Tcnα
C. difficile	TcdA					
	TcdB	48 (68)				
C. sordellii	TcsH	78 (88)	48 (68)			
	TcsL	48 (68)	76 (87)	49 (69)		
C. novyi	Tcnα	31 (51)	31 (51)	32 (52)	31 (51)	
C. perfringens	TpeL	42 (62)	40 (61)	43 (62)	41 (62)	33 (54)

Values represent the percent identities of amino acids (in parentheses are the percent homologies)

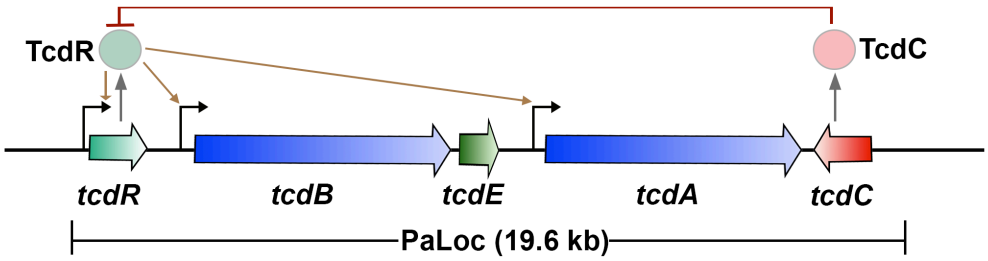

Figure 1-1: Organization of toxin genes. Schematic representation of the pathogenicity locus (PaLoc). Toxin-encoding genes, *tcdA* and *tcdB*, are indicated by blue arrows, regulatory genes are shown in light green (*tcdR*; positive) or red (*tcdC*; negative), and holin-encoding gene *tcdE* is shown in dark green. The direction of the arrows reflects the direction of transcription. TcdR positively regulates its own expression as well as the expression of *tcdA* and *tcdB* (indicated by brown arrows). TcdC is an anti-sigma factor that negatively regulates toxin expression by interfering with TcdR function. TcdE is involved in the secretion of toxins.

Non-toxigenic *C. difficile* strains, however, can acquire the PaLoc from toxigenic strains through horizontal gene transfer, resulting in the conversion of non-toxigenic strains to toxin producers (21). Changes in the toxin coding region within the PaLoc, including single nucleotide polymorphisms (SNPs), insertions, or deletions, have been used to classify naturally occurring *C. difficile* isolates (22). Based on comparison to a reference strain VPI10463, thirty-four *C. difficile* toxinotypes have been defined, highlighting the heterogeneity of the toxin coding region among *C. difficile* isolates (23).

In addition to the toxins, the PaLoc in most pathogenic strains encodes three proteins, TcdR, TcdC, and TcdE, which are thought to regulate toxin production and secretion (Figure 1-1) (6, 20, 24). TcdR is a member of the extracytoplasmic function (ECF) family of alternative sigma factors and plays a critical role in activating the expression of *tcdA* and *tcdB* (25, 26). Additionally, TcdR positively regulates its own expression (27). While there have been conflicting reports on the role of TcdC in toxin production, several studies suggest that TcdC functions as an anti-sigma factor that negatively regulates toxin expression (28, 29). The role of TcdE has also been controversial (30, 31). The protein shares homology with the bacteriophage holin proteins, which are involved in the release of progeny phages from the host bacterium (32). TcdA and TcdB do not possess any recognizable secretion signal, and toxin export does not require bacterial cell lysis (33). These observations have led to the suggestion that the toxins might be exported from the bacterial cell by a non-classic secretion pathway involving holin proteins. Several published studies now support this hypothesis (20, 30, 34).

C. difficile cells grown in rich media typically express TcdA and TcdB during the stationary phase (35-37). The toxin expression has been reported to be influenced by several environmental stimuli, including temperature (38), sub-inhibitory concentrations of certain antibiotics (39-42), quorum signaling (35), short-chain fatty acids such as butyric acid (43), the presence of a rapidly metabolizable carbon source (36), and certain amino acids (43-45). The

presence of a rapidly metabolizable carbon source such as glucose in the local environment of the bacterium inhibits toxin production via the carbon catabolite control protein A (CcpA) (46). Branched chain amino acids inhibit toxin production via the global transcriptional regulator CodY (24, 47). Finally, factors involved in the regulation of motility and sporulation have also been reported to modulate the production of TcdA and TcdB (48-55).

Role of TcdA and TcdB in disease

The individual role and relative importance of TcdA and TcdB in disease pathogenesis has been a topic of active investigation. TcdA was initially thought to be the key virulence factor in *C. difficile* pathogenesis based on animal studies performed using purified toxins. Addition of TcdA to rabbit ileal loops and colon recapitulated the hallmark features of CDI including inflammation, increased mucosal permeability, fluid secretion, and tissue damage (56, 57). TcdB had no effect in these studies. Similarly, when given intragastrically to hamsters and mice, TcdA caused inflammation, diarrhea, and eventual death, whereas TcdB caused no symptoms in these animals (58). TcdB was capable of causing death in hamsters, however, if prior intestinal damage was present or if sub-lethal doses of TcdA were co-administered (58). These findings suggested that TcdA and TcdB might act synergistically. It was proposed that TcdA acts first and disrupts epithelial integrity, which then allows TcdB to enter and mediate toxic effects within the host. Additional evidence supporting the importance of TcdA in disease pathogenesis comes from studies showing that passive immunization with antibodies against TcdA and active immunization with TcdA toxoids or peptides provided protection against CDI in hamsters (59-61). Furthermore, a strong humoral immune response against TcdA has been shown to correlate with reduced disease severity and recurrence in humans (62-64).

The importance of TcdA in CDI has been questioned following the detection of clinically significant *C. difficile* strains that produce TcdB, but not TcdA (A^-B^+) (65, 66). In humans, these pathogenic A^-B^+ strains cause the same spectrum of clinical illness that is associated with A^+B^+ *C. difficile* strains, ranging from mild diarrhea to the more severe outcomes such as pseudomembranous colitis and death (65). Interestingly, the majority of the A^-B^+ strains produce a modified form of TcdB, whose enzymatic domain shares homology and GTPase substrate specificity with TcsL of *C. sordelli* (67). It has been proposed that this variant TcdB, which, like TcdA, is able to modify Ras GTPases, might be able to carry out TcdA-specific glucosylation events in the absence of TcdA (68). The observation that A^-B^+ strains are virulent in infected individuals indicates that TcdB is sufficient for pathology in humans. Consistent with this, TcdB has been shown to disrupt epithelial integrity and cause tissue damage in human colon explants and in a chimeric mouse model where human intestinal xenografts were transplanted into immunodeficient mice (69, 70). In the xenograft model, challenge with either TcdA or TcdB elicited the hallmark features of CDI such as increased mucosal permeability and fluid secretion, cytokine production, neutrophil recruitment, and tissue damage (70). Furthermore, recent Phase III clinical trials show that a monoclonal antibody that neutralizes TcdB, bezlotoxumab, can reduce CDI recurrence in human patients (71). Overall, these studies indicate that TcdB plays an important role in *C. difficile* pathogenesis in humans.

The roles of TcdA and TcdB in disease have also been investigated by using isogenic *C. difficile* strains with defined toxin deletions in animal infection studies. In the first two studies, clindamycin-treated hamsters were infected with isogenic derivatives of *C. difficile* strain 630, a low toxin producing clinical isolate. In the first study, the wildtype strain (expressing both toxins) and mutants producing only TcdB were virulent and caused death in hamsters, but mutants producing only TcdA did not cause death in 80% of the infected animals (72). These findings suggested that TcdB was the major virulence factor of *C. difficile*. The second study supported

the importance of TcdB in *C. difficile* virulence by showing that a mutant producing only TcdB was comparable to wildtype in its ability to cause fulminant disease and death in hamsters (73). However, in contrast to the earlier study, an isogenic mutant producing only TcdA also resulted in disease and death in hamsters, although the time course of death was delayed compared to wildtype and $TcdA^{-}TcdB^{+}$ strains (73). This study also showed that an isogenic double mutant that did not produce TcdA and TcdB was avirulent in hamsters, consistent with the observation that naturally occurring $TcdA^{-}TcdB^{-}$ *C. difficile* strains are typically non-pathogenic in humans. Similar results were obtained in another study performed by the same group, which used isogenic mutants generated from an epidemic PCR ribotype 027 strain, R20291 (74). The first three studies utilized the hamster model of CDI and reported only survival or death of the infected animals. A fourth study used both mouse and hamster models of CDI, and performed detailed analyses of the tissue pathology and the host responses following infection (75). The wildtype and isogenic single and double toxin knockout strains used in this study were generated from another epidemic PCR ribotype 027 strain, M7404. Results from this study showed that both TcdA and TcdB were capable of inducing host innate immune and proinflammatory responses, but TcdB was the driver of fulminant disease (75). Strains expressing TcdB (wildtype and $TcdA^{-}TcdB^{+}$) caused significant weightloss and severe systemic disease in both the mouse and hamster models of infection. These findings are consistent with previous observations that purified TcdB causes cardiovascular damage and systemic disease in a zebrafish intoxication model (76), and that only anti-TcdB antibodies prevent systemic disease in piglets infected with *C. difficile* (77). In sum, the infection and intoxication studies show that while both TcdA and TcdB play a role in most infections, TcdB may be more important in the severe aspects of the disease.

Structure and mechanism of action of TcdA and TcdB

TcdA and TcdB are broadly classified as AB toxins, wherein a B subunit is involved in the delivery of an enzymatic A subunit into the cytosol of a target cell. The enzymatic A subunit of TcdA and TcdB is an N-terminal glucosyltransferase domain (GTD) that inactivates members of the Rho family of small GTPases by glucosylation. The B subunit is composed of three regions: a combined repetitive oligopeptides (CROPS) domain, a delivery/pore-forming domain, and an autoprotease domain (APD) (Figure 1-2A). The homologous proteins intoxicate host cells through a multi-step mechanism that involves 1) receptor binding and endocytosis, 2) pore formation and translocation of the GTD across the endosomal membrane, 3) autoprocessing and release of GTD into the cytosol, and 4) glucosylation of host GTPases (Figure 1-2B). These steps are discussed in more detail below.

Cellular receptors and receptor-binding domains

Historically, receptor binding has been associated with the CROPS domains located at the C-termini of TcdA and TcdB. The CROPS region contains multiple 19-24 amino acid short repeats (SRs) interspersed with four to seven long repeats (LRs) of 31 residues (78, 79). Analysis of the repetitive sequences in toxins from a reference strain (VPI10463) reveals that the CROPS domain spans residues 1812-2710 in TcdA and residues 1814-2366 in TcdB, with the TcdB CROPS being considerably shorter (Figure 1-3A). The TcdA CROPS domain contains 33 SRs and 7 LRs, and TcdB CROPS contains 21 SRs and 4 LRs. In 2005, a crystal structure of a fragment of TcdA CROPS (residues 2582-2709) comprising 4 SRs and 1 LR was solved (80). The five repeats form a beta-solenoid fold with each repeat consisting of a beta-hairpin

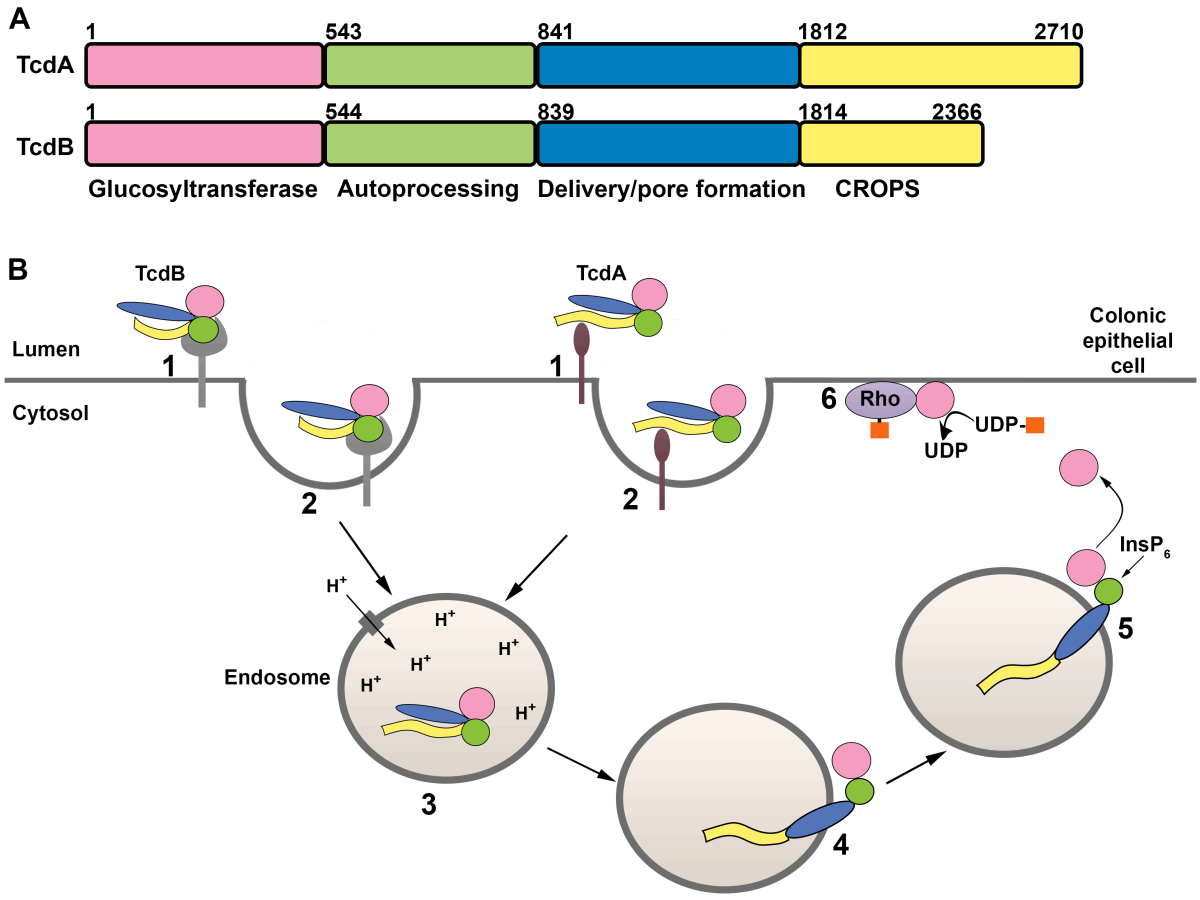

Figure 1-2: TcdA and TcdB primary structure and mechanism of action. A) TcdA and TcdB are organized into four functional domains: the glycosyltransferase domain (GTD; pink), the autoprocessing domain (APD; green), the delivery or pore-forming domain (blue), and the combined repetitive oligopeptides domain (CROPS; yellow). **B)** The four functional domains contribute to a multi-step mechanism of intoxication. TcdA and TcdB bind different cell surface proteins or sugars on the colonic epithelium (step 1) and are subsequently internalized into cells (step 2). The toxins reach acidified endosomes (step 3) and the low pH triggers a conformational change in the toxin delivery domain, resulting in pore formation and translocation of the GTD (and likely the APD) into the cytosol (step 4). Inositol hexakisphosphate ($InsP_6$) binds and activates the APD, resulting in the cleavage and release of the GTD (step 5). The GTD inactivates Rho family proteins by transferring the glucose moiety (orange squares) from UDP-glucose to the switch I region of the GTPase (step 6). Glucosylation disrupts GTPase signaling and leads to cytopathic 'rounding' effects and apoptotic cell death.

followed by a loop of 7-10 amino acids in SRs and 18 amino acids in LRs. The beta-hairpin of adjacent SRs contact each other but are rotated by 120°, resulting in a screw-like structure. In contrast, hydrogen-bonding interactions formed by the LR and the preceding SR lead to a 90° screw-axis transformation. Using this information, the Ng group constructed models of the complete TcdA and TcdB CROPS domains, which predicted an extended S-shaped structure for TcdA CROPS (Figure 1-3B) and a horseshoe-shaped structure for the shorter TcdB CROPS domain. Tertiary structures predicted by this model were later confirmed by electron microscopy studies of the holotoxins (Figure 1-3C) (81).

The idea that the CROPS domain can contribute to receptor-binding came from studies showing that the TcdA CROPS can bind carbohydrates present in mammalian cell surface glycoconjugates (78, 82-88). TcdA can bind to the human I, X, and Y blood antigens as well as a human glycosphingolipid, all of which have a core β-Gal-(1,4)-β-GlcNAc structure (87, 88). TcdA was also shown to bind α-Gal-(1,3)-β-Gal-(1,4)-β-GlcNAc, which is not present on human cells (85, 88). The crystal structure of a derivative of this trisaccharide in complex with a fragment of TcdA CROPS revealed that the sugar-binding occurs at the junctions formed between LRs and SRs (Figure 1-3D) (84). TcdA, therefore, has seven putative sugar binding sites, an observation that suggests a model wherein the toxin can form multivalent, high-avidity interactions with glycosylated receptors on the host cell. Whether TcdA binds multiple glycans simultaneously on host cells and whether such high-avidity interactions are important for toxin binding are not yet known. Additional evidence supporting a role for the TcdA CROPS domain in receptor-binding includes observations that, i) the isolated CROPS domain from TcdA can bind to host cells (89, 90), ii) excess TcdA CROPS competes with holotoxin in cell binding and cytopathic assays (89-91), and iii) the TcdA CROPS domain is highly immunogenic, and antibodies against this domain can block TcdA binding to cells and neutralize toxicity (59, 91-95).

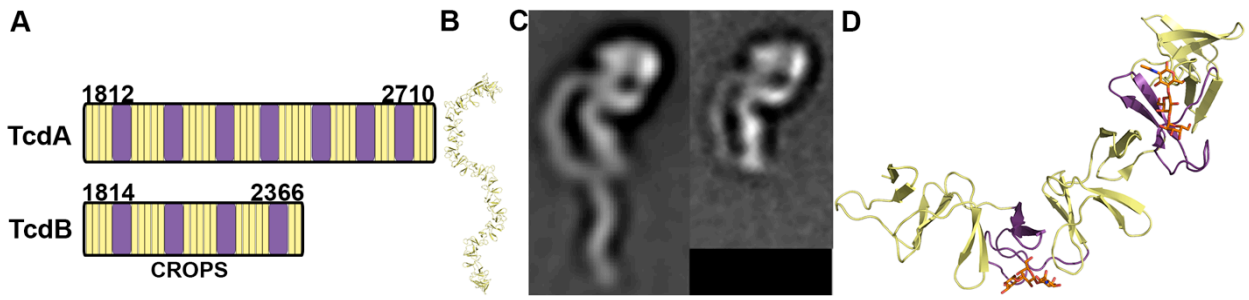

Figure 1-3: Structure of the CROPS domain. A) The CROPS domains of TcdA and TcdB consist of a series of short repeat (SR, yellow) sequences with interspersed long repeat (LR, purple) sequences. **B)** A model of the full TcdA CROPS based on a fragment structure (2F6E) is corroborated by **C)** negative stain electron microscopy images of TcdA (left) and TcdB (right) (81). **D)** The crystal structure of a CROPS fragment from the TcdA C-terminus (2G7C) shows how trisaccharides (orange carbons) bind at the vertices created at the intersection of a SR and LR. Figure credit: Dr. Borden Lacy.

Two cell surface proteins have been implicated as receptors for TcdA. The first is sucrase-isomaltase (SI), which is a glycoprotein located in the brush border of small intestines. SI was shown to mediate the binding of TcdA to rabbit ileum (86). Treatment with alpha-galactosidase inhibited binding of TcdA to SI, indicating that the toxin binds glycosyl modification(s) on the protein. SI, however, is not expressed in many cells and tissues that are sensitive to TcdA, including the human colonic epithelium (86, 96). A subsequent study performed by the same group identified glycoprotein 96 (gp96), a member of the heat shock protein family, as a binding partner for TcdA in human colonocytes (96). Heat shock protein gp96 is an endoplasmic reticulum paralog of cytosolic Hsp90 and is important for the proper folding and expression of many cell surface proteins including toll-like receptors (TLRs), integrins, and Wnt coreceptor LRP6 (97-99). Additionally, gp96 can translocate to the plasma membrane, where it can interact with bacterial surface-associated virulence factors to modulate pathogen adherence and entry into host cells (100-102). While Na *et al.* provided evidence that TcdA can bind gp96 *in vitro,* the specificity of this interaction was not evaluated (96). Furthermore, siRNA-mediated depletion of gp96 and blocking surface interaction using an anti-gp96 antibody conferred only partial resistance to TcdA-induced cytopathic effects, suggesting that TcdA binds additional cell surface proteins or sugars (96). Interestingly, gp96 is predicted to have five N-linked glycosylation sites but the identities of the glycan moieties are not known. It is likely that TcdA binds the sugar moieties on gp96 rather than the protein itself, but this needs to be investigated.

Unlike the CROPS domain of TcdA, evidence for carbohydrate binding by TcdB CROPS is limited to one study conducted with an electrospray mass spectrometry binding assay (82). However, the observation that bezlotoxumab, a TcdB-neutralizing antibody targeting the CROPS domain, blocks toxin binding to the host cell suggests a role for TcdB CROPS in receptor-binding (103). In line with this, a recent study identified chondroitin sulfate proteoglycan

4 (CSPG4) as a receptor for TcdB (104), and the binding interaction was mapped to the N-terminus of the CROPS domain (104, 105). In the initial study that identified CSPG4 as a receptor, Wei's group showed that $TcdB_{1500-2366}$, but not $TcdB_{1852-2366}$, was able to bind CSPG4 (104). A more recent study from the Min Dong group noted that while full length TcdB binds CSPG4, $TcdB_{1-1830}$ does not (105). Taken together, these studies suggest that the 1831-1851 region within the CROPS domain is important for TcdB binding to CSPG4. Notably, CSPG4 knockout cells were sensitive to high concentrations of TcdB, and NG2 (the rodent homolog of CSPG4) knockout mice succumbed to disease induced by TcdB (104), highlighting the existence of additional receptors for TcdB.

While the CROPS domain has historically been dubbed the receptor-binding domain, several recent studies have demonstrated that the receptor-binding function is not limited to this region of the toxin (90, 105-109). Truncated toxins ($TcdA_{1-1849,}$ $TcdA_{1-1874}$, $TcdB_{1-1811}$ and $TcdB_{1-1830}$) lacking most or all of the CROPS domain can still bind, enter, and perturb host cellular function (90, 105, 110). It appears that the CROPS domain contributes to but is not essential for host cell binding. Recently, Lambert and Baldwin reported that the region comprising residues 1361-1874 in TcdA is capable of binding and entering the host cell (111). Interestingly, a study by Olling *et al.* observed that the presence of TcdA holotoxin does not affect the binding of $TcdA_{1-1874}$ to cells in competition assays (90). This finding implies that the full length TcdA and the truncated toxin lacking the majority of the CROPS domain do not bind the same cellular receptors. It is possible that, in the presence of the extended CROPS domain, the alternate receptor-binding site is not accessible for interaction with a host receptor. Similar to TcdA, additional binding in TcdB may be mediated by the 300 to 350 residues preceding the CROPS domain. Studies using truncated TcdB toxins show that $TcdB_{1-1500}$ and $TcdB_{1-1529}$ are unable to induce cytopathic effects in cells, but the first 1500-1550 residues of TcdB are sufficient for intoxication when tethered with the diphtheria toxin receptor-binding domain (106, 107).

After the identification of CSPG4 as a receptor for TcdB, two other reports were published showing that poliovirus receptor-like protein 3 (PVRL3; also termed nectin 3) and frizzled proteins 1, 2 and 7 function as colonic epithelial receptors for TcdB (105, 108). Both PVRL3 and frizzled proteins bind TcdB outside the CROPS region (105, 108). It is, however, not known whether PVRL3 and frizzled proteins bind TcdB at distinct sites or compete for binding to the toxin. PVRL3 and frizzled proteins are both expressed on the surface of the human colonic epithelium (105, 108), and PVRL3 has been shown to co-stain with TcdB in tissues resected from a *C. difficile* infected patient (108). In contrast, CSPG4 is highly expressed in the intestinal subepithelial myofibroblasts and is not detectable in the surface epithelium (105, 112). During infection, it is likely that TcdB initially engages PVRL3 and/or frizzled proteins to enter and intoxicate the colonic epithelium. Upon damage to the epithelium or loss of tight junctions, the toxin could gain access to CSPG4 in the subepithelial myofibroblasts causing further damage to the mucosa. More work needs to be done to characterize the binding interactions between TcdB and its receptors and to define the role each receptor plays in the context of disease.

Cellular uptake and pore formation

After binding to their receptors, TcdA and TcdB are endocytosed into the host cell (Figure 1-2B). TcdB has been shown to enter cells by clathrin-mediated endocytosis, but the mechanism of TcdA uptake is unclear (113, 114). Once the toxins are internalized, they are trafficked to acidified endosomal compartments within the cell (115). Toxic cellular effects induced by TcdA and TcdB are inhibited by lysosomotropic agents and depend on the vacuolar H^+-ATPase, indicating a requirement for low pH in toxin action (90, 115-118). Other AB toxins that require low pH for action, such as diphtheria and anthrax toxins, have been shown to undergo conformational changes in an acidic environment that lead to the exposure of

hydrophobic regions that subsequently insert into the host membrane and form a pore (119, 120). Studies with *C. difficile* toxins A and B support a similar mode of action for these toxins.

Early evidence for pH-dependent conformational change and pore formation came from studies using TcdB. TcdB exhibited differences in native tryptophan fluorescence and protease susceptibility between neutral and acidic pH conditions, suggesting that the toxin undergoes structural changes at low pH. An increase in fluorescence of the probe 2-(p-toluidinyl) naphthalene-6-sulfonic acid, sodium salt (TNS) was also observed when TcdB was exposed to pH 5.0 or lower, indicating the exposure of hydrophobic regions (118). In addition to undergoing structural changes at acidic pH, TcdB was shown to form pores in cell membranes and artificial lipid bilayers (121). TcdA also undergoes conformational changes and forms pores at low pH (81, 122), but unlike TcdB, pore formation by TcdA requires cholesterol (122).

Pore formation and translocation are thought to be mediated by the central delivery domain (Figure 1-2A). A crystallographic structure of $TcdA_{4\text{-}1802}$ was recently published, revealing a structurally unique delivery domain (123). The domain begins after a three-helix bundle (residues 767-841) at the GTD-APD interface, and consists of a small globular sub-domain (residues 850-1025), an extended 'hydrophobic helical stretch' containing four α-helices (1026-1135), and a β-scaffold (1136-1802) which ends at the base of the APD (Figure 1-4A). Placement of the $TcdA_{4\text{-}1809}$ structure into the EM maps of TcdA holotoxin at neutral and low pH shows conformational flexibility at the junction between the APD, delivery domain, and the CROPs region (Figure 1-4B and C).

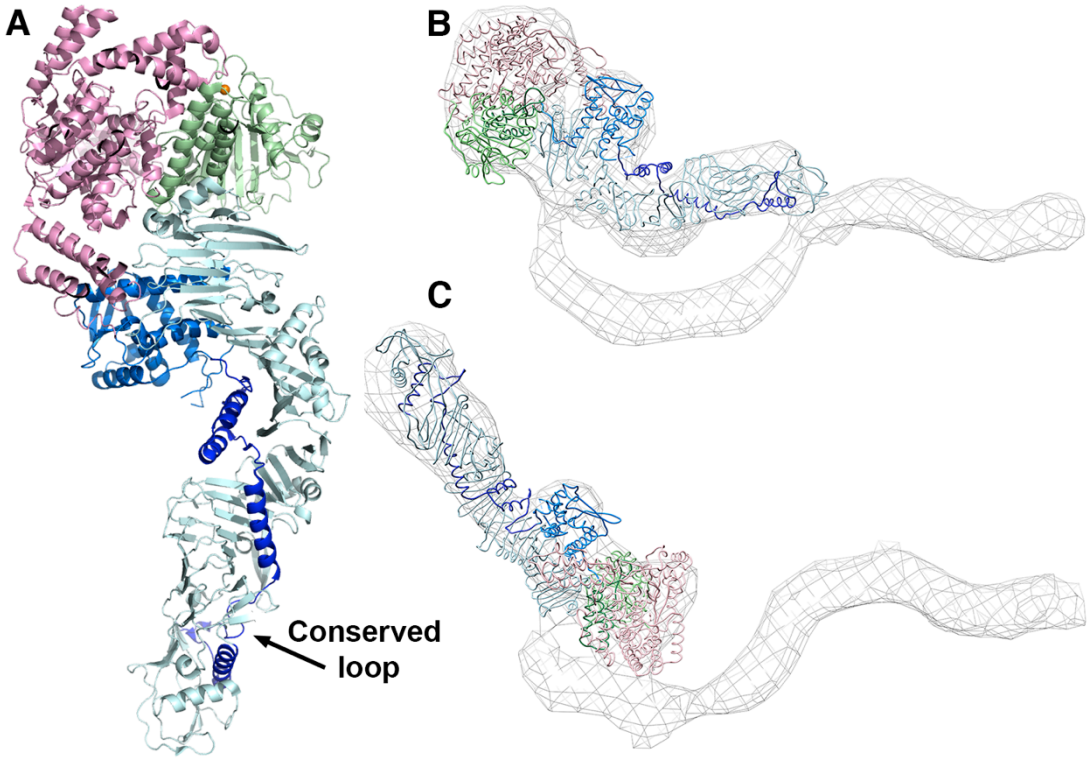

Figure 1-4. TcdA structure. A) The crystal structure of residues 4-1802 from TcdA (4R04) with the glucosyltransferase domain in pink and the autoprocessing domain in light green with its zinc atom depicted as an orange sphere. The delivery domain begins with a globular sub-domain (sky blue), followed by an extended stretch of four hydrophobic α-helices (navy blue). The α-helical stretch is scaffolded by an extended array of β-sheets (light blue). **B)** The $TcdA_{4-1802}$ structure docked into a 3D structure of the TcdA holotoxin obtained by negative stain electron microscopy (EM) at neutral pH. **C)** The $TcdA_{4-1802}$ structure docked into a 3D structure of the TcdA holotoxin obtained by negative stain EM at acidic pH indicates flexibility around the junction with the C-terminal CROPS domain. Figure credit: Dr. Borden Lacy.

The structure of the pore and the mechanism of pore formation by TcdA and TcdB have not yet been determined and remain a priority in the field. The delivery domain of TcdA and TcdB contain hydrophobic sequences (958-1130 in TcdA and 956-1128 in TcdB) that have been predicted to insert into the endosomal membrane with acidic pH (124). Mutational studies have shown that residues within this hydrophobic region, comprising the globular sub-domain and four α-helices, are important for TcdA and TcdB pore formation (107, 125). In the crystal structure of the TcdA delivery domain, the hydrophobic helices appear to wrap around the extended β-sheet structures, which could help maintain solubility while keeping them in a readily accessible conformation for subsequent membrane insertion. Notably, the hydrophobic helical stretch contains a surface loop that is strictly conserved across the large clostridial toxins (Figure1-4A). In both TcdA and TcdB, residues within this conserved loop have been shown to be critical for pore formation and cytotoxicity (123, 125). These findings suggest that targeting the conserved surface loop with antibodies or small molecules could provide a generalizable strategy for blocking the toxicity of the LCTs.

Translocation and autoproteolysis

Although TcdA and TcdB have been shown to form pores in cellular membranes, how these large, single polypeptide toxins deliver their effector domains to the host cytosol is not understood. The enzymatic domains of other pore-forming AB type toxins, such as diphtheria and anthrax toxin, have been shown to unfold at low pH, and the unfolding is thought be important for the translocation of these domains across the pore (119).

In 2003, Pfiefer and colleagues demonstrated that TcdB is proteolytically processed within the host cell, and only the N-terminal GTD domain was released into the cytosol upon translocation. Imaging and fractionation assays showed that the remainder of the toxin localized to endosomes (126). The cleavage occurs after a conserved leucine residue (542 in TcdA and

543 in TcdB), and results in the release of the GTD into the cytosol (127, 128). Rupnik *et al.* also observed that the cleavage reaction *in vitro* occurred at neutral pH and required the addition of host cell cytosol. Subsequently, Reineke and colleagues demonstrated that protein-free cytosolic extracts also induced toxin cleavage, and they identified inositol hexakisphosphate ($InsP_6$) as the inducer of this autocatalytic cleavage event (129). $InsP_6$ is a highly charged molecule that is abundant (10-60 μM) within mammalian cells (130). *In vitro* experiments show efficient autoprocessing of toxins at $InsP_6$ concentrations of 1-10 μM (131, 132), and support the idea that $InsP_6$ can induce autocatalytic cleavage of the toxins *in vivo*. The domain adjacent to the GTD in TcdA and TcdB shares sequence homology with the cysteine protease domain of the MARTX family of toxins, which is also activated by $InsP_6$ [reviewed in (133) and (134)]. This autoprotease domain (APD) was subsequently shown to induce the $InsP_6$-dependent cleavage and release of the GTD (131).

The APD has been described as a cysteine protease. The active site of the TcdA and TcdB APD has three conserved residues: a cysteine, a histidine and an aspartate (Figure1-5). Individual mutation of these residues (D589, H655, or C700 in TcdA; D587, H653 or C698 in TcdB) inhibits autoprocessing (131, 132). However, a recent report has shown that the conserved cysteine and histidine residues of TcdA and TcdB help to coordinate a zinc ion that is essential for autoprocessing activity (123). What serves as the nucleophile in this reaction is currently unclear, and warrants the use of the term autoprotease, instead of cysteine protease, when referring to this domain.

Crystal structures of the APD in the presence of $InsP_6$ reveal that $InsP_6$ binds a positively charged pocket that is separated from the active site by a structure termed the 'β-flap' (132, 135, 136). Binding of $InsP_6$ was shown to induce significant conformational changes by NMR and these changes were thought to be linked to protease activation (132). Through mutational analyses Shen *et al.* showed that this 'β-flap' structure transduces the allosteric change induced

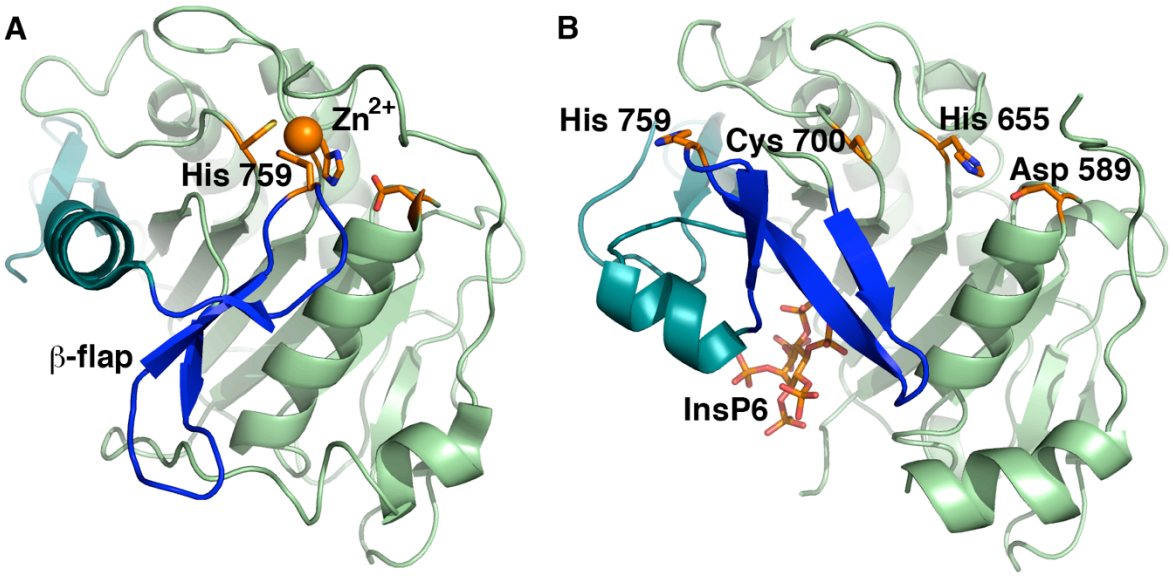

Figure 1-5. The autoprocessing domain (APD) undergoes a significant conformational change upon binding to $InsP_6$. The crystal structures of the TcdA APD in the **A)** absence (4R04) and **B)** presence of $InsP_6$ (3HO6) reveal significant changes in the central β-flap structure (blue) and the C-terminal sequence that follows (teal). The structure of the APD in the context of $TcdA_{4\text{-}1802}$ revealed the unexpected requirement for zinc (orange sphere) in TcdA and TcdB autoprocessing activity. Other key residues include Asp 589, His 655, and Cys 700 (side chains depicted with orange carbon atoms). His 759 is located at the tip of the β-flap and is bound to the zinc in the absence of $InsP_6$. It moves significantly upon $InsP_6$ binding. Figure credit: Dr. Borden Lacy.

by $InsP_6$ binding to the active site (137). Comparisons of the $InsP_6$-bound isolated TcdA APD structure with that of the APD from $TcdA_{4\text{-}1802}$ (crystallized in the absence of $InsP_6$) reveal that the β-flap (residues 746-765) rotates ~90°, and there is significant repositioning of the subsequent residues (766-802) following $InsP_6$ binding (Figure 1-5) (123). One effect of this structural change is an increase in positively charged residues at the $InsP_6$ binding site. $InsP_6$ binding also results in a 19 Å movement of H759, located at the tip of the β-flap (also involved in zinc binding), out of the active site (Figure 1-5). Mutation of H759 (or H757 in TcdB) leads to autoprocessing that is no longer dependent on $InsP_6$ concentration (123), suggesting that this residue in the β-flap is a key regulator of $InsP_6$-induced allostery in TcdA and TcdB.

While TcdA and TcdB APDs share the same mechanism of $InsP_6$-induced activation, cleavage is not equivalent between these two toxins. *In vitro*, TcdB holotoxin is more sensitive than TcdA to $InsP_6$-induced cleavage (127). Structural and biochemical studies indicate that autoprocessing of TcdA is repressed in the context of the holotoxin due to inter-domain interactions between CROPS and the N-terminus (123, 138, 139). This CROPS-mediated repression is alleviated upon acidification of the toxin-containing medium (138).

Mechanisms that modulate autoprocessing activity of the toxins can affect their virulence properties in the host. A study by Savidge *et al.* demonstrated that *C. difficile* toxins are S-nitrosylated at the conserved cysteine of the APD by the infected host, which inhibits the autoprocessing activity of the toxins in an $InsP_6$-dependent manner and reduces virulence (140). Nevertheless, it is important to note that autoprocessing deficient mutants of TcdA and TcdB are still able to inactivate some of their GTPase substrates and cause cytopathic effects in cells, albeit with delayed kinetics (127, 141, 142). In an *in vivo* intoxication study, virulence of a TcdB autoprocessing mutant is attenuated but not abolished (143). While autoprocessing can affect toxin potency by regulating the rate at which host cells targets are modified, it is not essential for the cytopathic and cytotoxic effects mediated by TcdA and TcdB. Interestingly, a study of the

autoprocessing mutant of TcsL (a homologous glucosylating toxin from *C. sordellii*) showed that this mutant, which is less toxic, can inactivate Rac but is impaired in its ability to glucosylate Ras GTPase (144). Rac has been reported to cycle to the endosomes where it is activated before trafficking back to the membrane, whereas Ras is trafficked to and remains at the plasma membrane (145, 146). In autoprocessing mutants, the GTD remains tethered to the endosomes and can access substrates that encounter the endosome. These findings suggest that the importance of autoprocessing in mediating toxin virulence in the host may vary depending on the localization of the GTD substrates.

Glucosylation and substrates

TcdA and TcdB encode a 63 kDa GTD at the N-terminus, which inactivates small GTPases from the Rho family (147, 148). GTPases targeted by TcdA, TcdB and other large clostridial toxins (LCTs) are listed in Table 1-2. GTPases are molecular switches that cycle between active GTP-bound and inactive GDP-bound states. This GTPase cycle is regulated by three classes of proteins: i) guanine nucleotide exchange factors or GEFs, which activate the GTPases by exchanging GDP for GTP, ii) GTPase activating proteins or GAPs, which facilitate the inactivation of the GTPases by stimulating their GTP hydrolyzing activity, and iii) guanine nucleotide dissociation inhibitors or GDIs, which extract the GTPases from the membrane and maintain the inactive GDP-bound form in the cytosol. In their active state, Rho family GTPases can interact with a wide-range of effector molecules such as kinases, phosphatases, lipases, and scaffolding proteins to regulate many cellular functions including assembly and organization of the actin cytoskeleton (149-151).

GTPases in their GDP-bound, membrane-associated form are the preferred substrates for the LCTs (152, 153). The toxins modify their targets through monoglucosylation of the conserved threonine in the switch I region of the GTPase (153, 154). This threonine residue is

involved in coordination of the Mg^{2+} ion required for GTP binding (155), and conformational changes in the switch I region subsequent to GTP binding affects interactions with regulatory proteins and effectors (149, 156). Consequently, glucosylation of the GTPases by the LCTs inhibits nucleotide exchange by GEFs (157), GAP-stimulated GTPase activity (158), GDI binding and cytosol-membrane cycling (152), and interaction with effector proteins (157-159). The above-mentioned glucosylation-induced effects disrupt GTPase signaling and have been linked to the cytopathic and cytotoxic effects observed with these toxins.

The LCTs use either uridine diphosphate (UDP)-glucose or UDP-GlcNac as the co-substrate for GTPase modification. Glucosylating toxins from *C. difficile* (TcdA/B) and *C. sordellii* (TcsH/L) use UDP-glucose as the glycosyl donor (153, 154, 160-162). TpeL from *C. perfringens* can use either UDP-glucose or UDP-GlcNAc (163), and α-toxin (Tcnα) from *C. novyi* uses UDP-GlcNAc as the sugar source (164). Mutational studies show that two amino acids near the catalytic cleft dictate the co-substrate specificity of the LCTs. TcdA, TcdB, and TcsL have isoleucine and glutamine in equivalent positions (Ile^{383}/Gln^{385} in TcdB and TcsL; Ile^{382}/Gln^{384} in TcdA), whereas TpeL and Tcnα have amino acids with smaller side chains at one or both positions (Ala^{383}/Gln^{385} in TpeL and Ser^{385}/Ala^{387} Tcnα), which can accommodate bulkier UDP-GlcNAc into the catalytic pocket. Replacing the bulky side chains with smaller groups and vice versa changes the donor substrate specificity (163, 165).

Crystal structures of the GTDs from TcdA, TcdB, TcsL, and Tcnα have been determined and have helped our understanding of the enzymatic mechanism (166-170). At the core of the structure is a Rossman fold, which is similar to that of the glucosyltransferase type A (GT-A) family of enzymes (Figure 1-6) (169, 171). Within this core is an Asp-X-Asp (DXD) motif, which is conserved in all LCTs and other GT-A members, and is essential for the enzymatic activity (172, 173). The DXD motif (Asp^{285}/ Asp^{287} in TcdA and Asp^{286}/ Asp^{288} in TcdB) is important for the coordination of the manganese cofactor, and the first Asp residue of the DXD motif also

Table 1-2. Substrate specificity of the large glucosylating toxins

Organism	Toxin	Strain	Targets	Reference
C. difficile	TcdA	VPI10463[a]	Rho, Rac, cdc42, Rap	(174)
	TcdB	VPI10463[a]	Rho, Rac, cdc42	(153, 174)
		1470[b]	Rac, cdc42, Rap, Ral, R-Ras	(67)
		8864[c]	Rac, cdc42, Rap, Ral, R-Ras	(175, 176)
		C34[d]	Rho, Rac, cdc42, Rap, Ral, R-Ras	(175)
		NAP1/RT027[e]	RhoA, Rac, cdc42, Rap, R-Ras	(177)
		NAP1$_V$/RT019	Rac, cdc42, Rap, R-Ras	(177)
C. sordellii	TcsL	VPI9048	Rac, cdc42, Rap, Ras	(160, 178)
		IP 82	Rac, Rap, Ral, Ras	(160, 162)
		6018	Rac, Rap, Ral, Ras	(178)
	TcsH	VPI9048	Rho, Rac, cdc42, Ras	(160, 179)
C. novyi	Tcnα	590, 19402	Rho, Rac, cdc42	(160, 164)
C. perfringens	TpeL	MC18	Rac, Rap, Ral, Ras	(163)

[a] Reference strain

[b] This strain has a nonsense mutation in the tcdA gene, which introduces a stop codon at amino acid position 47; Classified as TcdA negative (180)

[c] This strain has a 5.9-kb deletion in the 3' end of the tcdA region; Classified as TcdA negative (181)

[d] This strain has an insertion of approximately 2 kb in the tcdA gene that does not hinder expression of a fully active toxin (16)

[e] Epidemic strain

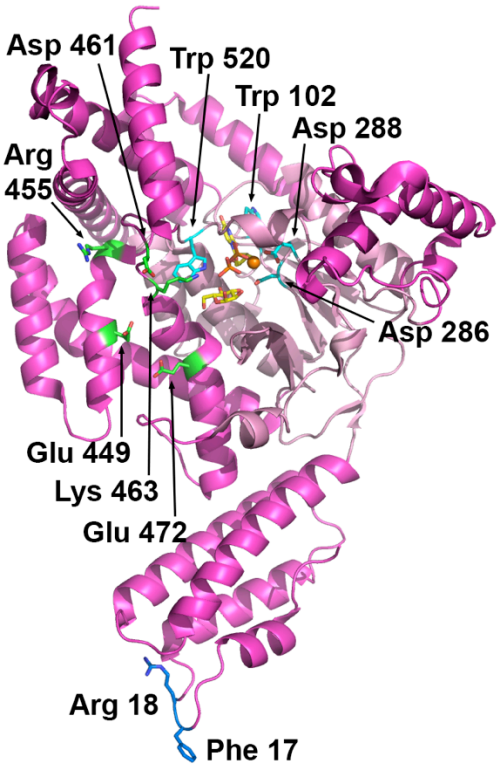

Figure 1-6. The glucosyltransferase domain. The crystal structure of the TcdB glucosyltransferase domain (2BVL) with hydrolyzed UDP-glucose (yellow carbon atoms) bound in the core GT-A fold (light pink). The side chains of key catalytic residues (Trp 102, Asp 286, Asp 288, and Trp 520; aqua carbon atoms) are indicated along with the manganese atom (orange sphere). Residues that have been implicated in GTPase substrate recognition include Glu 449, Arg 455, Asp 461, Lys 463, and Glu 472 (green carbon atoms). The membrane localization domain corresponds to the four α-helices at the base of the structure with the Phe 17 and Arg 18 residues implicated in membrane binding indicated with blue carbon atoms. Figure credit: Dr. Borden Lacy.

binds the 3′-hydroxyl group of the UDP-ribose and the glucose. UDP-binding involves additional residues that are conserved, including two tryptophans (Trp^{101}/Trp^{519} in TcdA and Trp^{102}/Trp^{520} in TcdB) that stabilize the uracil ring of the UDP by aromatic stacking or by binding the glycosidic oxygen. Mutation of these conserved residues results in significantly attenuated glycosyltransferase activity (182, 183).

In addition to the common GT-A family fold, LCTs have four α-helical sub-domains. The N-terminal sub-domain, also called the membrane localization domain (MLD), is a 4-helix bundle formed by the first ~90 residues of the GTD (Figure 1-6). The MLD has been shown to target the GTD to the cytosolic leaflets of cell membranes (such as the plasma membrane), where the enzyme can access its membrane-bound GTPase substrates (184-186). Mutation of conserved residues (particularly Phe17/Arg18) extending from the tip of the MLD 4-helix bundle has been shown to impair localization of the TcdB and TcsL GTDs to membrane lipids *in vitro* and in cells (187, 188). Additionally, MLD mutants of TcsL are defective in their ability to glucosylate GTPase substrates and cause cytotoxicity (144, 188), suggesting that localization to membranes is important for GTD-dependent cellular effects of LCTs.

The role of the other α-helical sub-domains is not known but they have been proposed to be involved in substrate binding (169). Specificity for Rho and Ras substrates varies among the LCTs (Table 1-2), but the molecular basis for these differences is not fully understood. In general, TcdB (from reference strains) and Tcnα exclusively modify Rho subfamily proteins, while TcdA and TcsH can also modify Ras GTPases (albeit to a lesser extent). TpeL and TcsL modify Ras GTPases and Rac but not Rho. Through mutagenesis and generation of chimeric GTDs, Jank *et al.* identified several charged residues located near the sugar binding pocket (Glu^{449}, Arg^{455}, Asp^{461}, Lys^{463} and Glu^{472}) that are important for substrate modification by TcdB and demonstrated that helix 17 contributes to RhoA recognition by TcdB (Figure 1-6) (183).

Interestingly, TcdB from reference (VPI10463) and variant (1470, 8864, C34 and NAP1/RT027) strains show significant differences in the GTPase substrate specificity (Table 1-2). TcdB sequences from variant strains have accumulated several mutations on the proposed substrate-binding surface compared to the classical TcdB, which likely contributes to recognition of Ras GTPases in addition to the Rho subfamily proteins (169). Of these variants strains, 1470 and 8864 lack functional TcdA and are classified as TcdA-TcdB+ (180, 181). TcdB isoforms from TcdA-TcdB+ strains have GTPase substrate specificity similar to that of TcsL in that they modify Ras and Rac but not Rho GTPases (Table 1-2). It has been proposed that these GTD variants may have arisen to compensate for the lack of functional TcdA, but the impact of the broader substrate specificity observed with TcdA is unclear.

Cellular effects of TcdA and TcdB

TcdA and TcdB disrupt the epithelial tight junctions and induce epithelial cell death, thereby causing direct injury to the colonic epithelium. Additionally, the toxins stimulate colonic epithelial cells to release proinflammatory cytokines and neutrophil chemoattractants, which lead to an acute innate inflammatory response with neutrophil recruitment, a key characteristic of the clinical pathophysiology of CDI (Figure 1-7) (189, 190). An impaired barrier in association with an active inflammation leads to increased intestinal and vascular permeability, and likely promotes fluid secretion. The loss of a protective barrier may also permit entry of toxins and/or bacteria into the lamina propria, resulting in further intestinal inflammation (Figure 1-7) (191). Prolonged exposure of the mucosal innate immune system to proinflammatory mediators can amplify the tissue damage, and may lead to severe disease outcomes (192-194). Disruption of the epithelial barrier, an intense inflammatory response with neutrophil infiltration into the lumen, and associated tissue damage are thought to contribute to the formation of pseudomembrane,

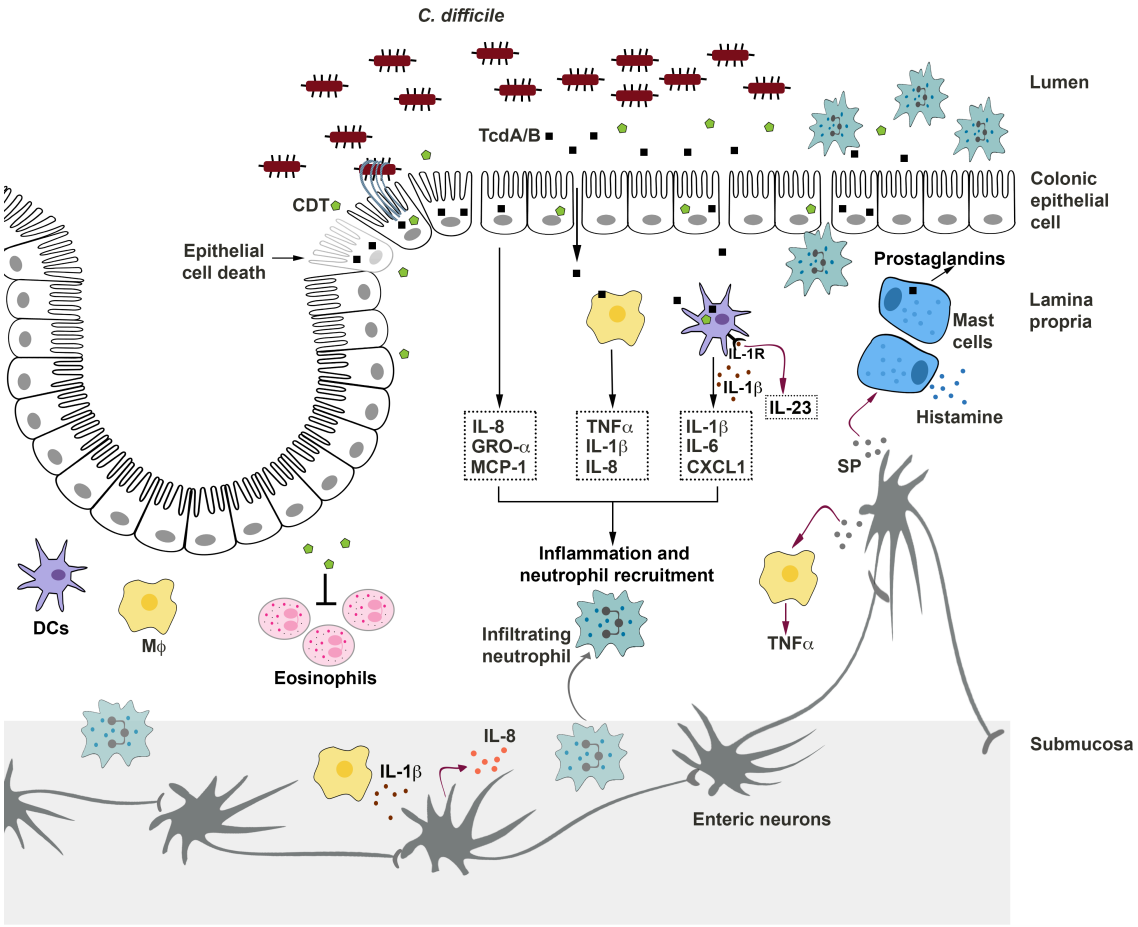

Figure 1-7. Cellular effects of *C. difficile* toxins. The toxins act on colonic epithelial cells and immune cells to induce inflammation and tissue damage. TcdA and TcdB disrupt the tight junctions and induce epithelial cell death, causing direct damage to the colonic epithelium. Additionally, the toxins stimulate epithelial cells to release inflammatory mediators that recruit neutrophils to the colonic mucosa. TcdA and TcdB can also enter the lamina propria following the disruption of the epithelial barrier and directly stimulate macrophages, dendritic cells, and mast cells to release inflammatory mediators, which further contribute to inflammation and neutrophil recruitment. Intoxication also results in the activation of enteric neurons and increased production of substance P (SP). SP can induce mast cell degranulation and can stimulate the lamina propria macrophages to release inflammatory cytokines. Prolonged intestinal inflammation can amplify tissue damage and contribute to neutrophil infiltration into the lumen, a key clinical feature of pseudomembranous colitis. The binary toxin CDT, expressed by some *C. difficile* strains, also induces cytopathic effects that lead to disruption of the tight junctions. Additionally, CDT can suppress a protective host eosinophilic response in the colon and can act synergistically with TcdA and TcdB to increase proinflammatory cytokine production by innate immune cells. Finally, CDT also contributes to *C. difficile* virulence by inducing the formation of microtubule-based cell protrusions that increase adherence of the bacteria.

which is observed in severe cases of CDI (190, 195, 196). The toxin-induced cytopathic and cytotoxic cellular effects and their underlying mechanisms are discussed below.

Glucosylation-dependent cytopathic and cytotoxic effects in epithelial cells

Rho GTPases regulate the assembly and organization of the actin cytoskeleton. RhoA induces the assembly of focal adhesions and actin stress fibers, whereas Rac1 and Cdc42 induce the formation of actin-rich surface protrusions lamellipodia and filopodia, respectively (150, 197). Additionally, Rho GTPases are important for the establishment of epithelial cell morphology and polarity (150). Consequently, GTPase inactivation by TcdA and TcdB results in the loss of the cytoskeletal structure, disassembly of focal adhesions, and disruption of tight junctions (69, 198-201). In tissue culture cells, these effects result in the characteristic cell rounding phenotype (also termed the cytopathic effect). The glucosylation-dependent cytopathic effect is thought to play an important role in the context of disease; toxin-induced disruption of tight junctions could result in impaired barrier function, increased intestinal permeability, and inflammation.

GTPase inactivation by TcdA and TcdB also affects cell cycle progression. Intoxication by TcdA and TcdB is associated with reduced expression of cyclin D1, which is required for progression through the G1 phase of the cell cycle, resulting in G1-S arrest (202, 203). Additionally, Rac1 has been shown to promote the activation of the mitotic kinase Aurora A and cyclin B/cyclin-dependent kinase (Cdk) I complex, which are required for mitotic entry, through its effector protein p21-activated kinase (PAK) (204, 205). Consequently, inactivation of Rac1 by *C. difficile* toxins delays activation of Aurora A and the CyclinB/Cdk1 complex in G2 phase and results in delayed G2-M transition (202, 204-208). Finally, RhoA inactivation by these toxins inhibits contractile ring formation and subsequent cytokinesis, resulting in the formation of bi-

nucleated cells (209). Thus, the toxins are capable of interfering with host cell proliferation by inactivating GTPases that regulate various stages of the cell cycle.

In addition to the cytopathic effect, inactivation of Rho GTPases by TcdA and TcdB can promote epithelial cell death (referred to as a cytotoxic effect). In tissue culture models, the glucosylation-dependent cell death induced by TcdA and TcdB is evident after 18-48 hours of intoxication and occurs by an apoptotic mechanism, with intoxicated cells exhibiting hallmark features including cell shrinkage, phosphatidylserine externalization, caspase activation, and DNA fragmentation (206, 208, 210-215). Apoptosis can occur via caspase-dependent and -independent mechanisms (216-219). Investigations with TcdA and TcdB show that the toxins induce the activation of executioner caspases 3 and 7 in a variety of cell lines (206-208, 211-213, 215, 220, 221). Activation of executioner caspases can occur via a death receptor-dependent extrinsic pathway (involving caspase 8) or by a mitochondria-dependent intrinsic pathway (involving caspase 9). TcdA and TcdB have been shown to induce mitochondrial outer membrane permeabilization (MOMP), cytochrome c release, and activation of caspase 9, and TcdA has also been shown to activate caspase 8 (206, 208, 211, 212, 220, 221). Although the toxin treatment induces caspase activation, the role of caspases in the apoptotic cell death caused by TcdA and TcdB is currently unclear. Experiments using caspase inhibitors and glucosyltransferase-deficient mutants have yielded conflicting results with both caspase-dependent and -independent apoptotic mechanisms having been reported for TcdA and TcdB (206, 208, 211, 213, 215, 220, 221). It is important to note that MOMP, which is regulated by pro- and anti-apoptotic B cell lymphoma 2 (Bcl-2) family members, can also promote apoptosis in a caspase-independent manner (218). MOMP can be induced by the cleavage and activation of Bid, a pro-apoptotic Bcl-2 family protein. Bid can be cleaved by caspase 8 or by non-caspase proteases such as cathepsins and calpains (216, 219). Interestingly, intoxication by TcdA also results in the cleavage of Bid, which was inhibited by a cathepsin/calpain inhibitor but not by

caspase inhibitors, suggesting a role for Bid in the caspase-independent apoptosis mechanism (208, 211, 212).

Glucosylation-independent cytotoxic effects in epithelial cells

TcdB has been shown to induce a bimodal cell death mechanism that is dependent on the toxin concentration (213). While at lower concentrations, TcdB induces apoptosis in a glucosylation-dependent manner, at higher concentrations (100 pM or above), TcdB causes a necrotic form of cell death that does not require either the autoprocessing or glucosyltransferase activities of the toxin (141, 213, 222, 223). The necrotic death can be observed in both cell culture and colon explant models after 2-4 hours of intoxication and is marked by rapid ATP depletion, early breakdown of the plasma membrane and cellular leakage, and chromatin condensation (141, 213, 222, 223). TcdB induces necrosis by triggering an aberrant production of reactive oxygen species (ROS) through the assembly of the NADPH oxidase (NOX) complex on endosomes (Figure 1-8) (123, 222, 223). High levels of ROS promote cellular necrosis likely though DNA damage, lipid peroxidation, protein oxidation and/or mitochondrial dysfunction (224-226). Interestingly, a TcdB mutant that is defective in pore formation is unable to induce cell death even at high nanomolar concentrations, suggesting that pore formation is important for the glucosylation-independent necrotic cell death caused by TcdB (125). Unlike TcdB, TcdA does not trigger ROS production via the NOX complex and causes a glucosylation-dependent apoptosis at all concentrations tested (213). The ability of TcdB, but not TcdA, to induce a necrotic cell death may explain why both a wildtype ($TcdA^+TcdB^+$) epidemic strain and an isogenic $TcdA^-TcdB^+$ mutant cause significantly more colonic tissue damage than an isogenic $TcdA^+TcdB^-$ mutant strain in animal models of infection (75). The glucosylation-independent mechanism of TcdB may play a similar role in the context of human disease; TcdB-induced

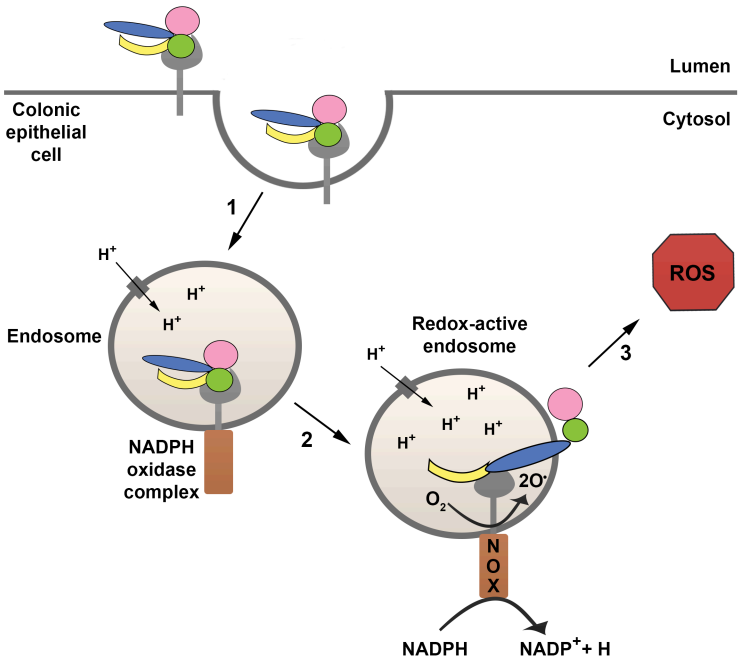

Figure 1-8. TcdB-induced necrosis. At higher concentrations (100 pM and above), TcdB causes a necrotic form of cell death that does not require the autoprocessing and glucosyltransferase activities of the toxin. TcdB induces necrosis by promoting the assembly of the NADPH oxidase (NOX) complex on endosomes (step 1). The fully assembled NOX complex in the redox-active endosome mediates the transfer of an electron from NADPH to molecular oxygen, resulting in the generation of superoxide (step 2) and production of reactive oxygen species (ROS) (step 3). High levels of ROS promote cellular necrosis likely though DNA damage, lipid peroxidation, protein oxidation and/or mitochondrial dysfunction.

necrosis likely contributes to the extensive gut damage observed in patients with severe forms of CDI.

Mammalian endocytic mechanisms

The plasma membrane of mammalian cells gates access to the cell's interior. Molecules on the outer leaflet of the plasma membrane respond to changes in extracellular environment and consequently their composition must be tightly regulated to achieve appropriate response to external stimuli. Endocytosis is the process by which cells regulate the turnover of membrane components. Endocytosis involves the *de novo* formation of internal membranes from the lipid bilayer, which subsequently undergo scission and release into the cytosol. In addition to regulating how cells communicate with their environment, endocytosis also plays a role in cell migration, cell division, intracellular signaling, and antigen presentation (227).

There are many ways to enter a cell. Figure 1-9 and Table 1-3 summarize key endocytic routes, some known cargoes and host factors implicated in these pathways. These pathways are described in detail in Doherty and McMahon (227), Mercer et. al (228) and Boucrot et. al (229). Pathogens such as viruses and bacteria and virulence factors such as bacterial toxins often exploit endogenous endocytic mechanisms to gain access to host cell cytosol. Internalization can occur by pinocytosis, which involves uptake of fluids and solutes. Pinocytic pathways include macropinocytosis, clathrin-mediated endocytosis, and several clathrin-independent mechanisms such as caveolae-mediated endocytosis, flotillin- or RhoA-dependent endocytosis. Some clathrin-independent pathways involve dynamin, a large GTPase that constricts the vesicle at the neck and allows for the scission and release into the cytosol.

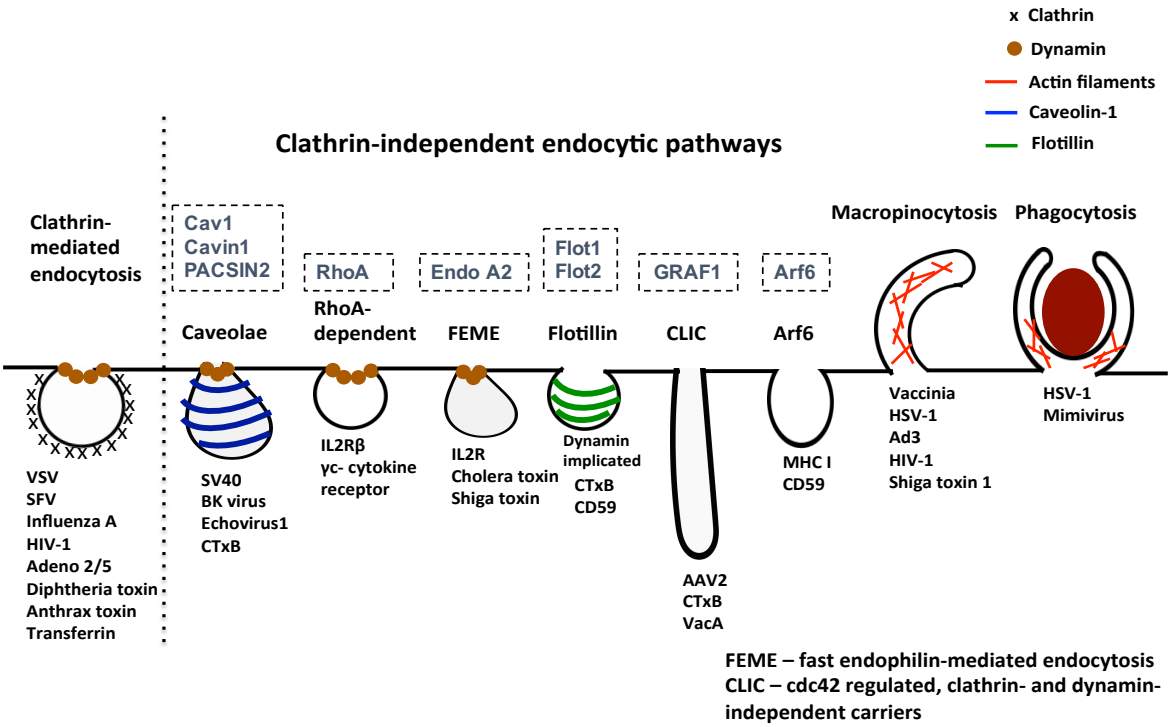

Figure 1-9. Endocytic routes. Endocytosis can occur via phagocytosis or by clathrin-dependent or –independent pinocytic mechanisms. Endogenous cargoes as well as pathogens and pathogenic agents that utilize these mechanisms are indicated below each pathway. Host factors important for the pathway are indicated in the dotted boxes above. Modified from Mercer, Schelhaas and Helenius (228).

Table 1-3. Endocytic pathways and associated cellular factors.

Endocytic pathways	Morphology	Dynamin required?	Associated proteins
Clathrin-mediated	Vesicular	Yes	Clathrin heavy and light chain, AP2, epsin, eps15, SNX9, synaptojanin, actin, amphiphysin, and many others.
Caveolae-dependent	Vesicular/tubulovesicular	Yes	Caveolins, cavin1/PTRF, PACSIN2, Scr, PKC, actin (many signaling proteins localize to these sites)
Clathrin-independent carriers (CLIC)	Tubular/ring like	No	Cdc42, ARHGAP10, actin, GRAF1, and other GRAFs.
Flotillin-dependent	Vesicular	Implicated but unclear	Flotillin 1 and 2
ARF6-dependent	Vesicular/ tubular	No	ARF6
IL-2Rβ pathway	Vesicular?	Implicated	IL-2Rβ, PAK1, PAK2
Fast endophilin-mediated endocytosis (FEME)	Tubulovesicular	Yes	Endophilin A2, actin, Rac, PI3K, Pak1
Macropinocytosis	Highly ruffled	No	Actin, PAK1, PI3K, Ras, Src
Phagocytosis	Cargo shaped	Implicated	Actin, IQGAP1, amphiphysin1, Rho kinase, adhesion proteins

Modified from Doherty and McMahon (227).

Large particles such as bacteria or viruses can also be internalized by phagocytosis, a process observed primarily in immune cells. Similar to many pathogens and pathogenic agents, TcdB exploits the clathrin pathway to gain access to host cell cytosol. However, the mechanism that promotes TcdA delivery to cytosol has remained elusive. A major focus of my thesis work was to determine the mechanistic and molecular details of the endocytic pathway utilized by TcdA. My investigations showed that TcdA did not utilize clathrin- or caveolae-mediated endocytosis. However, the endocytic mechanism did share some common features. TcdA utilized a pathway that required dynamin similar to that of the clathrin- and caveolae-mediated pathway. Additionally, the pathway also required PACSIN2/Syndapin II, a BAR (Bin/amphiphysin/rvs)-domain-containing protein that has been shown to be involved in membrane sculpting of caveolae and recruitment of dynamin for caveolae fission (230, 231). PACSIN2 interacts with dynamin and regulators of actin to induce membrane curvature and the formation of vesicular-tubular invaginations that can promote receptor-mediated endocytosis (232-234). In my data chapter, I will describe my efforts towards identification of PACSIN2 and dynamin as factors critical for TcdA entry and provide evidence that the endocytic route utilized TcdA is novel and distinct from clathrin- or caveolae-mediated pathways.

Research Objectives

The pathophysiology of *C. difficile* infection is primarily mediated by the actions of TcdA and TcdB. Consequently, there is a significant interest in understanding the unique and shared roles each toxin plays in disease. Building a molecular and mechanistic framework of how these toxins disrupt host cellular function is a priority among many in our field. Pathogenic cytopathic and cytotoxic effects induced by TcdA and TcdB require binding to cell surface receptors, internalization into host cells, and transport to acidified endosomal compartments within cells. When I began my work in the Lacy lab, efforts were already underway to identify host factors and signaling mechanisms that contribute to TcdB intoxication in colonic epithelial cells. Mitch LaFrance (a former graduate student in the Lacy lab) was investigating a TcdB receptor candidate (PVRL3), while Nicole Chumbler (a former graduate student) and Melissa Farrow (Research Assistant Professor) were working to elucidate mechanisms underlying TcdB-induced cytotoxicity. Furthermore, a year before I joined the lab, the Aktories group had published a report showing that TcdB entered the host cell by clathrin-mediated endocytosis (114). In contrast, the early events that occur during TcdA intoxication and the mechanism of TcdA-induced cytotoxicity were not known.

My goal was to investigate the early stages of TcdA intoxication and identify host factors and mechanisms utilized by TcdA to gain access to the host cell cytosol. My thesis work focused on three important questions with respect to toxin entry: 1) What are the cellular receptors for TcdA on colonic epithelial cells? 2) How does the toxin interact with its receptor(s)? and 3) How is TcdA internalized and delivered to acidified endosomal compartments with the cell? In Chapter II, I describe in detail my efforts to identify the endocytic pathway utilized by TcdA to gain entry into the host cell. I show that, unlike TcdB, TcdA entry is clathrin-independent. Instead, TcdA utilizes a previously uncharacterized host endocytic

process that is caveolae-independent but requires dynamin and PACSIN2 (or Syndapin II). PACSIN2 has been previously shown to be important for caveolae-mediated endocytosis; it contributes to the curvature of caveolae and the recruitment of dynamin for caveolae fission. The observation that PACSIN2 can function outside of the caveolae system suggests a novel mechanism of entry, one for which TcdA is now a known cargo. Consequently, studies on TcdA entry have the potential to inform us of mechanisms and additional factors critical for the formation, assembly, and/or function of the PACSIN2-and dynamin-dependent pathway. I have already begun work to identify additional factors involved in TcdA endocytosis, which I discuss in Chapter III. I also describe our ongoing and future efforts towards identification of TcdA receptors and understanding toxin interaction with the host cell. Results from these studies will be combined with ongoing work on TcdB to build a mechanistic framework of how both toxins disrupt epithelial function and cause tissue damage, and will guide the development of therapeutic strategies to prevent CDI.

CHAPTER II

CLOSTRIDIUM DIFFICILE TOXIN A UNDERGOES CLATHRIN-INDEPENDENT, PACSIN2-DEPENDENT ENDOCYTOSIS

Introduction

Clostridium difficile, a gram-positive, spore-forming anaerobe, is the most common cause of healthcare-associated infections and gastroenteritis-associated death in the United States (5, 235, 236). The pathogenesis of *C. difficile* is mediated by two large homologous exotoxins, TcdA and TcdB (308 kDa and 270 kDa, respectively), capable of causing epithelial cell death, fluid secretion and inflammation (190). Recent studies, using isogenic single and double toxin knockout strains, have shown that either TcdA or TcdB alone can cause disease in animal models, with TcdB linked to severe disease phenotypes (73-75). Most pathogenic isolates produce TcdA and TcdB emphasizing the need to consider both toxins when developing *C. difficile* therapeutics (23, 237).

TcdA and TcdB are broadly classified as AB toxins, wherein a B subunit is involved in the delivery of an enzymatic A subunit into the cytosol of a target cell. For *C. difficile* toxins, the A subunit is an N-terminal glucosyltransferase domain (GTD) that inactivates small GTPases, such as RhoA, Rac1 and Cdc42 (153, 154). The B subunit is composed of the combined repetitive oligopeptides (CROPs) domain, delivery/pore-forming and autoprotease domains. The CROPs has been proposed to function as the receptor-binding domain because it can bind cell surface carbohydrates (78, 82, 84), and antibodies against the CROPs region of TcdA and TcdB can neutralize toxicity (91, 103, 238). However, recent studies reveal that toxins lacking the CROPs domain can still bind, enter and perturb host cellular function, highlighting the presence

of alternative or additional receptor binding regions within the toxins (90, 107-109). Upon binding to cells, toxins are taken up by endocytosis and transported to acidified endosomal compartments (190). Acidification is thought to trigger a conformational change in the delivery domain, allowing it to insert into the membrane of the endosome and form a pore through which the enzymatic domains can be translocated (107, 118, 121). Once inside the cytosol, host inositol hexakisphosphate binds the autoprotease domain to induce cleavage and release of the GTD (129). The GTD transfers a glucose from UDP-glucose onto the switch I region of Rho family GTPases. This inactivation results in perturbation of the actin cytoskeleton and cell rounding (cytopathic effect) as well as apoptotic cell death (cytotoxic effect) (206, 212, 214, 215). At higher concentrations, TcdB is also capable of inducing aberrant production of reactive oxygen species, resulting in cell death by necrosis (141, 222).

Despite their homology, TcdA and TcdB appear to engage different receptors on the cell surface. Multiple receptors have been proposed for TcdA, including Galα1-3Galβ1-4GlcNac, rabbit sucrase-isomaltase and glycoprotein 96 (85, 86, 96). Three recent studies have shown that poliovirus receptor-like protein 3, chondroitin sulfate proteoglycan 4, and frizzled proteins can function as TcdB receptors on epithelial cells (104, 105, 108). Receptor binding by TcdB is followed by internalization via clathrin-dependent endocytosis (114), but the mechanism(s) by which TcdA enters cells has been less clear (113, 114).

In this study, I investigated TcdA cellular uptake by systematically perturbing the function of key host factors involved in various endocytic pathways using RNAi-based knockdown approaches and small molecule inhibitors, and by analyzing the toxin colocalization with markers of endocytic pathways by confocal microscopy. Results from this study indicate that cellular uptake of TcdA is mediated by a PACSIN2- and dynamin-dependent pathway and does not involve clathrin- or caveolae-mediated endocytosis. This work was published in PLoS Pathogens.

Results

TcdA and TcdB utilize distinct endocytic mechanisms to intoxicate epithelial cells

I first examined whether TcdA-induced cytotoxicity in colonic epithelial cells requires clathrin-mediated endocytosis (CME). Human colorectal adenocarcinoma (Caco-2) cells were transduced with non-targeting shRNA (ctrl shRNA) and shRNAs (sh489 and sh887) targeting two different sequences in the clathrin heavy chain (CHC). Expression of sh489 resulted in greater than 90% reduction in CHC protein levels, whereas sh887 did not alter CHC levels in cells (Figure 2-1A; inset). I challenged these shRNA-expressing cells with TcdA and TcdB concentrations ranging from 100 pM to 100 nM and assayed for cellular viability using CellTiterGlo. As expected, cells expressing sh489 (that were depleted of CHC) showed increased survival relative to cells expressing ctrl shRNA or sh887 when challenged with TcdB (Figure 2-1A; top panel). However, depletion of CHC did not affect TcdA-induced cell death across the range of concentrations tested (Figure 2-1A; bottom panel). A similar observation was made using a transient knockdown of CHC with small interfering RNA (siRNA) (Figure 2-2). Taken together, these data show that clathrin heavy chain is dispensable for TcdA-induced toxicity in Caco-2 epithelial cells.

The cytotoxicity data suggest that CME may not be required or involved in TcdA entry. To test this, I checked for colocalization of fluorescently labeled TcdA (TcdA-546) with labeled TcdB (TcdB-647) and CHC, markers of clathrin-mediated endocytosis. I verified that fluorescent labeling with Alexa dyes did not affect TcdA function prior to using TcdA-546 in the imaging assays (Figure 2-3). For the confocal assays, I intoxicated cells with 50 nM of TcdA-546 as it provided sufficient signal and dynamic range needed for image analyses (Figure 2-4).

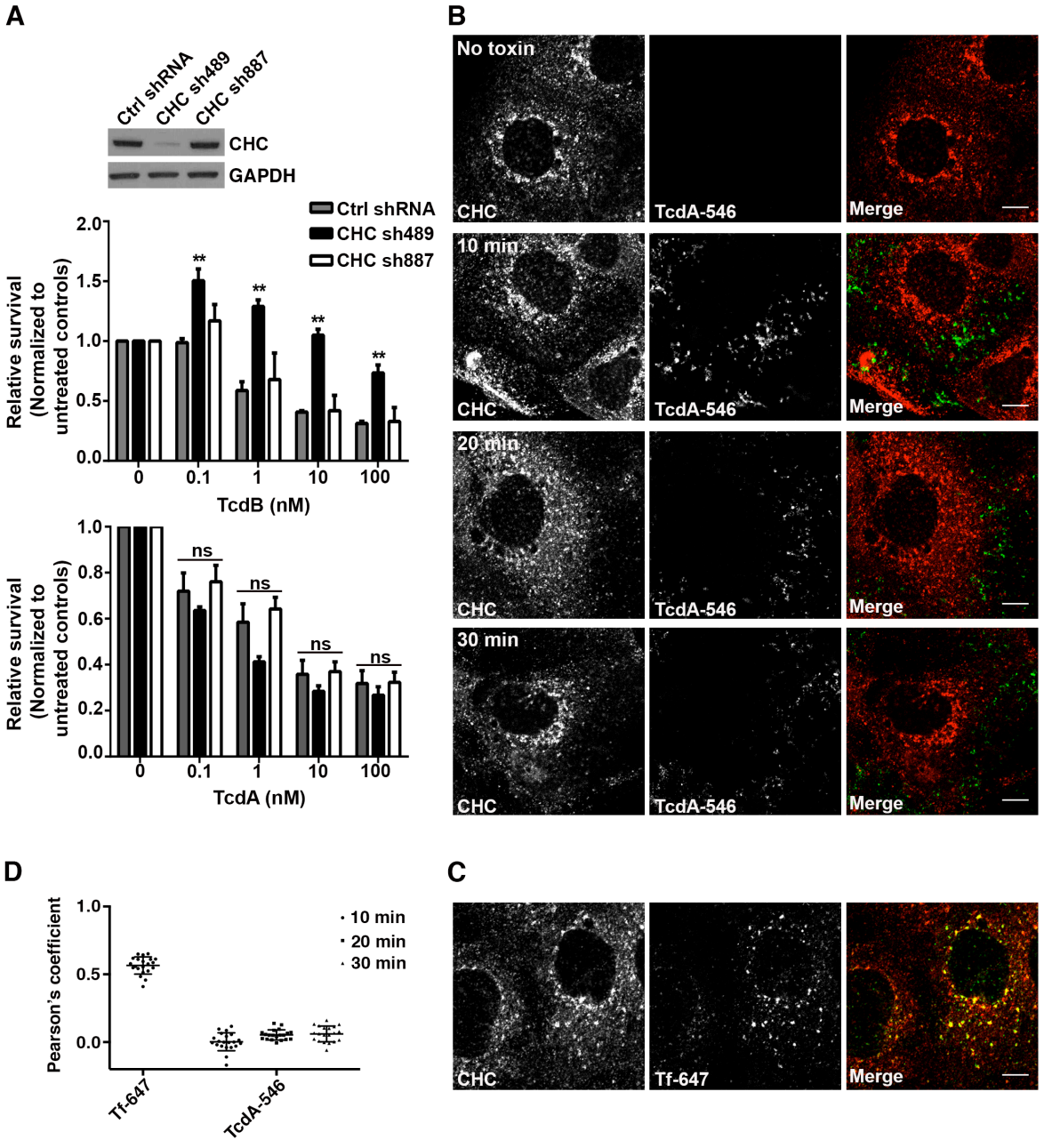

Figure 2-1. **TcdA and TcdB utilize distinct endocytic mechanisms to intoxicate colonic epithelial cells. (A) Depletion of clathrin heavy chain (CHC) does not affect TcdA-induced cytotoxicity.** Caco-2 cells expressing non-targeting shRNA (Ctrl shRNA) and shRNAs 489 and 887 targeting two different sequences in CHC were treated with indicated concentrations of TcdB or TcdA in triplicate. ATP levels were determined using CellTiterGlo and normalized to signal from untreated cells to assess the relative survival of cells post-toxin treatment. Results represent the mean and SEM of three independent experiments. Data were analyzed using two-way ANOVA and p-values were generated using Dunnett's multiple comparisons test in GraphPad Prism. **p<0.005; ns, not significant. Western blot of whole cell lysates from shRNA-expressing Caco-2 cells were probed with antibodies against CHC and GAPDH (loading control). Expression of shRNA489 targeting CHC results in significant reduction in CHC protein

levels as shown in the inset. **(B) TcdA does not colocalize with clathrin heavy chain during cell entry.** Caco-2 cells on glass coverslips were chilled at 10 °C for 45 min and then exposed to media containing 50 nM TcdA-546 or buffer (no toxin control). The toxin was allowed to bind to cells for 45 min at 10 °C. Unbound toxin was removed, and cells were shifted to 37 °C to allow internalization of toxin for the times shown. At each time point, cells were washed once with pre-warmed PBS, fixed and stained for CHC, and imaged by confocal microscopy. Merged images show clathrin in red and toxin in green. Scale bars, 10 μm. (**C) Transferrin colocalizes with clathrin-coated pits as expected.** Experiment was performed as in (B) with 20 μg/ml of transferrin-alexa647 (Tf-647; positive control for colocalization with clathrin). Transferrin internalization occurred at 37 °C for 10 min. Merged images show clathrin in red, transferrin in green and colocalization in yellow. Scale bars, 10 μm. The images shown in (B) and (C) are representative of multiple fields imaged from two independent experiments. **(D)** Pearson's correlation coefficient to assess the extent of colocalization between clathrin heavy chain and Tf-647 or TcdA-546. Data represent mean and SD of 20 individual cells.

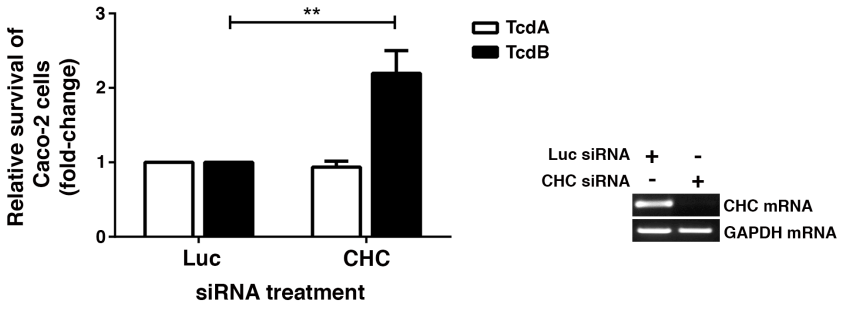

Figure 2-2. siRNA-mediated transient depletion of clathrin heavy chain does not affect TcdA-induced cell killing. Caco-2 cells were transfected with 10 nM siRNA against clathrin heavy chain (CHC) or luciferase (Luc; non-targeting control), exposed to 50nM TcdA (white bars) or TcdB (black bars) and then assayed for cellular viability using CellTiterGLO. Fold change of survival was obtained by normalizing the relative viability of samples to luciferase control. The data represent the average of ten independent experiments performed in triplicate with SEM indicated as error bars. Data were analyzed using Welch's t test. **$p<0.005$. RT-PCR confirms that siRNA treatment resulted in a decrease in CHC mRNA expression.

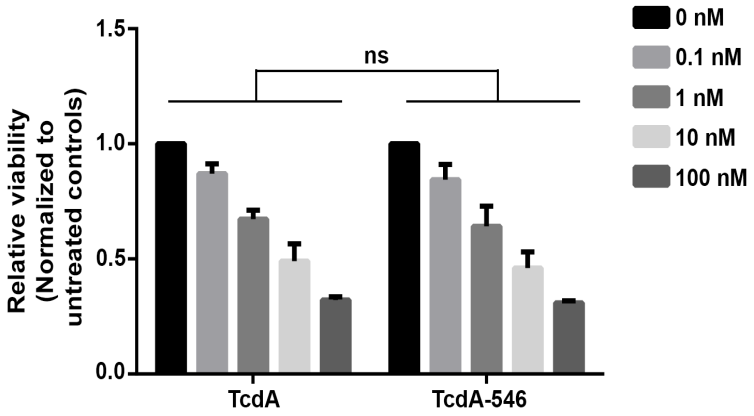

Figure 2-3. Labeling does not affect TcdA function. Caco-2 cells were treated with indicated concentrations of TcdA or TcdA-546 in triplicate. ATP levels were determined using CellTiterGlo and normalized to signal from untreated cells to assess the relative survival of cells post-toxin treatment. Results represent the mean and SEM of three independent experiments. Data were analyzed using two-way ANOVA and p-values were generated using Sidak's multiple comparisons test in GraphPad Prism. ns, not significant.

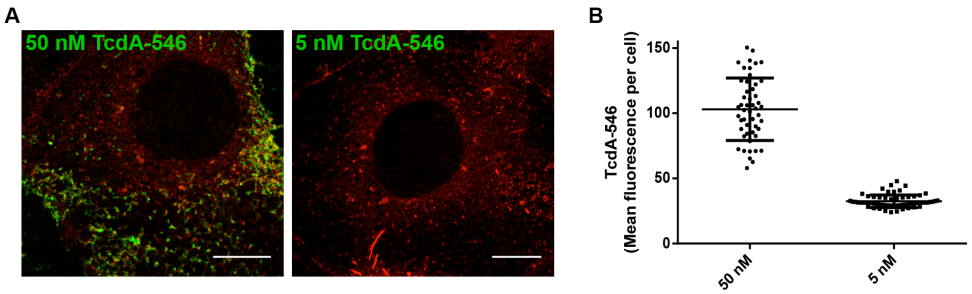

Figure 2-4. Comparison of TcdA fluorescence at 50 nM and 5 nM in Caco-2 cells. (A) Caco-2 cells were allowed to bind 50 nM or 5 nM TcdA-546 for 45 min at 10 °C. Cells were shifted to 37 °C for 4 min, washed, fixed and imaged using a LSM 510 Meta Inverted laser-scanning confocal microscope (Zeiss). In the images, TcdA-546 is shown in green and PACSIN2 in red. Scale bars, 10 μm. **(B)** Comparison of mean fluorescence intensities of TcdA-546 at 50 and 5 nM. Data represent mean and SD of 50 individual cells chosen at random.

Confocal microscopy revealed minimal to no detectable colocalization of TcdA-546 with TcdB-647 during cell entry (Figure 2-5). However, the labeling efficiency and signal intensity for TcdB was poor and less than desirable for colocalization and other imaging-based analyses. The technical challenges associated with obtaining higher labeling efficiencies while maintaining toxin function and internalization prevented me from using TcdB as a control in future immunofluorescence assays. As a result, in the subsequent experiment, transferrin (Tf-647) was used as a positive control for colocalization with CHC. As expected, Tf-647 exhibited significant colocalization with clathrin-positive vesicles (Figure 2-1C and D). However, in similar experiments, TcdA-546 did not colocalize with clathrin-positive structures during cell entry (Figure 2-1B and D). Taken together, these findings support a clathrin-independent mechanism of entry for TcdA and indicate that TcdA and TcdB utilize distinct endocytic mechanisms to intoxicate epithelial cells.

Clathrin-independent uptake of TcdA requires functional dynamin

Clathrin-independent endocytic (CIE) pathways can be dynamin-dependent or -independent (227, 239). Dynamin is a large GTPase that facilitates scission and release of newly formed endocytic vesicles from the plasma membrane. To determine if the clathrin-independent uptake of TcdA requires dynamin function, I perturbed dynamin activity in cells by siRNA depletion or pharmacological inhibition and studied the effect on toxin-induced Rac1 glucosylation and cell death. Caco-2 cells were transfected with siRNAs targeting dynamin-1 or luciferase (non-targeting control) and subsequently challenged with TcdA. I found that depletion of dynamin-1 improved survival of cells treated with TcdA by at least three-fold compared to the luciferase control (Figure 2-6A). I also verified that dynamin is important for the TcdA cytotoxic mechanism by using dynasore, a potent inhibitor of dynamin GTPases (240). Dynasore treatment prevented Rac1 glucosylation by TcdB in Caco-2 cells, consistent with the known role

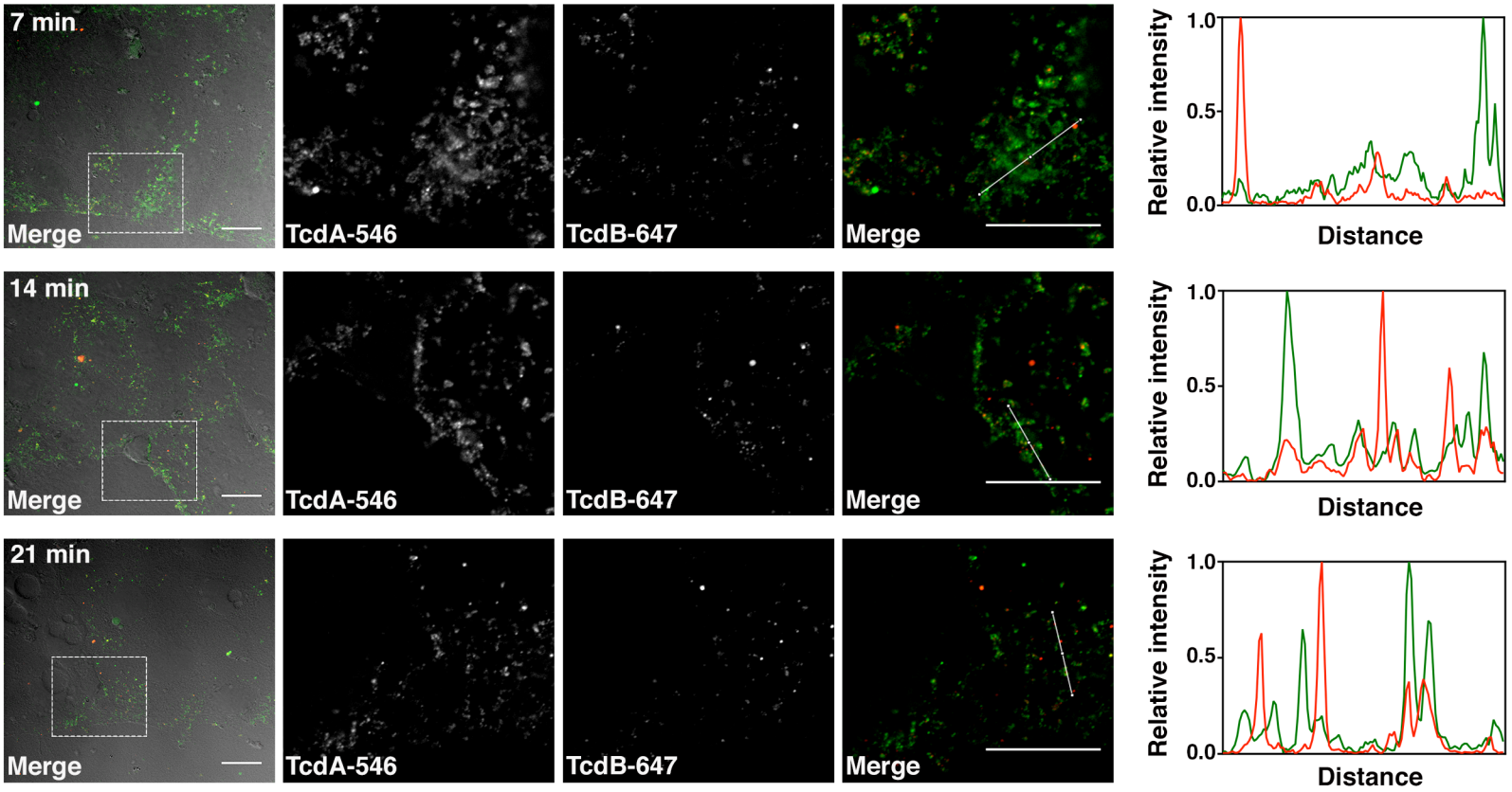

Figure 2-5. TcdB-647 signal intensity in cells is extremely low. Caco-2 cells were allowed to bind 50 nM TcdA-Alexa546 and TcdB-Alexa647 for 45 min at 10 °C. Unbound toxins were removed and cells were shifted to 37 °C to allow uptake for the times shown. At indicated times, cells were washed, fixed and imaged using a confocal Microscope. 1x merged images on the left show TcdB in red, TcdA in green and DIC in gray. White dotted boxes in the 1x merged images denote areas that were magnified. Scale bars, 20 µm. The profile analyses on the right represent the relative intensity of red and green pixels at each point along the line trace shown in the zoomed color images.

of dynamin in CME (Figure 2-6B and C). Furthermore, pretreatment of cells with dynasore completely inhibited Rac1 glucosylation by TcdA (Figure 2-6B and C), supporting my earlier observation that TcdA intoxication is dynamin-dependent.

To determine what step in the toxin pathway the inhibitor was affecting, I performed time-of-addition assays. Dynasore was added prior to intoxication (pretreatment), at the same time as toxin (0 min), or at various times post-intoxication, and Rac1 glucosylation in cells by TcdB (Figure 2-7A and B) and TcdA (Figure 2-7C and D) was measured. Results from these experiments show that inhibition of toxin-induced glucosylation can be bypassed by adding dynasore 5 to 10 min post-intoxication, suggesting that the inhibitor is acting at the stage of toxin entry. It is important to note that it takes several minutes for dynasore to appreciably inhibit dynamin-dependent pathways (240), which might explain the glucosylation occurring when the inhibitor and toxin are added together. In summary, these data indicate that TcdA entry and intoxication in epithelial cells require functional dynamin.

Depletion of caveolin1, cavin1 or PACSIN2 inhibits TcdA-induced toxicity in Caco-2 cells.

The above findings indicated that TcdA uptake occurs through a clathrin-independent and dynamin-dependent endocytic mechanism. Dynamin has been implicated or shown to be involved in several CIE pathways such as caveolar endocytosis, the RhoA-dependent pathway, flotillin-dependent endocytosis and endophilinA2-mediated endocytosis (FEME: fast endophilin-mediated endocytosis) (227, 229, 239, 241). To rapidly assess which of these pathway(s), if any, contribute to TcdA uptake, I performed siRNA-mediated depletion of a panel of host factors involved in these uptake mechanisms and examined their impact on TcdA-induced cell death.

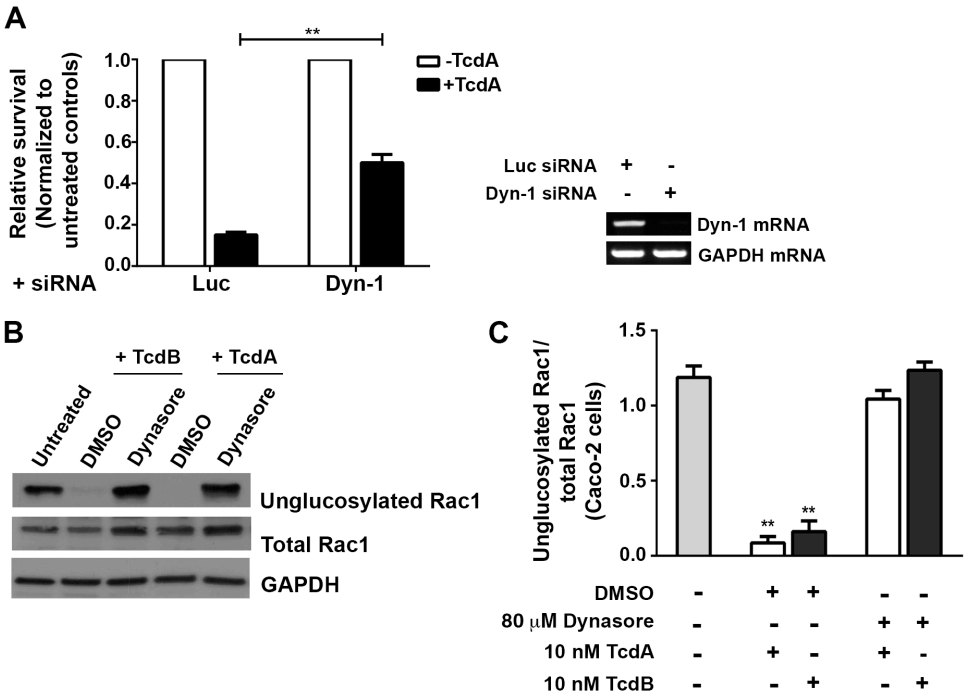

Figure 2-6. TcdA-induced Rac1 glucosylation and cytotoxicity are dynamin-dependent. (A) Depletion of dynamin-1 confers resistance to TcdA challenge. Caco-2 cells were transfected with 10 nM siRNA against dynamin-1 (Dyn-1) or luciferase (Luc; non-targeting control) and then intoxicated with 50 nM TcdA. ATP levels were determined using CellTiterGlo and normalized to signal from untreated cells to assess the relative survival of cells post-toxin treatment. The data represent the average of four independent experiments performed in triplicate with the SEM indicated as error bars. Data were analyzed using Welch's t test. **p<0.005. RT-PCR confirms that siRNA treatment resulted in a decrease in Dyn-1 mRNA expression. **(B) Pharmacological inhibition of dynamin GTPases prevents Rac1 modification by TcdA**. Caco-2 monolayers were pretreated with either 80 μM dynasore or with an equal amount of DMSO control for 1 h at 37 °C. Cells were switched to 4 °C for 1 h and then intoxicated with either 10 nM TcdA or TcdB (positive control). Toxins were allowed to bind at 4 °C for 1 h and then internalize at 37 °C. TcdA and TcdB treated cells were harvested after 25 min and 15 min, respectively. Whole cell lysates were prepared for SDS PAGE and Western blot. The blot was probed with antibodies against the unglucosylated and total Rac1, and GAPDH. Cells that did not receive toxin or treatment were used as a control. **(C)** Four replicates of the experiments shown in (B) were quantified by densitometry and represented as the ratio of unglucosylated and total Rac1 levels. Results reflect the mean and SEM, and were analyzed using one-way ANOVA. p-values were generated using Dunnett's multiple comparisons test in GraphPad Prism. **p<0.005.

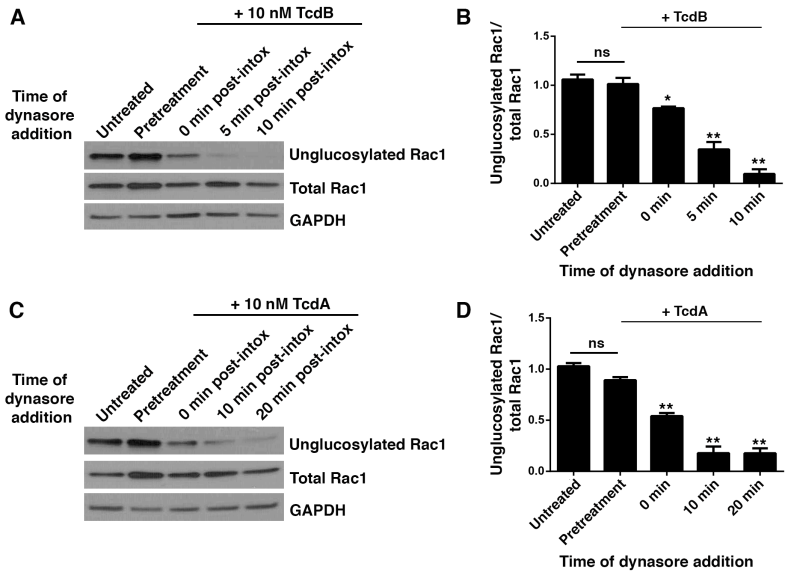

Figure 2-7. Dynasore time-of-addition assays reveal a block in toxin entry. Rac1 glucosylation assays were performed with 10 nM TcdB (A) or TcdA (C) as described in Fig. 2B but the time of addition of dynasore was varied. Dynasore was added 1 h prior to toxin treatment (pretreatment), or at the same time as toxin (0 min post-intox), or at various times post-intoxication. (B) and (D) Three replicates of the experiments shown in panels A and C were quantified by densitometry and represented as the ratio of unglucosylated and total Rac1 levels. Results reflect the mean and SEM, and were analyzed using a one-way ANOVA. p-values were generated using Dunnett's multiple comparisons test in GraphPad Prism. *p<0.05; **p<0.005; ns, not significant.

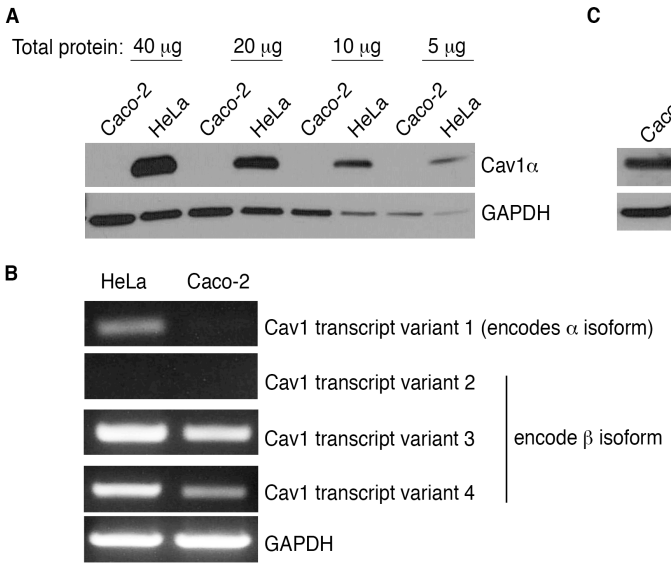

Figure 2-8. Caveolin-1 β isoform is expressed in Caco-2 cells. (A) Western blots of whole cell lysates from HeLa and Caco-2 cells probed with antibodies against the α isoform of caveolin-1 (sc-894) and GAPDH. **(B)** Total RNA from HeLa and Caco-2 cells were subjected to RT-PCR analyses to determine the mRNA expression of caveolin-1 transcript variants. GAPDH was amplified as a loading control. **(C)** Western blots of whole cell lysates from Caco-2 and caveolin1$^{-/-}$ mouse embryonic fibroblast (MEF) cells probed with antibodies against caveolin-1 (both isoforms, BD biosciences) and tubulin (loading control).

Caveolae-mediated endocytosis is a commonly studied clathrin-independent and dynamin-dependent pathway (227, 242). However, there are conflicting reports regarding the expression of caveolin1 (Cav1) in Caco-2 cells (243-245). Cav1 is typically expressed as two isoforms, Cav1α and Cav1β, and both isoforms can be found in caveolae (246). Western blotting and RT-PCR analyses show that Caco-2 cells preferentially express the beta isoform of Cav1 (Figure 2-8). Since Caco-2 cells express Cav1, I decided to include host factors from the caveolar pathway, namely Cav1, cavin1 and PACSIN2 (protein kinase C and casein kinase substrate in neurons 2), in the siRNA panel. Results from the siRNA screen show that depletion of flotillin1 or 2 (flotillin-dependent pathway), RhoA (RhoA-dependent pathway) or endophilinA2 (endoA2; FEME pathway) does not affect TcdA-induced cytotoxicity in Caco-2 cells. However, knockdown of Cav1, cavin1 or PACSIN2 protected cells from TcdA challenge (Figure 2-9). This protective effect was not observed for cells treated with TcdB, which enters via CME and was used as a negative control.

TcdA uptake is PACSIN2-dependent but occurs independent of caveolae-mediated endocytosis

Cav1, cavin1 and PACSIN2 are host proteins involved in caveolae-mediated endocytosis (230, 231, 247-249). Results from the siRNA screen, therefore, lead to the hypothesis that TcdA uptake in Caco-2 cells is mediated by caveolae-dependent endocytosis. However, Vogel *et al.* had previously shown that Caco-2 cells contain extremely few, if any, caveolae (245). Consistent with their finding, I observed that the cytoplasmic staining of cavin1 in Caco-2 cells was diffuse and atypical of caveolae-associated pools (Figure 2-10A). Caco-2 cells appear to lack caveolae despite expressing Cav1β and cavin1. Furthermore, I did not

observe appreciable colocalization of TcdA-546 with Cav1 or cavin1 in Caco-2 cells (Figure 2-10A).

To better understand the contribution of caveolae-mediated endocytosis to TcdA uptake, I decided to investigate TcdA entry in mouse embryonic fibroblast (MEF) cells, which are sensitive to TcdA and contain caveolae. Confocal microscopy revealed no detectable colocalization of TcdA-546 with Cav1 or cavin1 in MEFs (Figure 2-10B). Furthermore, investigation of TcdA-induced cell rounding in wildtype and Cav1-/- MEF cells shows that Cav1 is not required for the TcdA cytopathic mechanism (Figure 2-10C and D). A similar observation was made using a transient knockdown of Cav1 in wildtype MEF cells (Figure 2-11A and B). Taken together, these data suggest that TcdA uptake in MEFs is caveolae-independent. To test this directly, I measured toxin uptake in MEFs depleted of Cav1. MEF cells were transfected with control (luciferase) or Cav1 siRNA and allowed to internalize TcdA-546. Cav1 and TcdA-546 fluorescence intensities in cells were measured and compared between the two conditions to determine knockdown efficiency and extent of toxin uptake. I found that MEFs transfected with Cav1 siRNA showed a 67% decrease in Cav1 fluorescence staining compared to controls (Figure 2-11C and D). The toxin levels in cells remained unaffected by Cav1 depletion, however, supporting the idea of a caveolin-independent uptake mechanism for TcdA in MEFs (Figure 2-11C and E). In summary, data from both Caco-2 and MEF cells show that caveolae-mediated endocytosis does not contribute to cellular uptake of TcdA.

Interestingly, despite the lack of significant colocalization with Cav1-positive vesicles, TcdA-546 colocalized with PACSIN2 in wildtype MEF cells (Figure 2-12). PACSIN2/Syndapin-II is a BAR (Bin/amphiphysin/rvs)-domain-containing protein that has been shown to interact with dynamin and regulators of actin to induce membrane curvature and the formation of vesicular-tubular invaginations that can promote receptor-mediated endocytosis (232-234).

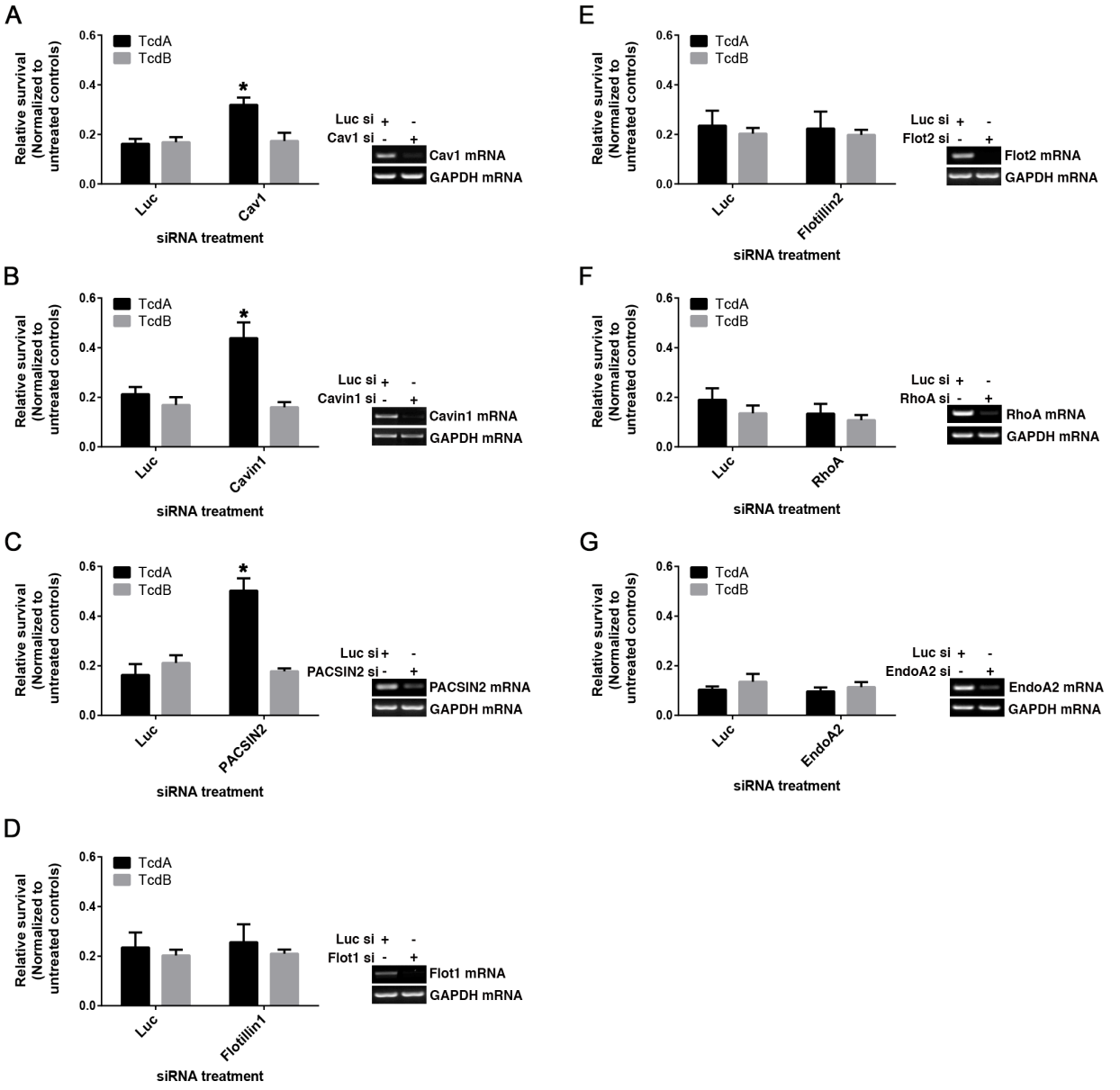

Figure 2-9. Depletion of caveolin1, cavin1 or PACSIN2 inhibits TcdA-induced toxicity in Caco-2 cells. Caco-2 cells were transfected with 10 nM siRNA against indicated endocytic host factors, exposed to 50 nM TcdA (black bars) or TcdB (gray bars) and then assayed for cellular viability using CellTiterGLO. Relative survival was obtained by normalizing the viability of treated cells to untreated (no toxin) controls. The data represent the average of at least three independent experiments performed in triplicate with the standard error of the mean indicated as error bars. Data were analyzed using t test. *p<0.05. RT-PCR confirms that siRNA treatment resulted in a decrease in the target mRNA expression.

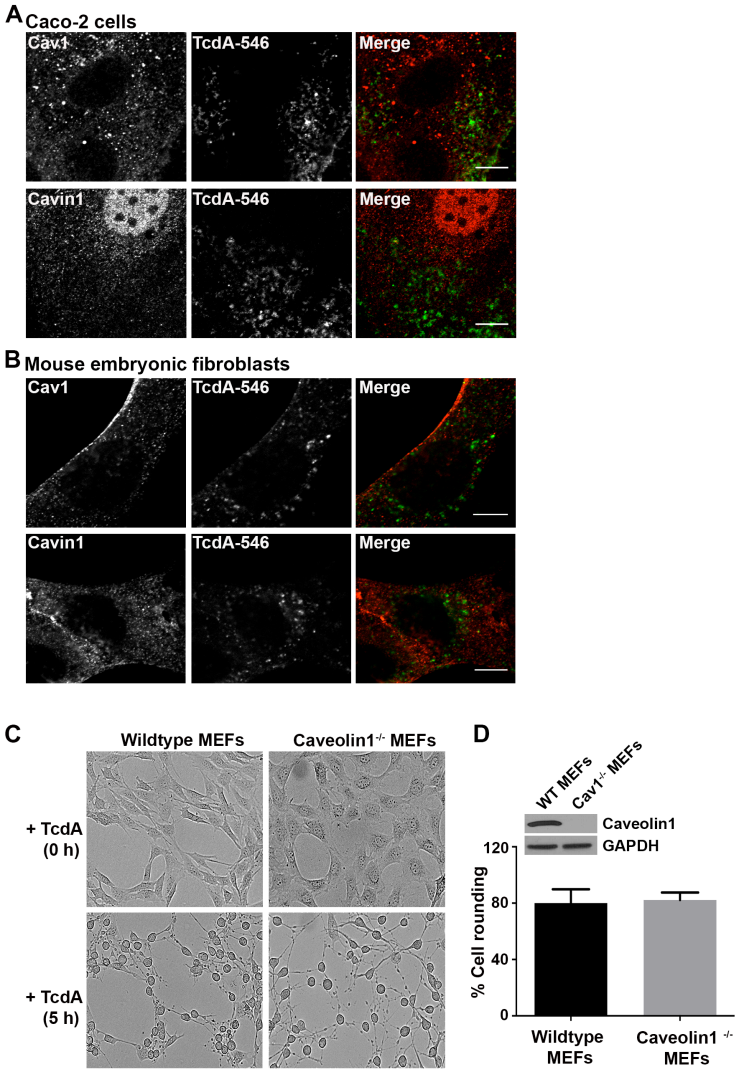

Figure 2-10. **TcdA entry does not involve caveolin-mediated endocytosis. (A) TcdA does not colocalize with caveolin1 (cav1) or cavin1 in Caco-2 cells.** Colocalization studies of TcdA and caveolar endocytic proteins, caveolin1 and cavin1, were performed by binding TcdA-546 to Caco-2 cells at 10 °C for 45 min and shifting cells to 37 °C to allow toxin uptake. After 10 min, cells were fixed and stained for caveolin1 or cavin1 and imaged using a confocal microscope. Merged images show caveolin1 or cavin1 in red and toxin in green. Scale bars, 10 µm. **(B) TcdA does not colocalize with caveolin1 or cavin1 in wildtype mouse embryonic fibroblast (MEF) cells.** Colocalization studies were performed in wildtype MEFs as described in (A). Toxin internalization occurred at 37 °C for 3 min. Scale bars, 10 µm. **(C) Caveolin1$^{-/-}$ MEFs are sensitive to TcdA-induced cell rounding.** Wildtype and caveolin1$^{-/-}$ MEFs were challenged with 10 nM TcdA and toxin-induced cell rounding effects were monitored using an imaging-based kinetic assay as described in Materials and Methods. Representative images of cells 0 h and 5 h post-toxin treatment for each cell type are shown. **(D)** The percentage of rounded cells 5 h post-toxin treatment was quantified for each cell type. Data represent mean and SD of at least 900 cells from three independent experiments. Knockout of cav1 was confirmed by probing western blot of whole cell lysates from wildtype and caveolin1$^{-/-}$ MEFs with antibodies against cav1 and GAPDH (loading control) as shown in inset.

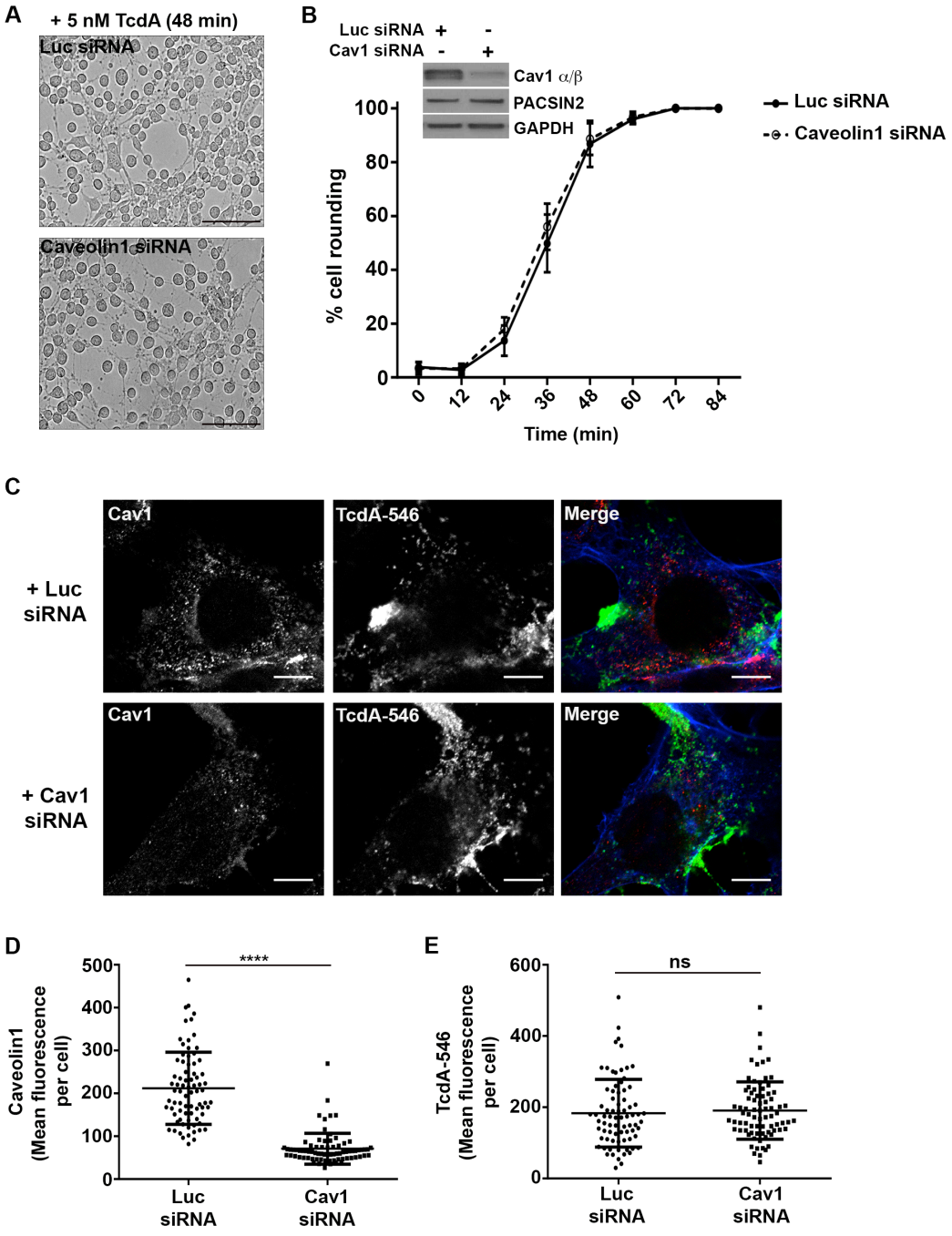

Figure 2-11. Caveolin1 is not required for TcdA uptake and toxin-induced rounding in wildtype MEF cells. (A) and (B) Depletion of Cav1 does not affect TcdA-induced cell rounding in wildtype MEF cells. MEF cells transfected with luciferase (non-targeting) or Cav1 siRNA were challenged with 5 nM TcdA, and toxin-induced cell rounding effects were monitored using an imaging-based kinetic assay as described in Materials and Methods. Representative images of cells 48 min post-toxin treatment are shown in **(A)**. Scale bars, 100 μm. **(B)** The percentage of rounded cells in each siRNA condition was quantified for the indicated time

points. Data represent mean and SD of at least 1200 cells from three independent experiments. Western blots of whole cell lysates shown in inset confirms that Cav1 siRNA transfection resulted in a significant decrease in Cav1 protein levels (87.9 ± 1.2 %) in cells. **(C), (D) and (E). Cav1 depletion does not affect TcdA uptake in MEF cells.** Wildtype MEF cells expressing luciferase (luc) or Cav1 siRNA were incubated with 50 nM TcdA-546 at 10 °C for 45 min. Cells were allowed to warm up to 37 °C for 2 min and then washed to remove unbound toxins and incubated with fresh media prewarmed to 37 °C. Bound toxins were allowed to internalize for 9 min at 37 °C. Cells were then fixed, stained for Cav1 and actin, and imaged by confocal microscopy. The images shown in **(C)** are representative of multiple fields imaged from two independent experiments. Merged images show Cav1 in red, TcdA-546 in green and actin (Phalloidin-647) in blue. Scale bars, 10 μm. **(D)** Comparison of mean fluorescence intensities of Cav1 between luc and Cav1 siRNA transfected cells. Data represent mean and SD of 77 individual cells. Student's t test ***p<0.0001. **(E)** Comparison of mean fluorescence intensities of TcdA-546 between luc and Cav1 siRNA transfected cells. Data represent mean and SD of 77 individual cells and were analyzed by student's t test. ns, not significant. Cells were chosen at random for intensity analyses.

Cell imaging studies show that there is a pool of PACSIN2 that colocalizes with Cav1-positive vesicles, consistent with the known role of PACSIN2 in caveolar endocytosis (Figure 2-12B and C). However, the PACSIN2 that colocalizes with TcdA-546 in MEF cells is not Cav1-associated (Figure 2-12B and C). I also found that PACSIN2 depletion, unlike that of Cav1, protects wildtype MEF cells from TcdA-induced cytopathic effects (Figure 2-13). To test whether PACSIN2 is involved in TcdA entry, I depleted PACSIN2 in wildtype MEFs by using siRNAs and examined the impact on TcdA binding and uptake. A 61% reduction in PACSIN2 staining had no impact on the overall toxin binding to cells (Figure 2-14). However, a 48% reduction in PACSIN2 fluorescence correlated with a 36% decrease in TcdA uptake (Figure 2-15). Similar uptake assays performed with transferrin, a clathrin-dependent cargo, show that transferrin uptake is not affected by PACSIN2 depletion, and indicates a specific role for PACSIN2 in TcdA entry (Figure 2-16).

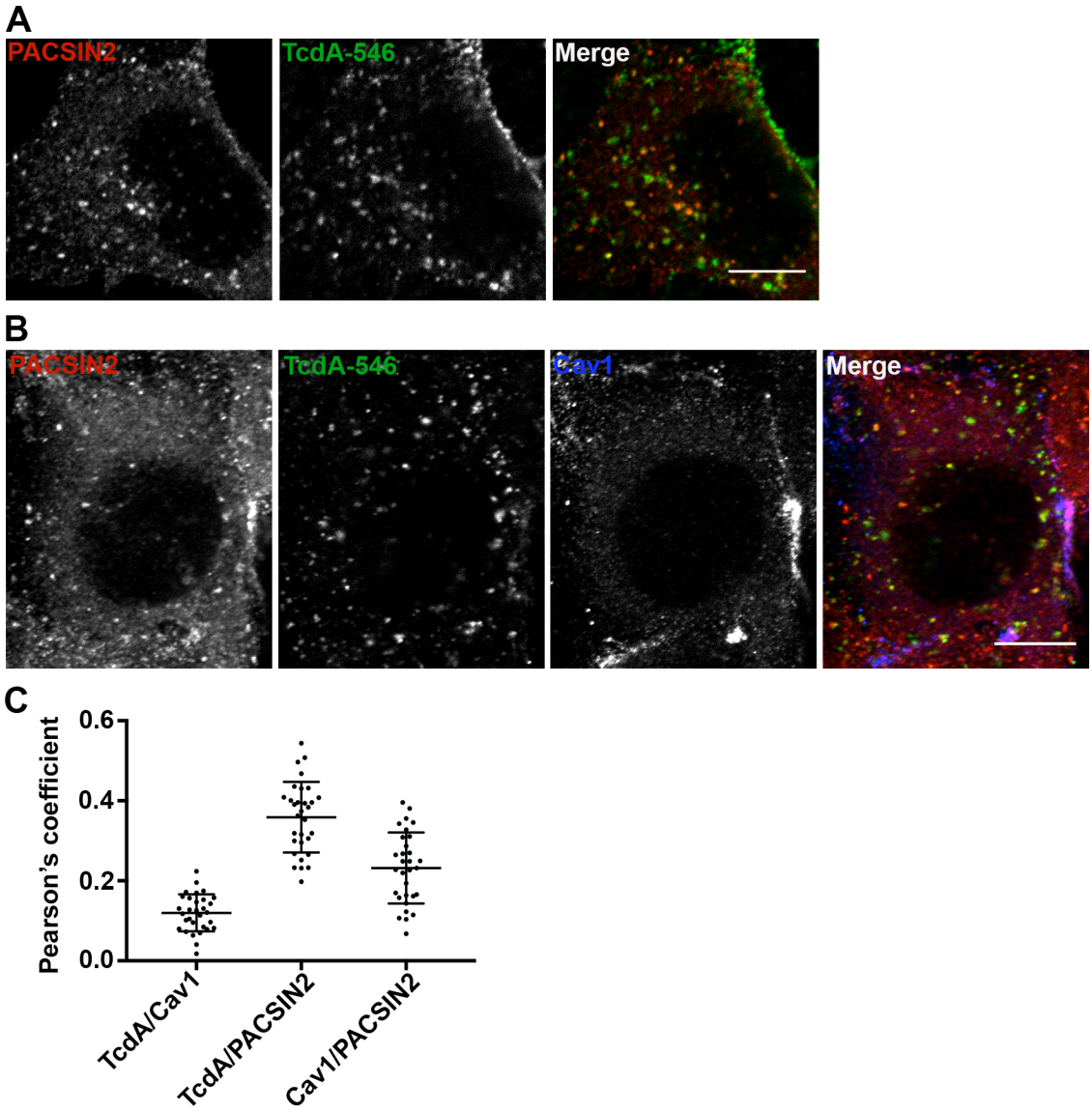

Figure 2-12. TcdA colocalizes with PACSIN2 in wildtype MEF cells. (**A**) Wildtype MEFs on glass coverslips were allowed to bind 50 nM TcdA-546 for 45 min at 10 °C, and cells were shifted to 37 °C to allow internalization of toxin for 3 min. Cells were fixed, stained for PACSIN2, and analyzed by confocal microscopy. Merged images show PACSIN2 in red, toxin in green, and colocalization in yellow. Scale bars, 10 μm. The images shown are representative of multiple fields imaged from two independent experiments. (**B**) Immunofluorescence assays were performed as described in (A), but cells were stained for cav1 in addition to PACSIN2. Merged images show PACSIN2 in red, toxin in green, and cav1 in blue. Yellow puncta in merged images denote TcdA- and PACSIN2-positive structures. Pink punta denote caveolae-associated PACSIN2. Scale bars, 10 μm. (**C**) Pearson's correlation coefficient to assess the extent of colocalization between PACSIN2, cav1 and TcdA-546 after 3 min toxin uptake. Data represent mean and SD of 31 individual cells chosen at random.

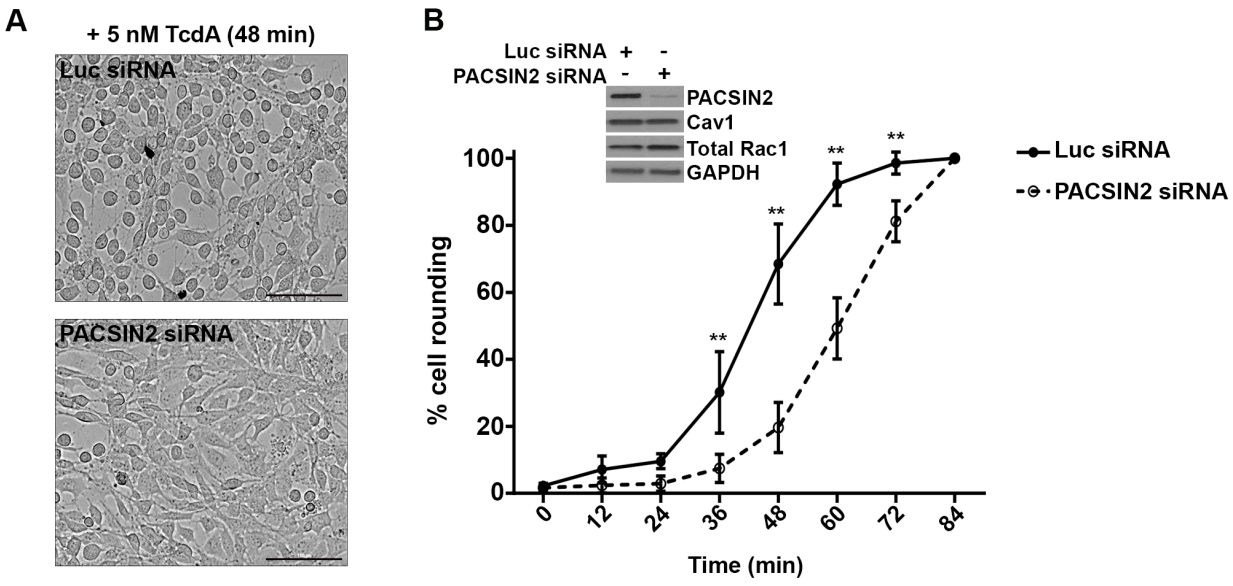

Figure 2-13. Depletion of PACSIN2 delays TcdA-induced cell rounding in wildtype MEF cells. MEF cells transfected with luciferase (non-targeting) or PACSIN2 siRNA were challenged with 5 nM TcdA, and toxin-induced cell rounding effects were monitored using an imaging-based kinetic assay as described in Materials and Methods. Representative images of cells 48 min post-toxin treatment are shown in **(A)**. Scale bars, 100 µm. **(B)** The percentage of rounded cells in each siRNA condition was quantified for the indicated time points. Data represent mean and SD of at least 1200 cells from three independent experiments. Data were analyzed using two-way ANOVA and p-values were generated using Sidak's multiple comparisons test in GraphPad Prism. **p<0.005. Western blots of whole cell lysates shown in inset indicate that PACSIN2 siRNA transfection resulted in a significant decrease (96.3 ± 2.8 %) in PACSIN2 protein levels but did not affect Cav1 or Rac1 levels in cells.

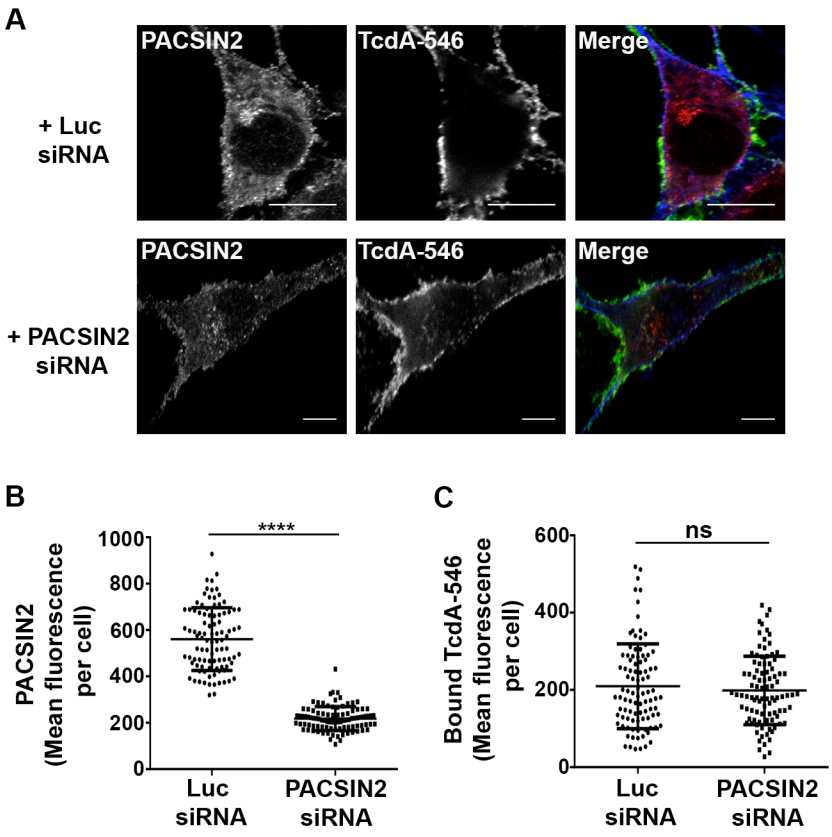

Figure 2-14. Depletion of PACSIN2 does not affect TcdA binding in MEF cells. (A) Wildtype MEF cells expressing luciferase (luc) or PACSIN2 siRNA were incubated with 50 nM TcdA-546 at 10 °C for 45 min. Cells were allowed to warm up to 37 °C for 2 min and then washed to remove unbound toxin and fixed. Cells were stained for PACSIN2 and actin (phalloidin-647). The images shown are representative of multiple fields imaged from three independent experiments. Merged images show PACSIN2 in red, TcdA-546 in green, and actin (Phalloidin-647) in blue. Scale bars, 10 μm. **(B)** Comparison of mean fluorescence intensities of PACSIN2 between luc and PACSIN2 siRNA transfected cells. Data represent mean and SD of 95 individual cells. Student's t test ***$p<0.0001$. **(C)** Comparison of mean fluorescence intensities of TcdA-546 between luc and PACSIN2 siRNA transfected cells. Data represent mean and SD of 95 individual cells and were analyzed by student's t test. ns, not significant. Cells were chosen at random for intensity analyses.

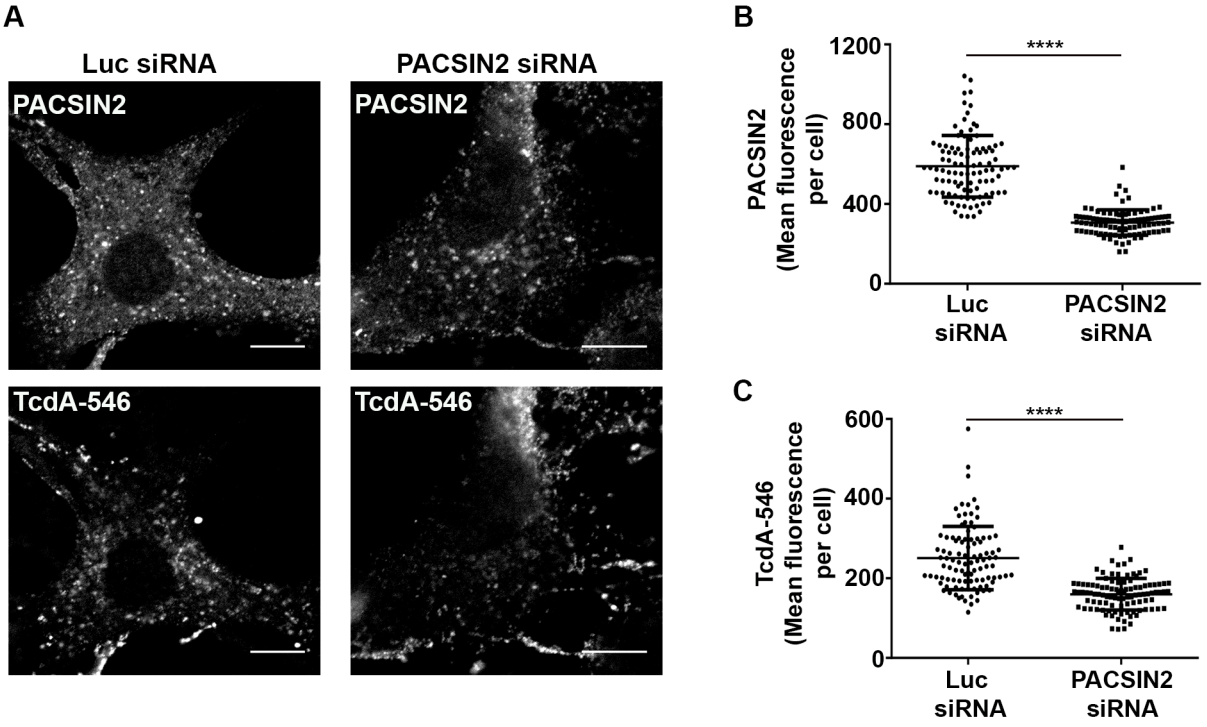

Figure 2-15. Depletion of PACSIN2 reduces TcdA uptake in MEF cells. Wildtype MEF cells expressing luciferase (luc) or PACSIN2 siRNA were incubated with 50 nM TcdA-546 at 10 °C for 45 min. Cells were allowed to warm up to 37 °C for 2 min and then washed to remove unbound toxins and incubated with fresh media prewarmed to 37 °C. Bound toxins were allowed to internalize for 9 min at 37 °C. Cells were then fixed, stained for PACSIN2 and imaged by confocal microscopy. PACSIN2 and TcdA-546 staining from each condition are shown in **(A)**. Scale bars, 10 μm. The images shown are representative of multiple fields imaged from two independent experiments. **(B)** Comparison of mean fluorescence intensities of PACSIN2 between luc and PACSIN2 siRNA transfected cells. Data represent mean and SD of 101 individual cells. Student's t test ***p<0.0001. **(C)** Comparison of mean fluorescence intensities of TcdA-546 between luc and PACSIN2 siRNA transfected cells. Data represent mean and SD of 101 individual cells. Student's t test ***p<0.0001. Cells were chosen at random for intensity analyses.

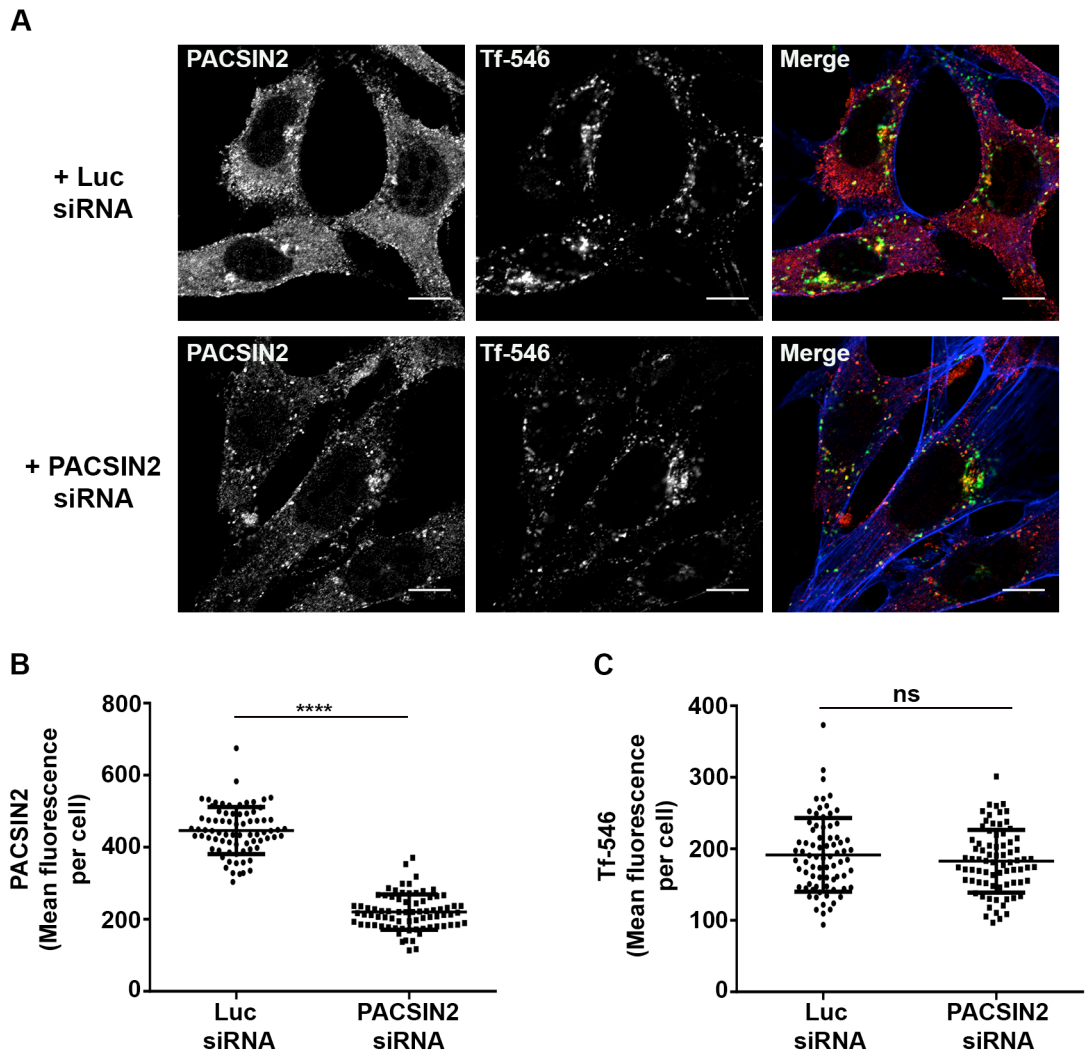

Figure 2-16. Depletion of PACSIN2 does not affect transferrin uptake in MEF cells. (A) Wildtype MEF cells expressing luciferase (luc) or PACSIN2 siRNA were incubated with 25 µg/ml of transferrin-alexa546 at 10 °C for 45 min. Cells were switched to 37 °C for 4 min, fixed and stained for PACSIN2 and actin (phalloidin-647). The images shown are representative of multiple fields imaged from two independent experiments. Merged images show PACSIN2 in red, transferrin-546 in green, and actin (Phalloidin-647) in blue. Scale bars, 10 µm. (B) Comparison of mean fluorescence intensities of PACSIN2 between luc and PACSIN2 siRNA transfected cells. Data represent mean and SD of 76 individual cells. Student's t test ***p<0.0001. (C) Comparison of mean fluorescence intensities of transferrin-546 between luc and PACSIN2 siRNA transfected cells. Data represent mean and SD of 76 individual cells and were analyzed by student's t test. ns, not significant. Cells were chosen at random for intensity analyses.

I next checked if PACSIN2 is involved in TcdA uptake in Caco-2 cells, which lack the caveolar pathway. Similar to our findings in MEF cells, I observed significant colocalization of TcdA-546 with PACSIN2-positive structures in Caco-2 cells by confocal microscopy (Figure 2-17). Unlike MEF cells, where TcdA colocalizes with PACSIN2 at 3 min, colocalization in Caco-2 cells was strongest at 10 min post-switch to 37 °C (Figure 2-17B and C). PACSIN2 has been shown to associate with Rac1 on early endosomes (250). It is possible that the TcdA-containing PACSIN2 structures in Caco-2 cells are early endosomes and that I was capturing colocalization at the stage of toxin translocation, where TcdA can access Rac1. To address this, I performed colocalization studies of TcdA-546 with PACSIN2 and early endosomal antigen 1 (EEA1) in Caco-2 cells. As expected, a fraction of PACSIN2 colocalized with EEA1 (Figure 2-18). However, these PACSIN2-positive early endosomes were distinct from the toxin-containing PACSIN2 structures observed at 0, 5, 10 and 15 min post-switch to 37 °C (Figure 2-18). Taken together, these data show that TcdA-546 colocalizes with a Cav1- and endosome-independent pool of PACSIN2 in Caco-2 cells.

Strong colocalization between TcdA-546 and PACSIN2 and inhibition of TcdA-induced cell death upon PACSIN2 depletion (Figure 2-9 and Figure 2-19) suggest that PACSIN2 is required for TcdA entry in Caco-2 cells. To test this, I depleted PACSIN2 and examined the effect on TcdA binding and uptake. Caco-2 cells were transduced with a non-targeting shRNA (ctrl shRNA) and shRNA 982 (sh982) targeting PACSIN2. Expression of sh982 resulted in 94.7 ± 2.1 % reduction in PACSIN2 protein levels by western blotting (Figure 2-20). Since TcdA binding to cells might be temperature-sensitive (251), I performed binding assays at two different conditions (10 °C and 37 °C). Irrespective of the temperature, I found that PACSIN2 depletion does not affect TcdA binding to cells (Figure 2-20). I then investigated the effect of PACSIN2 depletion on TcdA uptake by imaging-based approaches. Caco-2 cells stably

expressing shRNAs were allowed to bind and internalize TcdA-546 and were then stained for PACSIN2 (Figure 2-21). Expression of sh982 resulted in a 66% decrease in PACSIN2 fluorescence in cells (Figure 2-21C). In contrast to control cells, TcdA-546 signal in sh982-expressing cells was typically restricted to the cell periphery suggesting that toxin internalization is inhibited in these cells (Figure 2-21A). Consistent with that, cells expressing sh982 showed a 44% reduction in TcdA-546 fluorescence compared to cells expressing ctrl shRNA (Figure 2-21D). Despite similar cell surface binding, the overall levels of cell-associated toxin in PACSIN2-depleted cells were lower than that of controls. PACSIN2 depletion inhibited TcdA entry, and the toxin that is stuck on the outside and unable to enter the cells was likely lost in the subsequent wash steps. I also observed a strong correlation (R^2 = 0.8) between TcdA-546 and PACSIN2 fluorescence in cells (Figure 2-21B). Linear regression analyses show that an increase in PACSIN2 fluorescence correlated with a corresponding increase in toxin fluorescence (and vice versa), supporting the conclusion that TcdA uptake is PACSIN2-dependent. Lastly, to evaluate the specificity of the observations with PACSIN2, I performed colocalization and uptake assays in Caco-2 cells with transferrin (a clathrin-dependent cargo). Confocal assays reveal minimal to no colocalization between transferrin and PACSIN2 at 1 min post-switch to 37 °C (Figure 2-22B and C). However, the degree of colocalization increased with time. Transferrin has been previously shown to be transported to PACSIN2-positive perinuclear vesicles upon entry (250). Consistent with that, I found a significant portion of transferrin in PACSIN2-positive endosomes at 3 min post-entry (Figure 2-22A). This is in contrast to TcdA, which colocalizes with an endosome-independent pool of PACSIN2 in Caco-2 cells (Figure 2-18). It is important to note that while transferrin colocalizes with PACSIN2-positive endosomes, the uptake of this cargo in Caco-2 cells does not require PACSIN2 (Figure 2-23). In sum, these findings emphasize a specific requirement for PACSIN2 in the TcdA uptake mechanism.

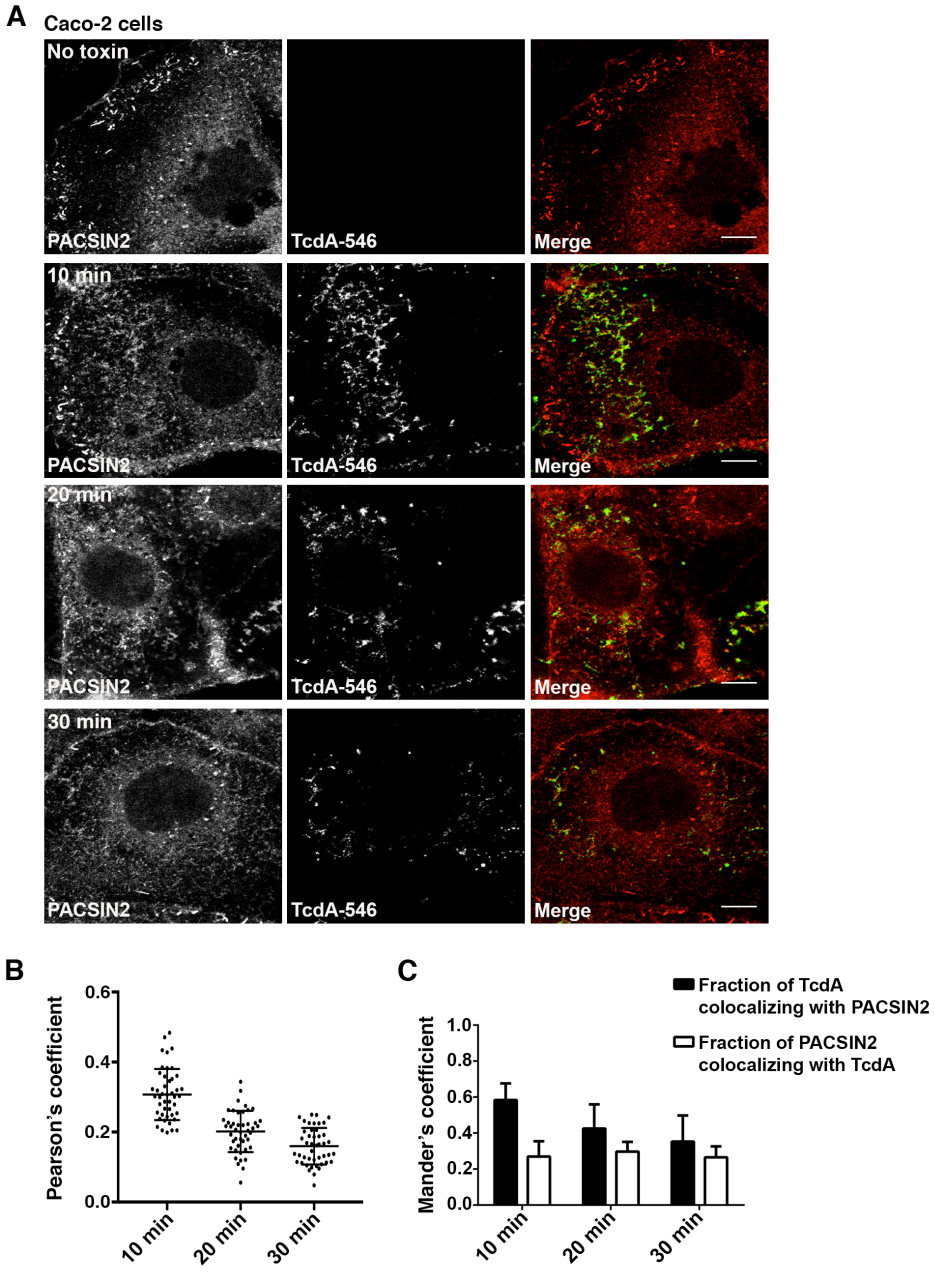

Figure 2-17. TcdA colocalizes with PACSIN2 during entry in Caco-2 cells. (A) Immunofluorescence assays were performed as described in Fig. 1B. At indicated time points, cells were fixed, stained for PACSIN2 and analyzed by confocal microscopy. Merged images show PACSIN2 in red, toxin in green and colocalization in yellow. Scale bars, 10 μm. The images shown are representative of multiple fields imaged from three independent experiments (**B**) Pearson's correlation coefficient to assess the extent of colocalization between PACSIN2 and TcdA-546 at the indicated time points. Data represent mean and SD of 45 individual cells. **(C)** Mander's coefficient to assess the fraction of TcdA-546 colocalizing with PACSIN2 and vice versa. A value of 1.0 indicates 100% overlap between the two colors. Data represent mean and SD of 45 individual cells. Cells were chosen at random for colocalizaton analyses.

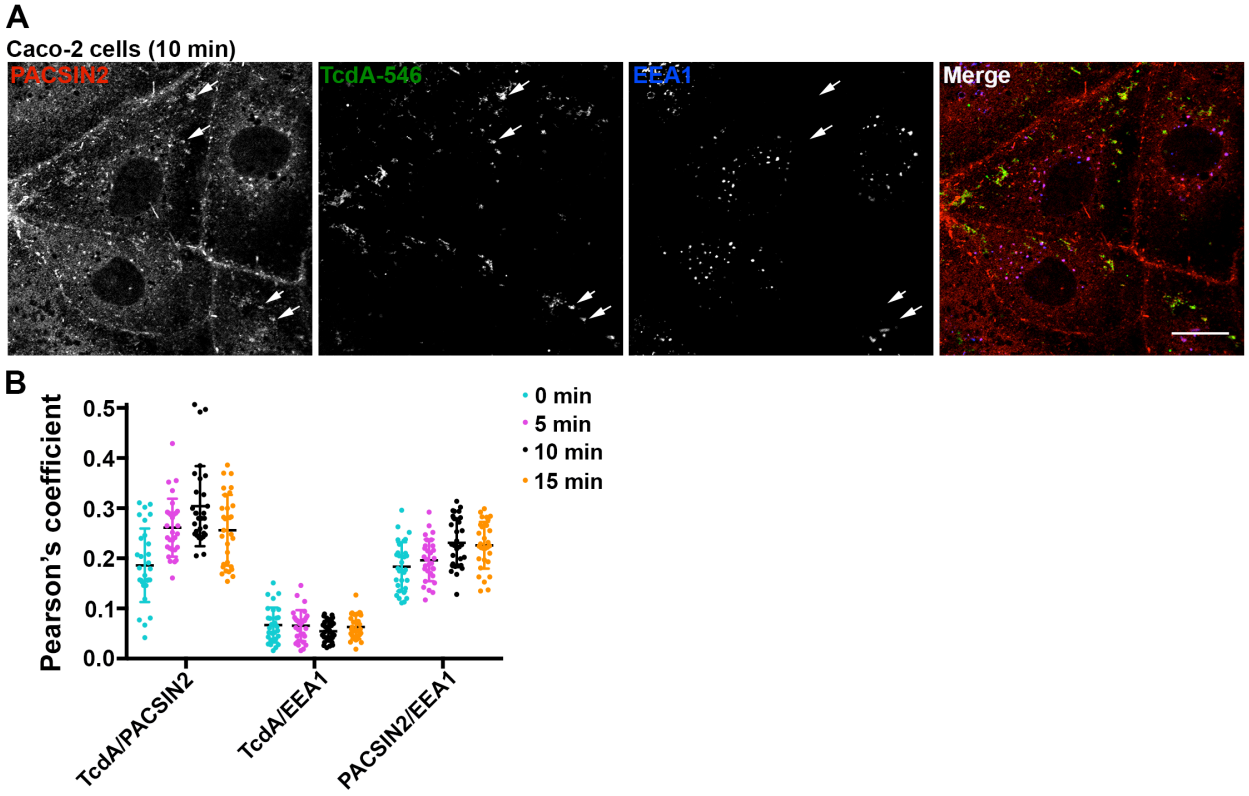

Figure 2-18. TcdA- and PACSIN2-positive structures at 5, 10 and 15 min post-switch to 37 °C are not early endosomes. (**A**) Caco-2 cells on glass coverslips were allowed to bind 50 nM TcdA-546 for 45 min at 10 °C. Unbound toxin was removed, and cells were shifted to 37 °C to allow internalization of toxin for 0, 5, 10 or 15 min. Cells were fixed, stained for PACSIN2 and early endosomal antigen 1 (EEA1) and analyzed by confocal microscopy. Merged images show PACSIN2 in red, toxin in green and EEA1 in blue. Yellow puncta in merged images denote TcdA- and PACSIN2-positive structures. Pink punta denote PACSIN2-positive endosomes. Scale bars, 20 μm. The arrowheads in the images highlight representative regions that are positive for TcdA and PACSIN2 but not EEA1. The images shown are from the 10 min time point and are representative of multiple fields imaged from two independent experiments. (**B**) Pearson's correlation coefficient to assess the extent of colocalization between PACSIN2, EEA1 and TcdA-546 at 0, 5, 10 and 15 min post-entry. Data represent mean and SD of 30 individual cells.

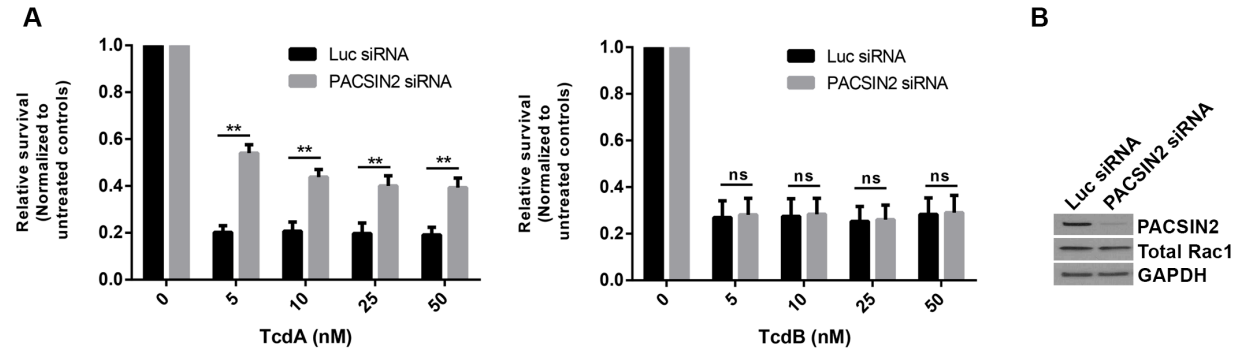

Figure 2-19. Depletion of PACSIN2 inhibits TcdA-induced cell killing at various concentrations tested. (A) Caco-2 cells were transfected with 10 nM siRNA against PACSIN2 or luciferase (Luc; non-targeting control) and then intoxicated with indicated concentrations of TcdA or TcdB. ATP levels were determined using CellTiterGlo and normalized to signal from untreated cells to assess the relative survival of cells post-toxin treatment. Results represent the mean and SEM of three independent experiments. Data were analyzed using two-way ANOVA, and p-values were generated using Sidak's multiple comparisons test in GraphPad Prism. **p<0.005; ns, not significant. **(B)** Western blot of whole cell lysates from siRNA-expressing Caco-2 cells probed with antibodies against PACSIN2, total Rac1 and GAPDH (loading control). PACSIN2 siRNA resulted in 94.4 ± 4.4 % reduction in PACSIN2 protein levels by densitometry.

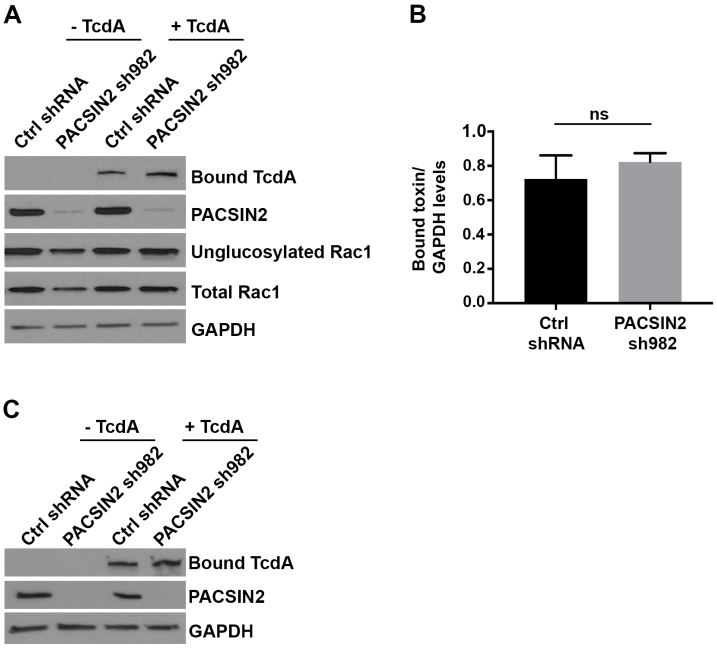

Figure 2-20. PACSIN2 depletion does not affect TcdA binding to Caco-2 cells. (**A**) Caco-2 monolayers expressing ctrl shRNA and PACSIN2 sh982 were allowed to bind 30 nM TcdA at 10 °C. Whole cell lysates were prepared for SDS PAGE and Western blot. The blot was probed with antibodies against TcdA CROPs, PACSIN2, unglucosylated Rac1, total Rac1 and GAPDH. Cells that did not receive any toxin were used as a control. (**B**) Experiments shown in (A) were quantified by densitometry and represented as the ratio of bound toxin and GAPDH levels. Results reflect the mean and SEM of three independent experiments and were analyzed using two-tailed t-test. ns, not significant. **(C)** Experiment was performed as in (A) with some modifications. After toxin binding at 10 °C, cells were switched to 37 °C for 4 min to warm the cells to 37 °C. Cells were then washed with PBS prewarmed to 37 °C to remove unbound toxins and collected for lysis and western blotting.

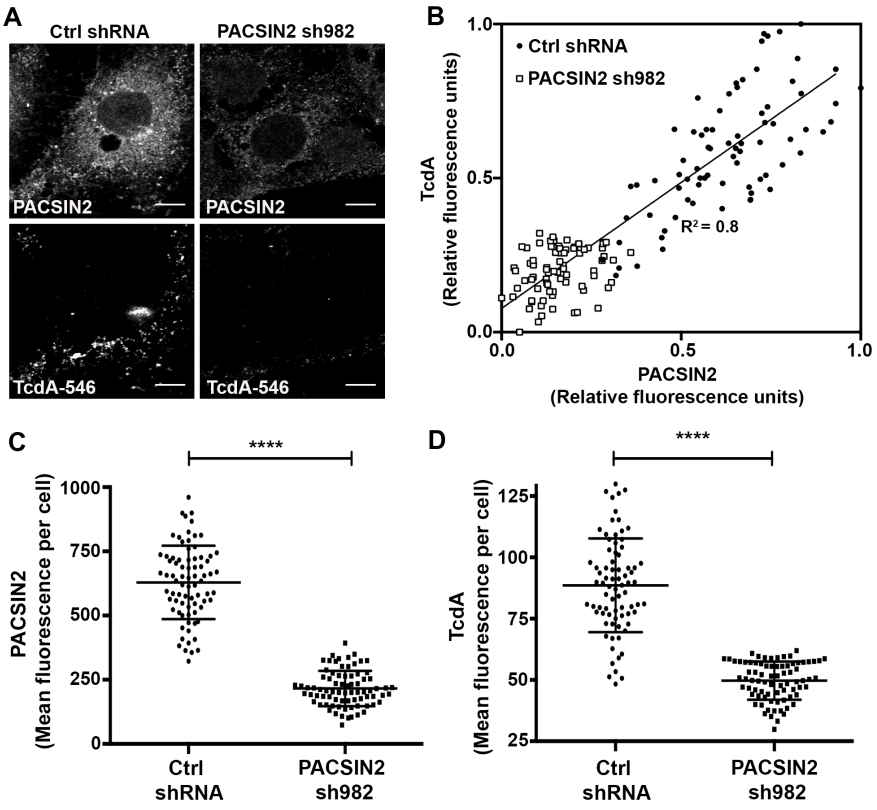

Figure 2-21. Depletion of PACSIN2 inhibits TcdA entry in Caco-2 cells. (A) Caco-2 cells expressing non-targeting shRNA (Ctrl shRNA) or shRNA 982 targeting PACSIN2 were incubated with 50 nM TcdA-546 at 10 °C for 45 min. Unbound toxins were removed and cells were shifted to 37 °C to allow internalization. After 20 min, cells were washed, fixed, stained for PACSIN2 and imaged by confocal microscopy. PACSIN2 and TcdA staining from ctrl shRNA and sh982 expressing cells are shown. Scale bars, 10 µm. The images shown are representative of multiple fields imaged from three independent experiments **(B)** Scatter plot of the relative fluorescence intensities of PACSIN2 and TcdA in ctrl shRNA (black circles) and PACSIN2 sh982 (white squares) expressing cells. Each data point represents an individual cell. A total of 78 cells per condition were chosen at random for analyses. Linear regression analysis was performed in GraphPad Prism and indicates a strong correlation between PACSIN2 and toxin levels in cells. **(C)** Comparison of mean fluorescence intensities of PACSIN2 between ctrl shRNA and PACSIN2 sh982 expressing cells. Data represent mean and SD of 78 individual cells. Student's t test ***p<0.0001. **(D)** Comparison of mean fluorescence intensities of TcdA between ctrl shRNA and PACSIN2 sh982 expressing cells. Data represent mean and SEM of 78 individual cells. Student's t test ***p<0.0001.

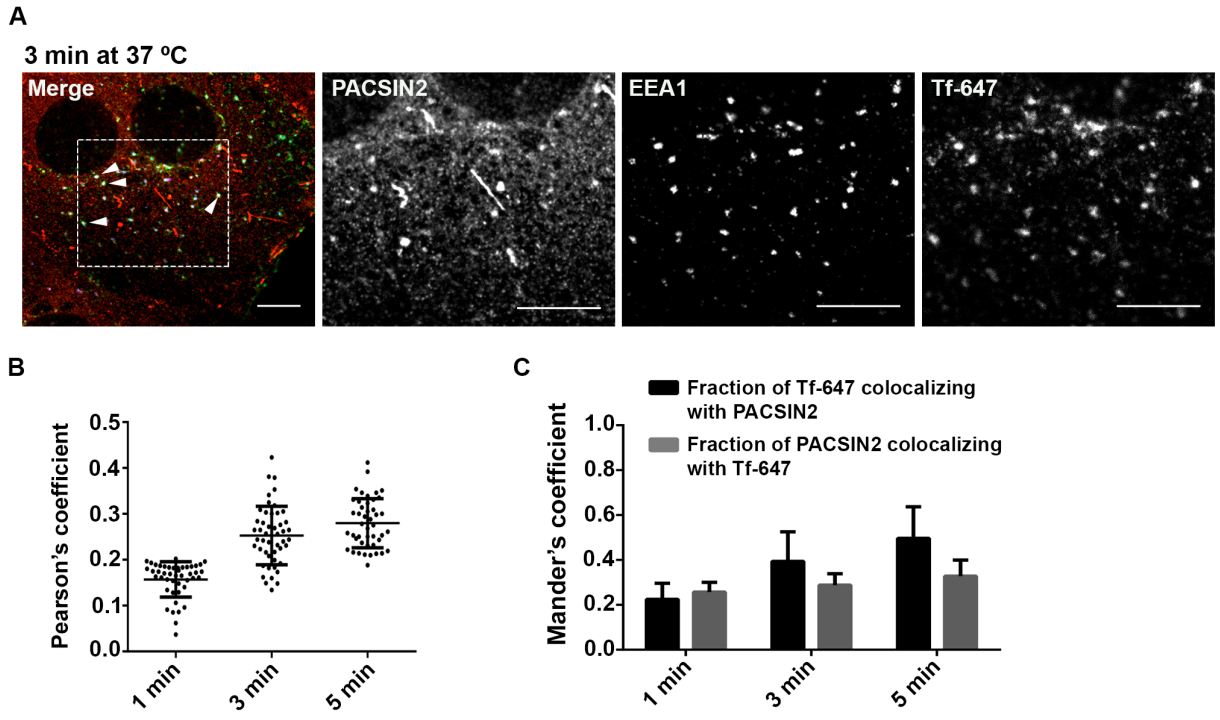

Figure 2-22. Transferrin colocalizes with PACSIN2-positive endosomes in Caco-2 cells. **(A)** Caco-2 cells on glass coverslips were allowed to bind 25 µg/ml of transferrin-alexa647 for 45 min at 10 °C. Cells were shifted to 37 °C to allow internalization for 1, 3 and 5 min. Cells were fixed, stained for PACSIN2 and early endosomal antigen 1 (EEA1) and analyzed by confocal microscopy. Merged images show PACSIN2 in red, transferrin in green, and EEA1 in blue. Scale bars, 10 µm. The arrowheads in the images highlight representative regions that are positive for transferrin, PACSIN2 and EEA1. The images shown are from the 3 min time point and are representative of multiple fields imaged from two independent experiments. **(B)** Pearson's correlation coefficient to assess the extent of colocalization between transferrin and PACSIN2. Data represent mean and SD of at least 43 individual cells. **(C)** Mander's coefficient to assess the fraction of transferrin colocalizing with PACSIN2 and vice versa. A value of 1.0 indicates 100% overlap between the two colors. Data represent mean and SD of 43 individual cells. Cells were chosen at random for colocalization analyses.

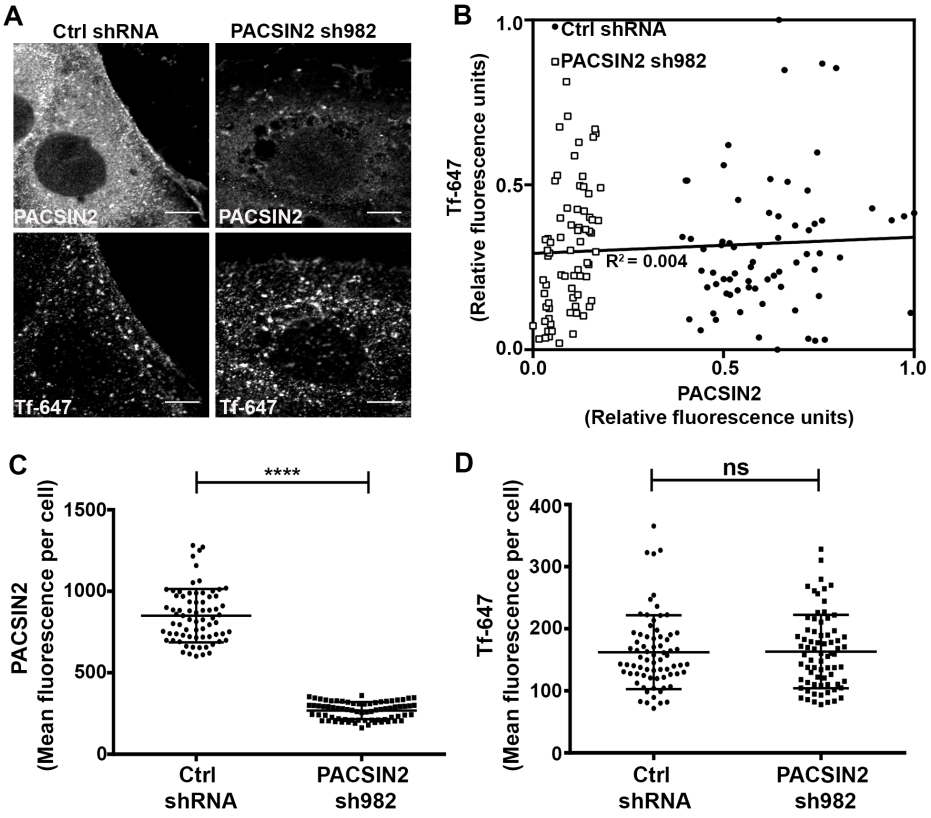

Figure 2-23. PACSIN2 depletion does not affect transferrin uptake in Caco-2 cells. (A) Caco-2 cells expressing non-targeting shRNA (Ctrl shRNA) or shRNA 982 targeting PACSIN2 were incubated with 25 µg/ml transferrin-647 (Tf-647) at 10 °C for 45 min. Cells were shifted to 37 °C to allow internalization. After 5 min, cells were washed, fixed, stained for PACSIN2 and imaged by confocal microscopy. PACSIN2 and Tf-647 staining from ctrl shRNA and sh982 expressing cells are shown. Scale bars, 10 µm. The images shown are representative of multiple fields imaged from three independent experiments. **(B)** Scatter plot of the relative fluorescence intensities of PACSIN2 and Tf-647 in ctrl shRNA (black circles) and PACSIN2 sh982 (white squares) expressing cells. Each data point represents an individual cell. A total of 72 cells per condition were chosen at random for analyses. Linear regression analysis was performed in GraphPad Prism and indicates a lack of correlation between PACSIN2 and Tf-647 levels in cells. **(C)** Comparison of mean fluorescence intensities of PACSIN2 between ctrl shRNA and PACSIN2 sh982 expressing cells. Data represent mean and SD of 72 individual cells. Student's t test ***p<0.0001. (D) Comparison of mean fluorescence intensities of Tf-647 between ctrl shRNA and PACSIN2 sh982 expressing cells. Data represent mean and SD of 72 individual cells and were analyzed by student's t test. ns, not significant.

Discussion

TcdA and TcdB are the key virulence factors that mediate the pathology associated with *C. difficile* infection (73, 75). Cellular intoxication by TcdA and TcdB depends on endocytosis and transport to acidified endosomal compartments within cells (107, 116, 118, 121). Since these toxins represent excellent targets for therapeutic intervention, understanding the mechanism of toxin entry is a significant priority.

TcdB has been shown to require clathrin-mediated endocytosis (CME) to induce Rac1-inactivation and cell rounding (114). However, the endocytic mechanisms utilized by TcdA for entry and intoxication have not been clearly defined. In this study, I have combined several independent approaches to obtain a detailed understanding of TcdA entry into cells. I perturbed the function of several key endocytic factors using RNAi-mediated depletion or pharmacological inhibition and determined the subsequent effect on TcdA uptake and toxin-induced downstream effects such as Rac1 glucosylation, cell rounding or cell death. The use of TcdB and transferrin as a controls in these assays allowed for comparative analyses of the endocytic factors (or pathways) relevant for the cytotoxic mechanism of both toxins and for evaluation of the specificity of the perturbations made. Additionally, I validated my findings from the perturbation studies by examining the colocalization of fluorescently labeled TcdA with markers of specific endocytic pathways.

Using these complementary approaches, I find that TcdA uptake in Caco-2 cells is independent of CME. First, both transient and stable depletion of CHC had no effect on TcdA-induced cytotoxicity. Second, TcdA did not colocalize with markers of the clathrin-mediated endocytic pathway. My results contradict previous reports that propose a role for CME in TcdA uptake (113, 114). While the first study reported that TcdA uptake occurs via CME (114), the second study has implicated both clathrin-dependent and –independent pathways in TcdA

uptake (113). Both studies relied primarily on pharmacological inhibition of CME by chlorpromazine to investigate the contribution of CME to TcdA entry. Pretreatment of HeLa or HT-29 cells with chlorpromazine was shown to reduce Rac1 glucosylation and cell rounding by TcdA (113, 114). Consistent with these studies, I observed that chlorpromazine treatment also reduced Rac1 glucosylation by TcdA in Caco-2 cells. While chlorpromazine has been widely used to disrupt clathrin-coated pits, several studies demonstrate that the drug can also interfere with clathrin-independent endocytic mechanisms (229, 252-254). It is therefore important to corroborate the data obtained by pharmacological inhibition with other more specific approaches. Interestingly, in contrast to their chlorpromazine experiments, Gerhard *et al.* did not observe a significant decrease in Rac1 glucosylation by TcdA in HT-29 cells depleted of CHC (113). This would argue that TcdA intoxication in HT-29 cells is independent of CME, consistent with my findings in Caco-2 cells.

Clathrin-independent endocytic (CIE) pathways can be subdivided based on whether or not they use a dynamin GTPase for vesicle scission (255, 256). Macropinocytosis, clathrin-independent carriers (CLIC) and Arf6-regulated pathways are dynamin-independent, whereas dynamin has been implicated or shown to be involved in caveolae-, RhoA-, flotillin- and endophilinA2-mediated endocytosis (227, 229, 239, 255, 256). Results from my perturbation studies indicate that TcdA internalization is dynamin-dependent. Using a siRNA-based screen of endocytic factors from dynamin-dependent pathways, I was able to identify Cav1, cavin1 and PACSIN2 to be important for TcdA-mediated cell death.

Cav1, cavin1 and PACSIN2 are key proteins involved in caveolae formation and endocytosis. Cav1 is a major structural component of caveolae membrane coats (249); disruption of Cav1 leads to loss of caveolae (247), and ectopic expression of Cav1 in cells lacking caveolae results in *de novo* formation of caveolae (257). Cavin1 or PTRF (polymerase I transcript release factor) is a caveolae-associated protein that is required for the formation of

caveolae via sequestration of caveolins into caveolae (248). PACSIN2/syndapin-II is a Fer-CIP4 homology-BAR (F-BAR) domain-containing protein that is involved in the membrane sculpting of caveolae and recruitment of dynamin for caveolae fission (230, 231). I found no evidence for a direct involvement of caveolae-mediated endocytosis in TcdA uptake. Imaging studies in Caco-2 cells showed no detectable colocalization between TcdA and Cav1 or cavin1. However, I made two observations worth noting. First, Caco-2 cells do not express the α isoform of Cav1. Fujimoto *et al.* reported that expression of the Cav1 α isoform, but not β isoform, resulted in the formation of caveolar invaginations in cells that lack endogenous caveolae, suggesting that the α isoform is required for functional caveolae formation (246). Second, I observed a strong nuclear but diffuse cytoplasmic staining for cavin1 in Caco-2 cells. These observations are in line with a previous report by Vogel *et al.* (245), which showed that Caco-2 cells lack functional caveolae. Lack of Cav1α and functional caveolae likely affects the localization and function of cavin1 in these cells resulting in the atypical staining pattern. I also did not observe colocalization between TcdA and Cav1 or cavin1 in mouse embryonic fibroblast cells that do contain functional caveolae. Furthermore, depletion of Cav1 does not affect TcdA uptake or TcdA-induced cytopathic effects in MEFs indicating that TcdA uptake can occur independent of caveolae-mediated endocytosis.

I speculate that Cav1 and cavin1 promote TcdA-induced toxicity in Caco-2 cells through indirect mechanisms. One possibility is that these proteins regulate the expression or function of endocytic factors involved in the TcdA uptake mechanism. There is emerging evidence for such crosstalk between caveolar proteins and other CIE pathways (258, 259). Additionally, Cav1 and cavin1 are involved in cholesterol trafficking and homeostasis (260-262). TcdA requires cholesterol for pore-formation and toxicity (122). Depletion of caveolar proteins may modulate the lipid composition of cell membranes leading to indirect effects on TcdA toxicity. However, Cav1 depletion does not affect TcdA-induced cytopathic effects in MEF cells, making this

unlikely to be the mechanism involved. Finally, caveolar proteins could be involved in signaling mechanisms or recycling of receptors that promote TcdA-induced toxicity. We currently do not know the receptor(s) or the exact uptake mechanism for TcdA in Caco-2 and MEF cells. Therefore, it is difficult to determine which of these indirect mechanisms, if any, contribute to the effects observed in our siRNA-viability assay.

Interestingly, I observed that TcdA uptake, while caveolae-independent, is dependent on PACSIN2. In MEF cells, which contain caveolae, TcdA colocalizes with PACSIN2, and depletion of PACSIN2 inhibits TcdA entry and toxin-induced downstream effects. I made similar observations in Caco-2 cells, which lack caveolae. Proteins in the PACSIN/syndapin family have an N-terminal F-BAR domain that mediates F-actin binding and membrane bending and a C-terminal Src homology 3 (SH3) domain that can interact with dynamin, synaptojanin and Neuronal Wiskott-Aldrich Syndrome Protein (N-WASP), a component of the actin polymerization machinery (232, 263-267). PACSIN2 is ubiquitously expressed, whereas PACSIN1 is mainly expressed in brain, and PACSIN3 is expressed predominantly in skeletal muscles, lung and heart (265, 268, 269). PACSINs form homo- and hetero- oligomers that allow them to function as adapter or scaffolding proteins that can link the actin cytoskeleton with the endocytic machinery (233, 234, 270). Previously, PACSIN2 has been shown to be involved in epidermal growth factor receptor (EGFR) internalization and cholera toxin B (CTxB) entry (231, 250, 271). Similar to the observations with TcdA, CTxB has been shown to colocalize with PACSIN2 in HeLa cells (250), and depletion of PACSIN2 results in a significant decrease in CTxB incorporation into HeLa cells (231). It is not clear from these studies however, whether PACSIN2 functions independently of caveolae-mediated endocytosis in promoting CTxB entry.

While PACSIN2 is required for TcdA uptake in both Caco-2 and wildtype MEF cells, the molecular and mechanistic details of this PACSIN2-dependent uptake may differ between these cells. In wildtype MEF cells, imaging studies show TcdA in PACSIN2-positive structures that

have a vesicular appearance, whereas in Caco-2 cells, I observed TcdA in PACSIN2 structures with different curvature. PACSIN2 is a BAR-domain protein that bends membranes. In addition to being associated with vesicular structures such as caveolae, PACSIN2 is also known to create tubular membrane invaginations (232). I speculate that in Caco-2 cells, TcdA is internalized into small tubules or tubular constrictions induced by PACSIN2, resulting in the extended structures observed in the images. I do not know why toxin is internalized into PACSIN2 structures with different curvatures in Caco-2 vs MEF cells, and this is an area for future investigation.

Overall, my data indicate that in Caco-2 and MEF cells TcdA uptake and intoxication occurs by a clathrin- and caveolae-independent endocytic mechanism that requires PACSIN2. While this work supports an important role for PACSIN2 and dynamin in TcdA uptake and cytotoxicity, I cannot conclude that TcdA entry occurs solely by this mechanism. Alternate routes of entry may exist for TcdA, but based on the perturbation studies, I anticipate that their contribution will be minor. This work also shows that TcdA and TcdB utilize distinct endocytic pathways to intoxicate epithelial cells. TcdA and TcdB bind different cell surface proteins and sugars (85, 86, 96, 104, 108), which likely explains their internalization by distinct endocytic pathways. Importantly, the differences in entry between TcdA and TcdB can have implications regarding their cytotoxic mechanisms. TcdB is more than potent than TcdA in cell culture and animal models (75, 272, 273). TcdB causes necrosis and extensive damage to the colonic epithelium by inducing the production of reactive oxygen species (ROS). ROS generation by TcdB requires internalization of TcdB-receptor complexes and the activated NADPH oxidase complex via CME and the subsequent formation of a redox active endosome (222). TcdA, however, is unable to induce ROS (222). I speculate that the clathrin-independent, PACSIN2-dependent entry mechanism utilized by TcdA prevents the assembly of the redox active endosomes, resulting in reduced toxicity compared to TcdB.

Many aspects of this PACSIN2- and dynamin-dependent endocytic mechanism remain to be elucidated, including how PACSIN2 mediates vesicle formation. Recently, Boucrot *et al.* and Renard *et al.* described a new endocytic route (FEME pathway) mediated by endophilinA2, which is a BAR domain-containing protein similar to PACSIN2 (229, 241). The FEME pathway is a clathrin-independent and dynamin-dependent pathway that mediates internalization of various clathrin-independent cargoes including Shiga and cholera toxins (229, 241). Binding to cargo receptor and recruitment of dynamin is mediated by the SH3 domain of endophilin, membrane curvature is induced by the BAR domain, and membrane scission is achieved by the cooperative actions of endophilin, actin and dynamin (229, 241, 274). I speculate that PACSIN2 can mediate vesicle formation and release in a manner similar to that of endophilin. I also do not know how TcdA is able to gain entry by this pathway and what other host proteins in addition to PACSIN2 and dynamin are required for this process. For future studies, it will be important to identify the TcdA receptor and characterize the toxin-receptor interactions that are necessary for entry by this pathway. We hope to use TcdA as a tool to screen for host proteins that play a role in this pathway.

In conclusion, this study identifies an important route of entry for TcdA in cells that could be targeted for therapeutic purposes, and expands our understanding of PACSIN2's role in endocytosis. In the future, it will be important to investigate how this PACSIN2 pathway is regulated and if this is a generalized mechanism that TcdA can utilize in cell types other than Caco-2 and MEF cells.

Materials and Methods

Cell culture. Caco-2 cells (ATCC HTB-37) were maintained in Minimum Essential Medium (MEM) supplemented with 10% fetal bovine serum (FBS; Atlanta Biologicals), 1% MEM non-essential amino acids (M7145; Sigma), 1% Hepes buffer (15630080; Gibco) and 1% sodium pyruvate (S8636; Sigma). HeLa cells (ATCC CCL-2), HEK 293T cells (ATCC CRL-11268), wildtype (ATCC CRL-2752) and caveolin1$^{-/-}$ mouse embryonic fibroblast (MEF) cells (ATCC CRL-2753) were grown in Dulbecco's Modified Eagle's Medium (DMEM) supplemented with 10% FBS. Dynasore (D7693; Sigma) was dissolved in DMSO to obtain a 25 mM stock and was used at a final concentration of 80 μM. Dynasore experiments were performed under serum-free media conditions as the inhibitor binds to serum proteins and loses activity (275).

Toxin expression and purification. Plasmids encoding wildtype TcdA and TcdB were transformed into *Bacillus megaterium* according to the manufacturer's instructions (MoBiTec). Recombinant toxins were expressed and purified as described previously with some modifications (168). *B. megaterium* expression strains were grown in LB containing 10 mg/L tetracycline and 35 mL overnight culture was used to inoculate 1 L of media. Bacteria were grown at 37 °C with shaking at 220 rpm. Toxin expression was induced with 5 g D-xylose once the culture reached OD_{600}= 0.5. Cells were harvested after 4 h and resuspended in 200 mL of binding buffer (20 mM Tris [pH 8.0], 100 mM NaCl for TcdA and 20 mM Tris [pH 8.0], 500 mM NaCl for TcdB) supplemented with DNase, 400 μL of lysozyme (10 mg/mL) and protease inhibitors (P8849; Sigma). Cells were lysed using an Emulsiflex homogenizer, and lysates were centrifuged at 48,000 g for 30 min. The proteins were purified from the supernatant by Ni-affinity, anion exchange and size exclusion chromatography. Toxins were eluted and stored in 20 mM HEPES (pH 7.0), 50 mM NaCl.

Viability assays. Caco-2 cells were seeded at a density of 1,000 cells per well in a 384-well plate and incubated at 37 °C for 48 h. Cells were then challenged with serial dilutions of TcdA (unlabeled or alexa546 labeled) or TcdB in triplicate. ATP levels of TcdB- and TcdA-treated cells were quantified 24 h and 48 h post intoxication, respectively, by addition of CellTiter-Glo (G7571; Promega) and used as a measure of cellular viability. Luminescence was read using a BioTek Synergy 4 plate reader. Relative cell survival was determined by normalizing the ATP levels of toxin-treated cells to untreated controls.

siRNA assays. For viability assays, Caco-2 cells (1000 cells/well) were reverse-transfected with 10 nM siRNA against luciferase (non-targeting; negative control) or various targets (Thermo Fisher Scientific) using RNAiMax transfection reagent (13778075; Thermo Fisher Scientific) as described previously (222). Transfections were performed in a 384-well plate format, with 8 wells per target and toxin treatment. Three wells received mock treatment and three wells received 50 nM of TcdA for 48 h or 50 nM TcdB for 24 h and viability was assayed using CellTiter-Glo. Cells from the remaining two wells were collected and used for RNA isolation and RT-PCR analyses. Relative cell survival was determined by normalizing the ATP levels of toxin-treated cells to untreated controls (which is at a value of 1.0). In some instances, cytotoxicity data are represented as fold change of survival, which was obtained by normalizing the relative viability for each target to that of luciferase control. For immunofluorescence assays, wildtype MEF cells (14,000 cells/well) were reverse-transfected with 20 nM siRNA against luciferase, Cav1 or PACSIN2 (Thermo Fisher Scientific) using lipofectamine RNAiMax (1.5 μL per well) as described by the manufacturer. Cells were seeded on 12 mm glass coverslips (# 1.5; Fisherbrand) in 24-well plates and incubated at 37 °C for 48 h to achieve sufficient knockdown. Transfected cells were subsequently used for toxin binding and uptake analyses.

Lentivirus production and transduction of Caco-2 cells. Non-targeting control shRNA (RHS4346) and shRNAs targeting sequences in clathrin heavy chain (V2LHS_67887 and V3LHS_359489) were purchased from GE Healthcare Dharmacon, Inc. PACSIN2 shRNA (TRCN0000037982; Sigma) was a gift from Matt Tyska (Vanderbilt University, Nashville, TN). The packaging plasmids ΔR8.91 and pCMVG were a kind donation from Chris Aiken (Vanderbilt University Medical Center, Nashville, TN). For stable knockdowns, shRNA plasmids were packaged into lentiviral particles for transduction. Briefly, HEK293T cells were plated in a 10 cm dish and transfected with 1 mL of serum free media containing 30 µg total DNA (15 µg shRNA plasmid + 11.25 µg ΔR8.91 + 3.75 µg pCMVG) preincubated with 90 µL of 1 mg/mL of PEI. After 48 h of transfection, a total of 10 mL media containing virus particles was collected and passed through a 0.45 µm filter and stored in 1 mL aliquots at – 80 °C. Caco-2 cells were plated in 75- cm2 flasks such that they were 60% confluent on the day of transduction. Cells were incubated with 1.5 mL of virus supernatant diluted in 3 mL of conditioned media containing 4 µg/mL of polybrene (107689; Sigma) at 37 °C for 4 h, then supplemented with 5 mL of conditioned media and incubated overnight. Infected cells were passaged and allowed to recover for 2 days. Transduced Caco-2 cells were then selected by culturing in media containing 10 µg/mL puromycin (P8833; Sigma) for 96 h. To confirm knockdown, whole cell lysates were probed with antibodies against the target protein and GAPDH (loading control).

RT-PCR analyses. Total RNA was extracted using the RNeasy Mini Kit (74104; Qiagen). Target mRNAs were amplified from 10 ng of template RNA using a OneStep RT-PCR kit (210212; Qiagen). Primers used are listed in Table 2-1. GAPDH mRNA was amplified as a loading control. The RT-PCR products were resolved on a 1-1.5% agarose gel and imaged using the KODAK EDAS 290 digital camera system.

Cell binding assays. Caco-2 cells expressing ctrl shRNA and PACSIN2 sh982 were seeded at a density of 400,000 cells/well in a 6-well plate format and incubated at 37 °C for 48 h. For the binding assay, cells were switched to 10 °C for 1 h and then intoxicated with 30 nM TcdA. Toxins were allowed to bind at 10 °C for 1 h. Media containing unbound toxin inoculum were then removed and cells were washed twice with ice cold PBS. Cells were dislodged by using a cell scraper, collected and pelleted at 1000 g for 5 min. Cell pellets were homogenized to obtain lysates for SDS PAGE and Western blot. For assays performed at 37 °C, cells were initially incubated with toxin suspension for 30 min at 10 °C and then switched to 37 °C for 4 min. The brief incubation warms the cells to 37 °C but does not allow for appreciable toxin internalization. Cells were then washed twice with PBS prewarmed to 37 °C to remove unbound toxins and collected for lysis and western blotting. The blot was probed with antibodies against TcdA, PACSIN2, unglucosylated Rac1, total Rac1 and GAPDH. Additionally, cells that did not receive any toxin were used as control.

Western blotting. To prepare samples for western blotting, cell pellets were suspended in 60 µL of lysis buffer (10mM Tris-Cl, pH 7.4, 250 mM sucrose, 3 mM Imidazole) supplemented with protease inhibitor cocktail (1:100, P8340; Sigma) and homogenized by passing 20-times through a 27G needle fitted to a sterile 1 mL syringe. Nuclei and debri were pelleted and removed by spinning at 1500 g for 15 min. Samples were then diluted with Laemmli sample buffer containing 2-mercaptoethanol and heated at 95 °C for 5 min. Equal volumes were loaded on a 4-20% Mini-Protean gradient gels (Bio-Rad). Proteins were transferred in Tris-Glycine buffer to PVDF membranes at 100 V for 1 h and blocked with 5% milk in PBS containing 0.1% Tween-20 (PBST) overnight. Primary antibodies against clathrin heavy chain (1:2000, ab21679; Abcam), GAPDH (1:3000, sc-25778; Santa Cruz), unglucosylated Rac1 (1:1000, 610650; BD Biosciences), total Rac1 (1:1000, 05-389; Millipore), caveolin1α (1:2000, sc-894; Santa Cruz), caveolin1α/β (1:1000, 610060; BD Biosciences), PACSIN2 (1:2000, AP8088b; Abgent),

Table 2-1. Primers used for RT-PCR analyses.

Oligo name	Sequence (5' to 3')
CHCf	CCCAGCCCAGCCAGGTCAAAC
CHCr	CATCTGCAACTTGAGGCGCATGC
Dyn1f	CGTAGGCAGGGACTTCTTGCC
Dyn1r	CGCAGGGGGAGCAGCTTGTTC
Cav1v1f	GTTCTCACTCGCTCTCTGCT
Cav1v1r	AGATGTCCCTCCGAGTCTACG
Cav1v2f	GGAGTGTCCGCTTCTGCTAT
Cav1v2r	CGGTGTAGAGATGTCCCTGCG
Cav1v3f	GTAGCTGTCGGAGCGGTTAG
Cav1v3r	AGTCAATCTTGACCACGTCATCG
Cav1v4f	CTGTCGGAGCGGGACATC
Cav1v4r	AAAGAGTGGGTCACAGACGG
Cavin1f	AAATCATCGGGGCCGTAGAC
Cavin1r	GCAGCTTCACTTCATCCTGGTA
PACSIN2f	ACGGAGTGTGCGACGGAT
PACSIN2r	GTTCCCGACCTCCCAGAAGC
Flotillin1f	GCGTCCCGGAAGCTCCAGCCTG
Flotillin1r	GGCTTTAGCTTCCCGGATCCC
Flotillin2f	CGACACTCAGAGGATTTCCC
Flotillin2r	ACTGGTCCCGGTCCTGATAA
EndoA2f	CAGTTCTACAAGGCGAGCCA
EndoA2r	CCAGCAATGCGTCACCAAAG
RhoAf	GATGGAAAGCAGGTAGAGTTGG
RhoAr	GCAGCTCTCGTAGCCATTTCA
GAPDHf	CGCGGGGCTCTCCAGAACATC
GAPDHr	TGGTGGTCCAGGGGTCTTACTCC

TcdA (1:1000, NB600-1066; Novus Biologicals) and tubulin (1:5000, 3873S; Cell Signaling) were diluted in 5% milk-PBST and incubated with the membranes for 2 h at room temperature. Membranes were washed four times with PBST and then incubated with anti-mouse (7076S; Cell Signaling) or anti-rabbit (7074S; Cell signaling) HRP-linked secondary antibodies for 1 h at room temperature (1:2000 for TcdA, PACSIN2, Rac1, caveolin1 and CHC; 1:5000 for GAPDH and tubulin). Membranes were washed four times with PBST and HRP was detected using ECL Western Blotting Substrate (32106; Pierce). Images of film scans were converted to grayscale and cropped using Photoshop (Adobe Systems).

Fluorescent labeling of toxins. Purified toxins in 20 mM HEPES (pH 7.0), 50 mM NaCl were incubated with a five-fold molar excess (over the cysteines) of thiol-reactive Alexa Fluor dyes (A10258 and A20347; Thermo Fisher Scientific) at room temperature for 2 h in the dark. Excess dye was removed by dialysis overnight at 4 °C using slide-A-lyzer dialysis cassettes (66380; Thermo Fisher Scientific). Toxin concentration and degree of labeling were determined according to manufacturer's instructions and stored at – 80 °C for future use.

Immunofluorescence staining. $1x10^4$ cells were seeded on 12 mm glass coverslips (# 1.5; Fisherbrand) in 24-well plates and incubated at 37 °C for 48 h. For internalization assays, cells were chilled at 10 °C for 45 min and then incubated with media containing 50 nM labeled toxin or buffer (no toxin control) at 10 °C for 45 min. Unbound toxins were removed, and cells were switched to 37 °C for various time intervals to allow internalization of toxin. Caco-2 cells lose their actin cytoskeleton and begin to round after 30 min of toxin treatment. Therefore, for imaging experiments 30 min was chosen as the last time interval for staining and image analyses. At each time interval, cells were washed once with pre-warmed PBS and fixed with 4% paraformaldehyde in PBS at 37 °C for 15 min. Following fixation, cells were quenched with

0.1 M glycine in PBS, washed three times with PBS and permeabilized with 0.2% Triton X-100/PBS for 3 min at room temperature (RT). Cells were washed three times with PBS and blocked overnight at 4 °C in PBS containing 4% BSA, 5% normal goat serum (Life technologies), 0.1% Tween-20. The following day, cells were washed once in BSA-PBST (1% BSA, 0.1% Tween-20 in PBS). Primary antibodies anti-CHC (1:1000, ab21679; Abcam), rabbit anti-caveolin1 (1:50 for Caco-2 cells and 1:250 for wildtype MEFs, 610060; BD Biosciences), mouse anti-caveolin1 (1:25 for wildtype MEFs (Fig 4), 610493; BD Biosciences), anti-cavin1 (1:100, ab48824; Abcam), anti-EEA1 (1:250, 610457; BD Biosciences) and anti-PACSIN2 (1:100, AP8088b; Abgent) were diluted in BSA-PBST and incubated with cells for 2 h at RT. Primary antibody was removed and cells were washed four times with BSA-PBST, and incubated with goat anti-rabbit Alexa Fluor 647 (A-21245; Life Technologies), goat anti-mouse Alexa Flour 488 (A-11029; life Technologies) or goat anti-rabbit Alexa Fluor 546 (A-11035; Life Technologies) in BSA-PBST for 1 h at RT (1:1000 for CHC; 1:500 for caveolin1, cavin1, EEA1 and PACSIN2). Cells were washed twice in BSA-PBST and twice in PBS and then mounted using Prolong Gold Antifade Mountant (P36931; Life Technologies). For actin staining, cells were incubated with 1:100 dilution of Phalloidin-647 (A2287; Thermo Fisher Scientific) for 30 min at RT. The phalloidin incubation step was performed after secondary antibody staining and washes. After 30 min incubation, cells were washed twice in BSA-PBST and twice in PBS and then mounted using Prolong Gold Antifade Mountant.

Confocal microscopy. Slides were imaged using a 63x/ 1.40 numerical aperture (NA) Plan-Apochromat oil immersion objective on a LSM 710 Meta Inverted laser-scanning confocal microscope (Zeiss) located in the Vanderbilt Cell Imaging Shared Resource (CISR) Core. Alexa488 was excited using the 488 nm line of an Argon laser. Alexa546 was excited at 561 nm and Alexa647 was excited at 633 nm using a HeNe laser. Fluorescence emission was detected

using filters provided by the manufacturer. Pinhole size was identical for the fluors used. Single sections of 0.49 µm thickness from a Z-stack are presented. For the purpose of presentation, raw images were exported in tiff format and brightness and contrast were adjusted to the same extent using Fiji (276).

Image analyses and quantification. For measurements of colocalization, individual cells were demarcated and Pearson's correlation coefficient and Mander's overlap coefficients were determined using the Colocalization plugin in Fiji. The Mander's coefficient determines the fraction of channel1 that overlaps with channel2 and vice versa, with 100% overlap resulting in a value of 1. Nuclei were excluded from the colocalization analyses. Qualitative analyses of colocalization were performed using the plot profile feature in Fiji. The pixel intensities along the line were obtained from the original 12-bit image for each channel and plotted as relative intensities over distance using GraphPad Prism. PACSIN2, Cav1, transferrin and TcdA signals in siRNA- or shRNA-expressing cells were determined by demarcating individual cells and measuring the mean fluorescence intensities for each channel using Fiji. The mean fluorescence intensities of PACSIN2 and TcdA (or transferrin) for each cell were converted to relative intensity values and plotted against each other to generate the scatter plot. To determine the correlation between PACSIN2 and TcdA (or transferrin) in cells, a linear regression analysis was performed on the entire data set and R^2 value for best fit is represented. Cells were chosen at random for colocalization and intensity analyses.

Cell rounding assay. Wildtype and caveolin1$^{-/-}$ MEF cells were seeded, in triplicate, at 200,000 cells/well in 6-well plates. The following day, cells were chilled at 10 °C for 45 min and allowed to bind 10 nM TcdA for 45 min. Plates were then moved to a Cytation 5 Cell Imaging Multi-Mode Reader (BioTek), and bright field images of cell morphology were captured at 15 min intervals

for a 5 h time period, using a 20x/ 0.45 NA objective (1220517; BioTek). A total of 4 frames per well were captured at each time point. The chamber was maintained at 37 °C with 5% CO_2 for the duration of this experiment. Real-time videos of cells rounding in response to toxin were generated using Fiji. For quantification, a total of 36 frames from three independent experiments were analyzed for each cell type and results were expressed as the percentage of rounded cells. Cell rounding assays with siRNA transfected cells were performed as described above with a few modifications. Wildtype MEF cells (200,000 cells/well) were reverse-transfected with 20 nM siRNA against luciferase (non-targeting; negative control), Cav1 or PACSIN2 (Thermo Fisher Scientific) using RNAiMax transfection reagent (7 μL per well) as described by the manufacturer. After 48 h, cells were intoxicated with 5 nM TcdA and images were captured every 12 min for a total of 2 h. For quantification, a total of 12 frames (> 100 cells/frame) from three independent experiments were analyzed for each time point and siRNA condition, and results were expressed as the percentage of rounded cells.

Statistical analyses. Statistical analyses are described in figure legends. A p-value of ≤ 0.05 was considered significant.

CHAPTER III

CONCLUSIONS AND FUTURE DIRECTIONS

Conclusions

C. difficile is the leading cause of hospital-acquired diarrhea and pseudomembranous colitis worldwide. Most clinical isolates produce two homologous toxins, TcdA and TcdB, which enter host colonocytes to induce pathogenic effects that result in fluid secretion, inflammation, and necrosis of the colonic mucosa. As a toxin-mediated disease, there is significant interest in understanding the unique and shared roles each toxin plays in pathogenesis. A mechanistic framework of how these toxins disrupt host cellular function is a priority among many in our field.

Disruption of cellular function by TcdA and TcdB requires entry into the host cell. When I began my graduate work, it was generally accepted in the field that TcdA and TcdB interacted with distinct receptor structures on colonic epithelial cells. Upon binding to different cellular receptors, it was thought that both the toxins utilized similar endocytic mechanisms to gain entry into the host cell. This view was based on a report from the Aktories group that stated that the large clostridial glucosylating toxins enter cells by clathrin-mediated endocytosis (CME) (114). However, while developing assays to identify cellular factors important for TcdA-induced toxicity, I discovered that TcdA intoxication does not depend on clathrin heavy chain, a critical component of CME. On close inspection, most of the experiments in the report published by the Aktories group were conducted with TcdB. Mainly by analogy it was concluded that TcdA also utilizes the same endocytic mechanism. My observation that TcdA intoxication does not require clathrin suggested that TcdA and TcdB likely entered host cells by distinct mechanisms. I then

began a systematic evaluation of all documented entry mechanisms to uncover the route of TcdA entry. What I found is something quite novel: a process that depends on the presence of dynamin and PACSIN2 but is independent of clathrin- or caveolae-mediated endocytosis (Chapter II). PACSIN2 (also termed Syndapin II) is a F-BAR domain protein previously shown to be important for caveolae-mediated endocytosis; it contributes to the curvature of caveolae and the recruitment of dynamin for caveolae fission. The observation that PACSIN2 can function outside of the caveolae system suggests a novel mechanism of entry, one for which TcdA is now a known cargo. Consequently, TcdA could serve as a valuable cell biology tool in furthering our understanding of this uncharacterized host endocytic process. Cholera toxin and epidermal growth factor receptor also depend on PACSIN2 for internalization, opening up the exciting possibility that this endocytic mechanism could be used by multiple host and pathogenic factors for internalization.

Many questions remain regarding TcdA entry mechanism and the regulation of the PACSIN2- and dynamin-dependent endocytic pathway. Identification of the TcdA receptor that mediates host cell entry via the PACSIN2-dependent route and characterization of receptor-toxin interactions will be a priority for future studies in this area. Furthermore, elucidating signaling events following receptor ligation and identifying additional host factors involved in TcdA host cell entry are also key to building a molecular and mechanistic model of critical early events occurring during intoxication. Our expectation is that these future studies using TcdA will also allow a better understanding of this as-yet uncharacterized host endocytic process. My efforts and ideas to address these questions are discussed next.

Future Directions

Identify host cellular factors important for TcdA entry

As discussed earlier, except for PACSIN2 and dynamin, host factors involved in TcdA entry into host cells are not known. These factors include cell surface receptors, signaling and scaffolding proteins that may regulate internalization of receptor-toxin complexes, and other intracellular proteins that may work in concert with PACSIN2 and dynamin to mediate formation and scission of toxin-containing membrane-associated endocytic structures. To identify host factors important for TcdA entry I took a discovery-based approach and conducted a genetic screen using a mutant library generated by the gene-trapping technology. Gene-trapping involves mutagenizing mammalian cells with a replication-deficient retroviral gene-trap vector that carries a promoterless neomycin resistance gene. Insertion of the vector into an actively transcribed region of the chromosome disrupts expression of the gene into which it has inserted and confers resistance to neomycin (G418). Screens using gene-trap libraries have been successful in identifying the receptor for *C. difficile* transferase (CDT) binary toxin (277) and key host factors that promote *C. perfringens* epsilon toxin (278). The Lacy lab has used this approach to identify 43 mammalian genes that contribute to TcdB-induced cytotoxicity - one of which (Polio virus receptor-like 3 or Nectin3) was determined to be a receptor for TcdB and published in PNAS (108).

To identify host factors that confer susceptibility to TcdA, I optimized and performed a preliminary screen using a Madin-Darby Canine Kidney gene-trap library (MDCK GT). This library was generated and provided to us by Jinsong Sheng and Don Rubin (Vanderbilt University). Briefly, the library was incubated in media supplemented with G418 and treated with 5 nM of TcdA. After 9 hours, toxin-resistant clones (which are still flat and adherent) were selected for growth by removing detached (rounded cells) and dead cells and allowed to recover

for 10-14 days. The toxin treatment was repeated two more times and a small fraction of the surviving clones was propagated until sufficient DNA could be isolated for sequencing analyses. I picked around twenty clones for propagation but only eight survived. Mapping the insertion with vector-specific primers identified seven genes that were disrupted (VMP1 was disrupted in two clones). Results are presented in Table 3-1. The remaining toxin-resistant clones (>60) were pooled and frozen for future deep sequencing analyses. Analyses of these clones should yield additional host targets for validation and mechanistic evaluation. Our collaborators have also generated a gene-trap library using Caco-2 cells, which we now have access to. Should there be issues with reviving the frozen MDCK mutant cells, we can perform the screen using Caco-2 cells, which are also more physiologically relevant.

The next step is to confirm that the candidate genes obtained from the MDCK screen are indeed critical for TcdA intoxication in human colonic epithelial cells. This can be done by using the siRNA-based viability assay described in my previous study (Chapter II). Our laboratory currently has two whole-genome siRNA arrays (siGENOME and ON TARGET plus SMART pools, Dharmacon), which can be used for this validation step. I have already performed the secondary validation assays for the seven targets we received from the initial round of sequencing. After 48 h of treatment with target-specific siRNA pools, I challenged Caco-2 cells with TcdA and calculated fold change of cell survival. Of the seven candidates tested, only depletion of four and a half LIM domains protein 2 (FHL2) and neuron navigator 2 (NAV2) conferred significant protection (greater than 1.5-fold compared to luciferase siRNA-treated controls) against TcdA challenge in Caco-2 cells (Table 3-1; last column). Similar validation approaches will be used for other targets that we identify from our future sequencing analyses.

NAV2 is one of the three members of the neuron navigator family (NAV1, NAV2 and NAV3). The full-length protein is 261 kDa with several functional domains (Figure 3-1) (279, 280).

Table 3-1. Host factors identified from the MDCK gene-trap screen.

Gene Name	Gene Description	Proposed Function(s)	RNAi validation[1] Mean fold survival (s.d.)
FHL2	Four and a half LIM domains protein 2	Protein-protein interactions; signal transduction	2.40 (0.4)
NAV2	Neuron navigator 2	Cell growth and migration; endocytosis	3.16 (0.9)
VMP1	Vacuole membrane protein 1	Regulation of autophagy	1.01 (0.3)
ADNP	Activity-dependent neuroprotector homeobox	Regulation of gene expression	1.00 (0.3)
TAB1	TGF-beta activated kinase 1 (MAP3K7) binding protein 1	Signaling	1.04 (0.3)
PHAX	Phosphorylated adaptor for RNA export	RNA export from nucleus	1.34 (0.4)
BCAT1	Branched chain amino-acid transaminase 1, cytosolic	Amino acid metabolism; cell proliferation	1.09 (0.3)

[1] RNAi validation results are represented as fold-change of survival, which was obtained by normalizing the percent viability for each target to that of luciferase non-targeting control. Mean fold-change of 1.5 or greater is considered protective. Data represent average of at least 7 independent experiments with the standard deviation indicated within parenthesis. Validation assays were performed in Caco-2 cells.

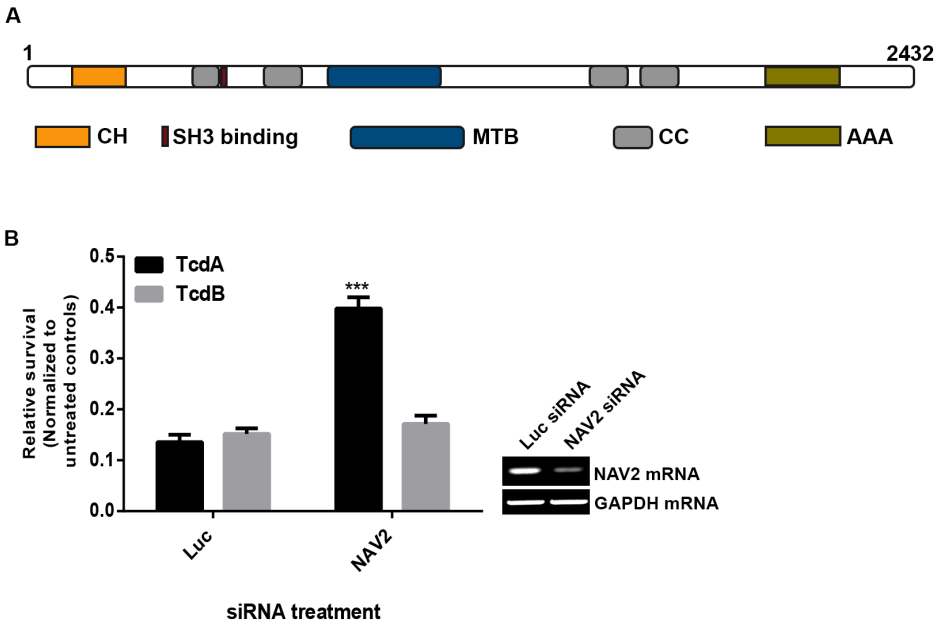

Figure 3-1. Neuron navigator 2 (NAV2) is important for TcdA-induced cytotoxicity. A) Domain organization of human NAV2**.** CH, calponin-homology domain that is often found in cytoskeletal (actin-binding) and signal transduction proteins; SH3 binding motif, capable of mediating protein-protein interactions; MTB domain, a cytoskeletal interacting domain that enables binding to microtubule (MT) plus ends; CC, coiled-coil regions, which function as oligomerization domains for a wide variety of proteins such as motor proteins and transcription factors, and a AAA ATPase domain. Adapted from Muley *et al.* (280) and Van Haren *et al.* (281). **B)** Caco-2 cells were transfected with 10 nM siRNA, exposed to 50 nM TcdA (black bars) or TcdB (gray bars) and then assayed for cellular viability using CellTiterGLO. Relative survival was obtained by normalizing the ATP values of treated cells to untreated controls. The data represent the average of nine independent experiments performed in triplicate with the standard error of the mean indicated as error bars. Data were analyzed using t test. ***p<0.005.

All three mammalian navigator proteins are microtubule plus-end tracking proteins (281). NAV2 also contains an AAA ATPase domain at the C-terminus. AAA ATPases are involved in a wide range of biological processes including DNA replication, protein degradation, membrane fusion, and vesicle transport (cytoplasmic dynein) (282). The physiological functions of NAV2 are largely unknown but it has been proposed to regulate cytoskeletal dynamics during cell migration, outgrowth, and endocytosis (280, 283). NAV2 is a homolog and an ortholog of *C. elegans* UNC-53, which has been shown to localize to the cytoskeleton, bind F-actin *in vitro*, and interact with the actin cytoskeleton regulator, ABI-1 (Abelson kinase interactor-1) (280, 283, 284). In addition to modulating cytoskeletal dynamics at the leading edge of migrating or outgrowing cells, UNC-53 is proposed to play a role in receptor-mediated endocytosis. Defects in uptake of different ligands have been observed under UNC-53 knockdown conditions (283, 285), supporting a role for this protein and potentially NAV2 in endocytosis. Based on these observations, I propose that NAV2 is involved in TcdA entry and this hypothesis will be evaluated in the future. If NAV2 contributes to TcdA internalization in cells, it will be important to determine whether NAV'2 role in toxin mechanism is dependent on its ATPase activity and/or binding to cytoskeletal structures.

FHL2 is a member of the FHL family of proteins that also includes FHL1, FHL3, FHL4 and ACT (activator of cyclic AMP response element modulator (CREM) in the testis) (286). LIM domain contains two zinc finger loops that mediate protein-protein interactions. FHL2 is expressed in both the nucleus and the cytoplasm and is involved in signal transduction and regulation of actin cytoskeletal dynamics and gene expression (286, 287). FHL2 has been shown to interact with receptors and signaling and structural proteins including the cytoplasmic domains of α and β integrins, focal adhesion kinase (FAK), and actin (288-291). FHL2 is also involved in integrin-mediated signaling events at focal adhesions (292). Interestingly, siRNA-

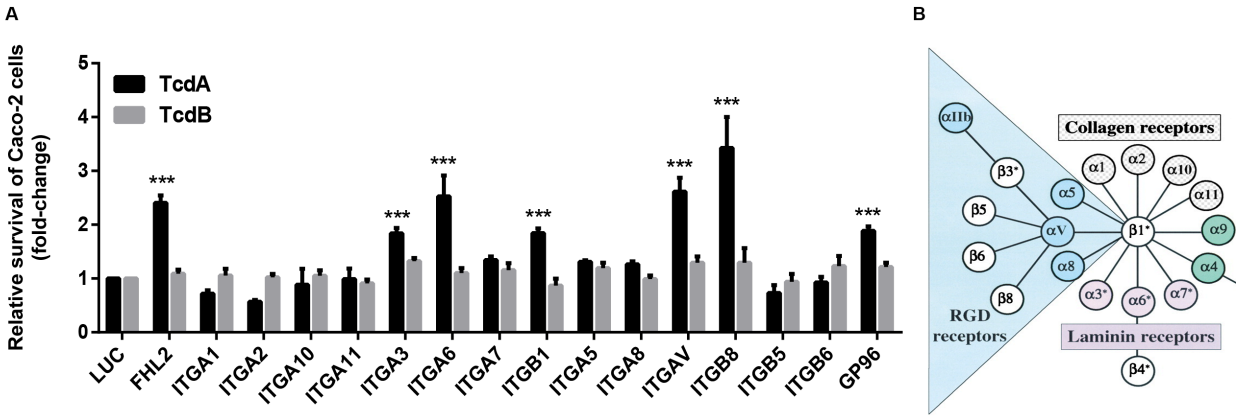

Figure 3-2. Host factors important for TcdA-induced toxicity in Caco-2 cells. A) Caco-2 cells were transfected with 10 nM siRNA against indicated host factors, exposed to 50 nM TcdA (black bars) or TcdB (gray bars) and then assayed for cellular viability using CellTiterGLO. Fold change of survival was obtained by normalizing the relative viability of samples to luciferase control. The data represent the average of at least four independent experiments performed in triplicate with the standard error of the mean indicated as error bars. Data were analyzed using one-way ANOVA. p-values were generated using Dunnett's multiple comparisons test in GraphPad Prism. ***p<0.005. **B)** Integrins are αβ heterodimers. The figure depicts the mammalian subunits and their αβ associations. Adapted from Richard O Hynes, Cell, 2002 (293).

mediated depletion of integrins alpha 3, alpha 6, beta 1, alpha V, and beta 8 also conferred significant protection against TcdA challenge in Caco-2 cells, suggesting a role for integrins in TcdA mechanism (Figure 3-2A). Integrin receptors exist as heterodimers of α and β subunits (Figure 3-2B), and have been shown to promote attachment and/or cell entry of several viruses, including rotavirus, human cytomegalovirus, human metapneumovirus, and reovirus (294-297). Whether integrins contribute to TcdA-induced toxicity by mediating attachment and/or internalization of TcdA is a question for future study.

In summary, I have identified several host factors that are important for TcdA-induced pathogenic effects in human colonic epithelial cells. Notably, depletion of these factors inhibited TcdA-induced cytotoxicity but had no effect on TcdB intoxication (Figure 3-1B and Figure 3-2A). As discussed earlier, it is likely that some of these factors may contribute to TcdA entry. Moving forward, we will directly determine if these identified factors (and any additional factors that we obtain from our future sequencing efforts) mediate entry of TcdA into host cells. In the preliminary entry assay, siRNAs will be used to knockdown selected candidates in Caco-2 cells. Cells will be incubated at 4 °C for 1 hour (to inhibit endocytosis) and exposed to either mock (buffer) or Alexa Fluor 546 labeled TcdA at 4 °C for 1 hour, washed and then incubated in fresh media at 37 °C. Surface bound toxins will be stripped and internalized toxin signal will be quantified by using flow cytometry. I have optimized conditions and developed a protocol for efficient stripping of surface-bound toxins. Additionally, I have validated this procedure by using a known inhibitor of toxin entry (Figure 3-3). We will adapt this protocol to a flow cytometry-based read out to obtain measurements of toxin and target host factor levels within whole cells under control and different knockdown conditions. We will corroborate these results with data obtained from colocalization studies. Host factors that are important for TcdA entry will be mechanistically evaluated to elucidate their role in TcdA cell binding and/or entry. Priority will be

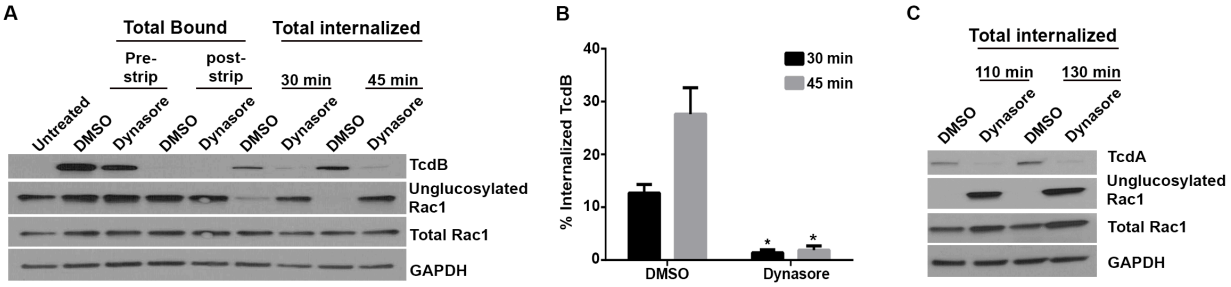

Figure 3-3. Validation of the entry assay using dynasore. A) Caco-2 monolayers were pretreated with either 80 μM dynasore or with an equal amount of DMSO control for 1 h at 37 °C. Cells were switched to 4°C for 1 h and then intoxicated with 25 nM 3xFLAG-TcdB$_{C698A}$ (cleavage-defective mutant of TcdB). Toxins were allowed to bind at 4°C for 1 h and then internalize at 37 °C for the indicated time points. To assess the bound toxin levels, cells were washed twice with PBS, dislodged by using a cell scraper, collected and homogenized to obtain lysates. To assess internalized toxin levels, the medium was removed and cells were washed once with PBS and then incubated with an acid solution (0.2 M acetic acid, 0.5 M NaCl in PBS) for 45 s. The acid solution was then removed and cells were washed twice with PBS, and further treated with trypsin solution to facilitate proteolysis and removal of any toxin still bound to the surface post-acid treatment. Cells were then collected and lysates were prepared for SDS-PAGE and Western blot. The blot was probed with antibodies against the toxin (anti-FLAG), unglucosylated and total Rac1, and GAPDH. The efficiency of the stripping procedure was assessed by comparing the total bound toxin levels before and after acid wash and trypsin treatment. **B**) Three independent replicates of the experiments shown in **a** were quantified by densitometry. The relative amounts of internalized TcdB were determined by normalizing the internalized toxin signal to that of total bound toxin (pre-strip), and the values were expressed as a percentage. Results reflect the mean and SEM, and were analyzed using two-tailed t-test. *$p<0.05$. **C)** Similar experiment performed with 3xFLAG-TcdA$_{C700A}$ show that dynasore treatment prevents toxin entry.

given to cell surface proteins as they are likely to serve as receptors for TcdA. In addition to the genetic screen described above, we are pursuing biochemical approaches to identify receptors that mediate TcdA binding and entry. Our additional efforts toward receptor identification are discussed next.

Identify determinants of cell binding

Receptor-binding is a critical first step in TcdA mechanism. Identifying cellular receptors for TcdA and determining structural features or regions within the toxin that are critical for TcdA interaction with the host cell surface are key to understanding and preventing toxin entry. Our current and future efforts in these areas are discussed below.

Identify TcdA receptor(s) on human colonic epithelial cells

The entry mechanism is often directed by the cell surface receptor. Three receptors have been recently identified for TcdB, but the human epithelial cell receptor (or receptors) for TcdA is currently unknown and represents an important question for future study. A previous report showed that TcdA can interact with heat shock protein gp96 (96). Depletion of gp96 inhibits TcdA-induced cytotoxicity in Caco-2 cells (Figure 3-2A). However, it is currently unclear whether gp96 promotes entry of TcdA into human colonic epithelial cells. Gp96 is also present within the cell, where it facilitates proper folding and expression of many cell surface proteins including integrins and Wnt coreceptor LRP6 (97-99). Consequently, depletion of gp96 could have indirect effects on TcdA cytotoxic mechanism. Moving forward, we will evaluate the role of gp96 in TcdA cell binding and entry using colocalization studies and antibody-blocking experiments. The specificity of the anti-gp96 antibody will be determined prior to use in the

assays. Even if gp96 could serve as a receptor for TcdA and promote entry via the PACSIN2-dependent pathway, the modest inhibition of TcdA-induced cytopathic effects observed in the presence of an anti-gp96 antibody suggests the existence of additional receptor structures (96). Interestingly, while investigating the role of a host factor identified in my gene-trap screen I made the observation that integrins α3, α6, αV, β1, and β8 play a role in TcdA cytotoxic mechanism (*discussed in the previous section*). We will also evaluate whether integrins contribute to TcdA cell binding and entry. However, both gp96 and integrins are multi-functional proteins, and it is possible that they contribute to TcdA-induced cytotoxicity through mechanisms other than mediating toxin binding and/or entry. Furthermore, it is also possible that TcdA binds multiple surface proteins, which may make it difficult to identify receptor candidates through the genetic screen described above. Therefore, we have decided to also pursue a biochemical approach which will involve, 1) cross-linking desthiobiotinylated TcdA to the cell surface, 2) solubilizing cells with a detergent-based buffer, 3) pull-down using magnetic streptavidin beads to enrich for the complex, and 4) elution with biotin (desthiobiotin binds streptavidin with lower affinity than biotin) and downstream analyses by mass spectrometry. I have already generated a TcdA construct with a N-terminal AviTag, which is recognized by an *E. coli* biotin ligase, BirA. I have optimized a protocol to add a biotin or D-desthiobiotin to the tagged toxin enzymatically using BirA. Additionally, I have confirmed that the procedure does not affect toxin function (Figure 3-4). Candidates obtained through this cell-based pull-down approach will be validated and mechanistically evaluated using *in vitro* binding assays, and cell-based binding and entry assays in the presence of function blocking antibodies or siRNA.

Elucidate the role of sugar-binding and CROPS C-terminus in cell surface binding

There are several lines of evidence that show that the CROPS domain mediates TcdA interaction with the host cell surface. The isolated CROPS domain from TcdA can bind to host

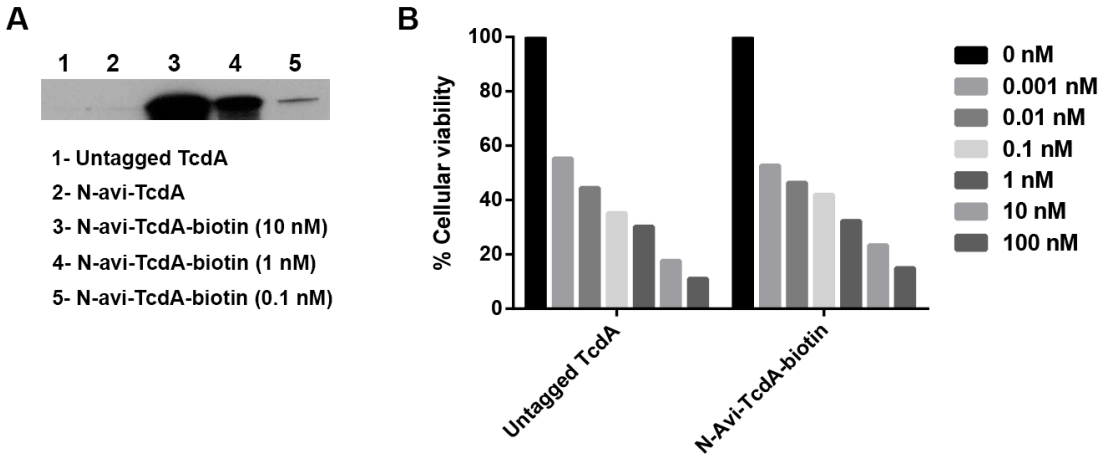

Figure 3-4. N-terminal AviTag and enzymatic biotinylation do not affect TcdA function. A) Western blotting using streptavidin-HRP confirms biotinylation of N-terminal AviTagged TcdA**.** Purified TcdA_avi was incubated at a final concentration of 3 μM. The biotinylation reaction occurred overnight at room temperature. Biotinylated toxins were then separated from the reaction mixture by size-exclusion chromatography and probed for biotin using streptavidin-HRP (BD biosciences). **B)** Young adult mouse colonic epithelial cells were intoxicated with indicated concentrations of untagged (control) or biotinylated AviTagged TcdA and then assayed for cellular viability using CellTiterGlo. Result indicates that the cytotoxicity of untagged holotoxin and biotinylated AviTagged toxin is comparable across toxin concentrations.

cells (89, 90), and excess TcdA CROPS competes with holotoxin in cell binding and cytopathic assays (89-91). TcdA CROPS contains seven putative sugar binding sites and it has been shown to bind carbohydrates known to be present in mammalian cell surface glycoconjugates (78, 82-88). A widely-held view in the field is that this sugar-binding property of CROPS is critical for TcdA's interaction with the host cell. However, recent studies on TcdA neutralizing anti-CROPS antibodies have questioned the importance of carbohydrate-binding in mediating toxin interaction with the cell surface.

We recently elucidated the mechanism of TcdA neutralization by a monoclonal anti-CROPS antibody, PA50 (298). Structural and functional analyses showed that PA50 Fab binds the C-terminus of TcdA CROPS, specifically repeats 5, 6, and 7 (R5, R6, and R7), and neutralizes toxin function by blocking receptor-binding (Figure 3-5). It is important to note that PA50 Fab does not occlude the carbohydrate binding site on CROPS (Figure 3-6). Studies by other groups on two neutralizing single-domain antibodies (sdAbs), A20.1 and A26.8, show that these sdAbs also bind the C-terminus of TcdA CROPS (299). A20.1 binds a region that overlaps with the PA50 epitope (Figure 3-6), whereas, A26.8 binds a site in R7 located at the extreme C-terminus of the CROPS. Notably, A20.1 and A26.8 binding do not impair trisaccharide binding by TcdA (93). These observations suggest that there are sugar-independent interactions that are critical for binding and entry of TcdA. To test this hypothesis, we plan to generate a TcdA construct that can no longer bind trisaccharides and perform side-by-side comparisons of cell binding and entry with wildtype toxin. To generate such a toxin construct, we need to mutate the seven putative sugar binding sites in the CROPS region. Unfortunately, repetitive sequences within this region make mutagenesis difficult. To address this issue, we generated a CROPS sequence with reduced repeating motifs using a codon optimization tool (cool.syncti.org), had it synthesized by GenScript, and inserted it into our toxin vector by Gibson Assembly to generate holotoxin A with this new CROPS (TcdA opti-CROPS).

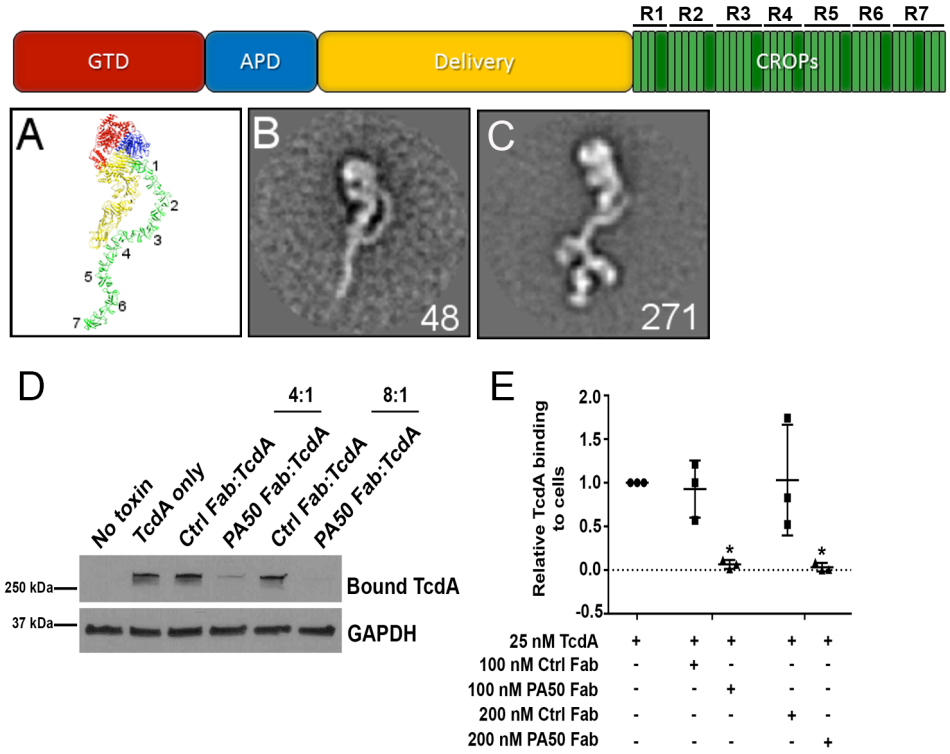

Figure 3-5. PA50 Fab binds C-terminus of TcdA CROPS and blocks toxin binding to the cell surface. Top schematic shows TcdA domain organization. CROPS short repeats (SRs) are in light green and long repeats (LRs) are in dark green. There are a total of 33 SRs and 7 LRs organized into seven repeat regions R1-7. **A)** Cartoon model of TcdA holotoxin, following the coloring in the domain schematic. **B)** Reference-free class showing TcdA holotoxin alone or **C)** the complex with Fab bound to CROPs-R5-R6-R7. Panels A-C were contributed by Dr. Heather Kroh, postdoctoral fellow in the Lacy lab. **D)** Purified TcdA (25 nM) was pre-incubated with 4- or 8-fold excess of PA50 Fab or an isotype control Fab. Caco-2 monolayers were allowed to bind TcdA-Fab complexes for 1 h at 10 °C (lanes 3-6). Unbound toxins were washed and whole cell lysates were prepared for SDS-PAGE and Western blot. The blot was probed with antibodies against TcdA and GAPDH. Cells that did not receive toxin and cells that received only toxin without any antibody were used as controls (lanes 1-2). **E)** Experiments shown in (A) were quantified by densitometry and binding of TcdA to cells was determined by normalizing bound TcdA levels to that of GAPDH. Relative TcdA binding to cells was determined by normalizing the binding values to that of the toxin only controls (*$p<0.05$). (C) and (D) Similar experiments performed with TcdA-Fab complexes (*$p<0.05$). Results reflect the mean ± SD of three independent experiments and were analyzed using one-way ANOVA.

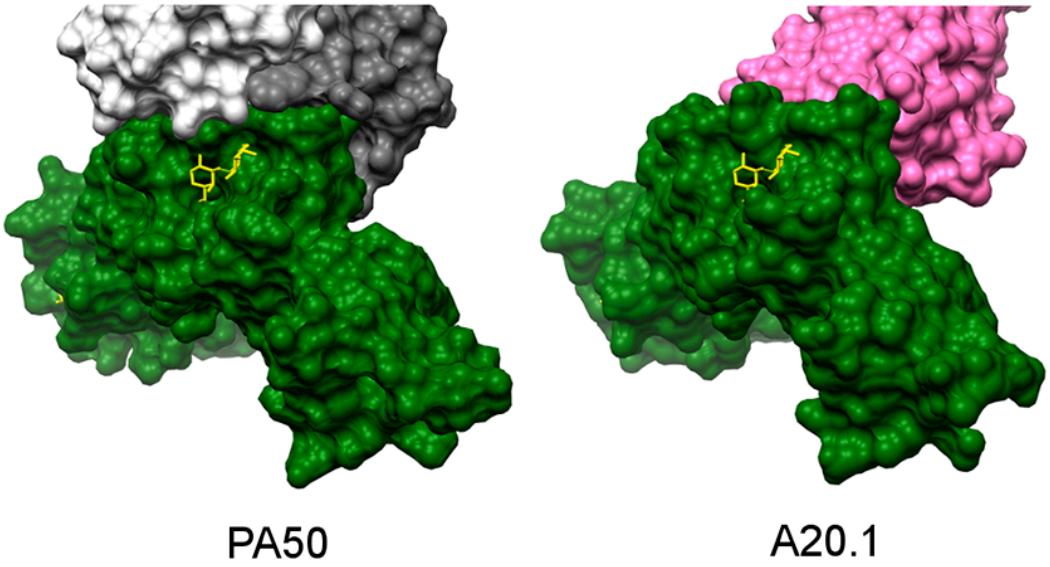

Figure 3-6. PA50 Fab and sdAb A20.1 epitopes on TcdA CROPS do not occlude the sugar binding site. Surface view of the relative location of the different antibodies to the trisaccharide binding pocket (yellow sticks) at CROPs-R6. TcdA-CROPs (green), PA50 Fab heavy (gray) and light (light gray) chains, A20.1 (pink). Figure credit: Dr. Heather Kroh.

We have fully sequenced TcdA opti-CROPS construct to confirm that no extraneous mutations were introduced during the cloning process. We will purify this toxin and perform cell-based assays to confirm that TcdA opti-CROPS functions similar to wildtype TcdA. Next, we will mutate the sugar binding sites by site-directed mutagenesis, confirm the lack of sugar binding using an *in vitro* assay (such as microscale thermophoresis or surface plasmon resonance), and test cell binding and internalization of TcdA opti-CROPS (vs wildtype TcdA).

In addition to sugar-binding, we are investigating the role of the C-terminal region of TcdA CROPS in host receptor-binding. A recent study showed that a CROPS truncation construct containing only R5, R6, and R7 ($TcdA_{2323-2710}$) bound cells with an apparent K_d equal to that of full length CROPS and was internalized into epithelial cells (300). In the same study, a CROPS construct lacking R5, R6, and R7 was unable to bind or enter cells. These observations suggest a critical role for the C-terminal portion of CROPS in TcdA binding and entry, which is consistent with results from the studies on anti-CROPS antibodies discussed above. It is likely that the C-terminus of TcdA CROPS comprising R5, R6, and R7 mediates the proposed sugar-independent interaction with the host cell surface. We plan to test this hypothesis in the future.

Overall, the studies described in this subsection will allow a better understanding of how the toxin interacts with the host cell surface and will inform development of strategies (such as monoclonal antibodies) to prevent toxin binding to host cells. Furthermore, if the C-terminus of TcdA CROPS mediates sugar-independent interactions with the host cell, then toxin constructs generated for those studies (holotoxin with no sugar binding sites or CROPS R5-R6-R7 with no sugar binding sites) can be used in our receptor identification studies discussed earlier.

Investigate the role of microtubule and microtubule-based motors in TcdA entry

One of the observations I made while investigating TcdA entry by colocalization studies is that, in Caco-2 cells, TcdA was often found in PACSIN2-positive structures that did not have the typical vesicular appearance. PACSIN2 is a BAR-domain protein that bends membranes. In addition to being associated with vesicular structures such as caveolae, PACSIN2 is also known to create tubular membrane invaginations (232). I speculate that in Caco-2 cells, TcdA is internalized into PACSIN2-positive tubules, resulting in the extended structures observed in the images. Interestingly, recent work by the Kenworthy lab shows that microtubules and microtubule motor dynein provide mechanical force for plasma membrane tubulation during clathrin-independent endocytosis of cholera toxin B subunit (CTxB) (301). Microtubules and dynein are also involved in the internalized of Shiga toxin B subunit (STxB) via endophilin A2-positive tubules (241). It is possible that microtubules, dynein, and PACSIN2 may work in concert to generate the tubular structures that contain TcdA. Moving forward, we will test if an intact microtubule network and dynein activity are required for the clathrin-independent, PACSIN2-dependent endocytosis of TcdA. Determining whether microtubules are involved in TcdA internalization will also help us mechanistically evaluate the role of NAV2, a microtubule plus-end binding ATPase, in TcdA intoxication.

In summary, receptor-binding and host cell entry are key events in the intoxication mechanism. The studies described in this chapter are likely to contribute significantly to our understanding of how TcdA intoxicates host cells. Results from these studies will be contrasted with ongoing work on TcdB to build a mechanistic framework of how both toxins cause toxicity in epithelial cells. Identifying mechanisms that are unique or shared by TcdA and TcdB will be critical towards the development of therapeutic strategies to prevent pathology associated with CDI.

APPENDIX

List of Publications

Chandrasekaran R and Lacy DB (2017). The role of toxins in *Clostridium difficile* infection. **FEMS Microbiology Reviews**.

Kroh HK, Chandrasekaran R, Rosenthal K, Woods R, Jin X, Ohi MD, Nyborg AC, Rainey J, Warrener P, Spiller BW and Lacy DB (2017). Use of a neutralizing antibody helps identify structural features critical for binding of *Clostridium difficile* toxin TcdA to the host cell surface. **The Journal of biological chemistry** 292(35):14401-12

Chandrasekaran R, Kenworthy AK and Lacy DB (2016). *Clostridium difficile* toxin A undergoes clathrin-independent, PACSIN2-dependent endocytosis. **PLoS Pathog** 12(12): e1006070.

LaFrance ME, Farrow MA, Chandrasekaran R, Sheng J, Rubin DH and Lacy DB (2015). Identification of an epithelial cell receptor responsible for *Clostridium difficile* TcdB-induced cytotoxicity. **Proc Natl Acad Sci U S A** 112(22): 7073-7078.

List of Manuscripts Under Review

Kroh, HK*, Chandrasekaran R*, Zhang Z, Rosenthal K, Woods R, Jin X, Nyborg AC, Rainey J, Warrener P, Melnyk RA, Spiller BW and Lacy DB. A neutralizing antibody that blocks *Clostridium difficile* toxin TcdB enzyme delivery. *In revision*. **** Co-first authors***

BIBLIOGRAPHY

1. Hall IC, O'Toole E. Intestinal flora in new-born infants: With a description of a new pathogenic anaerobe, bacillus difficilis. American Journal of Diseases of Children. 1935;49(2):390-402.

2. Bartlett JG, Moon N, Chang TW, Taylor N, Onderdonk AB. Role of Clostridium difficile in antibiotic-associated pseudomembranous colitis. Gastroenterology. 1978;75(5):778-82.

3. George WL, Sutter VL, Goldstein EJ, Ludwig SL, Finegold SM. Aetiology of antimicrobial-agent-associated colitis. Lancet (London, England). 1978;1(8068):802-3.

4. Martin JS, Monaghan TM, Wilcox MH. Clostridium difficile infection: epidemiology, diagnosis and understanding transmission. Nature reviews Gastroenterology & hepatology. 2016;13(4):206-16.

5. Lessa FC, Mu Y, Bamberg WM, Beldavs ZG, Dumyati GK, Dunn JR, et al. Burden of Clostridium difficile infection in the United States. The New England journal of medicine. 2015;372(9):825-34.

6. Smits WK, Lyras D, Lacy DB, Wilcox MH, Kuijper EJ. Clostridium difficile infection. Nature reviews Disease primers. 2016;2:16020.

7. He M, Miyajima F, Roberts P, Ellison L, Pickard DJ, Martin MJ, et al. Emergence and global spread of epidemic healthcare-associated Clostridium difficile. Nature genetics. 2013;45(1):109-13.

8. Fawley WN, Knetsch CW, MacCannell DR, Harmanus C, Du T, Mulvey MR, et al. Development and validation of an internationally-standardized, high-resolution capillary gel-based electrophoresis PCR-ribotyping protocol for Clostridium difficile. PloS one. 2015;10(2):e0118150.

9. Lawson PA, Citron DM, Tyrrell KL, Finegold SM. Reclassification of Clostridium difficile as Clostridioides difficile (Hall and O'Toole 1935) Prevot 1938. Anaerobe. 2016;40:95-9.

10. Giel JL, Sorg JA, Sonenshein AL, Zhu J. Metabolism of bile salts in mice influences spore germination in Clostridium difficile. PloS one. 2010;5(1):e8740.

11. Sorg JA, Sonenshein AL. Bile salts and glycine as cogerminants for Clostridium difficile spores. Journal of bacteriology. 2008;190(7):2505-12.

12. Theriot CM, Young VB. Interactions Between the Gastrointestinal Microbiome and Clostridium difficile. Annual review of microbiology. 2015;69:445-61.

13. Khanna S, Pardi DS. "Community-acquired Clostridium difficile infection: an emerging entity". Clinical infectious diseases : an official publication of the Infectious Diseases Society of America. 2012;55(12):1741-2.

14. Awad MM, Johanesen PA, Carter GP, Rose E, Lyras D. Clostridium difficile virulence factors: Insights into an anaerobic spore-forming pathogen. Gut microbes. 2014;5(5):579-93.

15. Barth H, Aktories K, Popoff MR, Stiles BG. Binary bacterial toxins: biochemistry, biology, and applications of common Clostridium and Bacillus proteins. Microbiology and molecular biology reviews : MMBR. 2004;68(3):373-402, table of contents.

16. Braun V, Hundsberger T, Leukel P, Sauerborn M, von Eichel-Streiber C. Definition of the single integration site of the pathogenicity locus in Clostridium difficile. Gene. 1996;181(1-2):29-38.

17. Hammond GA, Johnson JL. The toxigenic element of Clostridium difficile strain VPI 10463. Microbial pathogenesis. 1995;19(4):203-13.

18. Dingle KE, Griffiths D, Didelot X, Evans J, Vaughan A, Kachrimanidou M, et al. Clinical Clostridium difficile: clonality and pathogenicity locus diversity. PloS one. 2011;6(5):e19993.

19. Elliott B, Reed R, Chang BJ, Riley TV. Bacteremia with a large clostridial toxin-negative, binary toxin-positive strain of Clostridium difficile. Anaerobe. 2009;15(6):249-51.

20. Monot M, Eckert C, Lemire A, Hamiot A, Dubois T, Tessier C, et al. Clostridium difficile: New Insights into the Evolution of the Pathogenicity Locus. Scientific reports. 2015;5:15023.

21. Brouwer MS, Roberts AP, Hussain H, Williams RJ, Allan E, Mullany P. Horizontal gene transfer converts non-toxigenic Clostridium difficile strains into toxin producers. Nature communications. 2013;4:2601.

22. Rupnik M, Avesani V, Janc M, von Eichel-Streiber C, Delmee M. A novel toxinotyping scheme and correlation of toxinotypes with serogroups of Clostridium difficile isolates. Journal of clinical microbiology. 1998;36(8):2240-7.

23. Rupnik M, Janezic S. An Update on Clostridium difficile Toxinotyping. Journal of clinical microbiology. 2016;54(1):13-8.

24. Bouillaut L, Dubois T, Sonenshein AL, Dupuy B. Integration of metabolism and virulence in Clostridium difficile. Research in microbiology. 2015;166(4):375-83.

25. Mani N, Dupuy B. Regulation of toxin synthesis in Clostridium difficile by an alternative RNA polymerase sigma factor. Proceedings of the National Academy of Sciences of the United States of America. 2001;98(10):5844-9.

26. Moncrief JS, Barroso LA, Wilkins TD. Positive regulation of Clostridium difficile toxins. Infection and immunity. 1997;65(3):1105-8.

27. Mani N, Lyras D, Barroso L, Howarth P, Wilkins T, Rood JI, et al. Environmental response and autoregulation of Clostridium difficile TxeR, a sigma factor for toxin gene expression. Journal of bacteriology. 2002;184(21):5971-8.

28. Carter GP, Douce GR, Govind R, Howarth PM, Mackin KE, Spencer J, et al. The anti-sigma factor TcdC modulates hypervirulence in an epidemic BI/NAP1/027 clinical isolate of Clostridium difficile. PLoS pathogens. 2011;7(10):e1002317.

29. Matamouros S, England P, Dupuy B. Clostridium difficile toxin expression is inhibited by the novel regulator TcdC. Molecular microbiology. 2007;64(5):1274-88.

30. Govind R, Dupuy B. Secretion of Clostridium difficile toxins A and B requires the holin-like protein TcdE. PLoS pathogens. 2012;8(6):e1002727.

31. Olling A, Seehase S, Minton NP, Tatge H, Schroter S, Kohlscheen S, et al. Release of TcdA and TcdB from Clostridium difficile cdi 630 is not affected by functional inactivation of the tcdE gene. Microbial pathogenesis. 2012;52(1):92-100.

32. Tan KS, Wee BY, Song KP. Evidence for holin function of tcdE gene in the pathogenicity of Clostridium difficile. Journal of medical microbiology. 2001;50(7):613-9.

33. Mukherjee K, Karlsson S, Burman LG, Akerlund T. Proteins released during high toxin production in Clostridium difficile. Microbiology (Reading, England). 2002;148(Pt 7):2245-53.

34. Govind R, Fitzwater L, Nichols R. Observations on the Role of TcdE Isoforms in Clostridium difficile Toxin Secretion. Journal of bacteriology. 2015;197(15):2600-9.

35. Darkoh C, DuPont HL, Norris SJ, Kaplan HB. Toxin synthesis by Clostridium difficile is regulated through quorum signaling. mBio. 2015;6(2):e02569.

36. Dupuy B, Sonenshein AL. Regulated transcription of Clostridium difficile toxin genes. Molecular microbiology. 1998;27(1):107-20.

37. Hundsberger T, Braun V, Weidmann M, Leukel P, Sauerborn M, von Eichel-Streiber C. Transcription analysis of the genes tcdA-E of the pathogenicity locus of Clostridium difficile. European journal of biochemistry / FEBS. 1997;244(3):735-42.

38. Karlsson S, Dupuy B, Mukherjee K, Norin E, Burman LG, Akerlund T. Expression of Clostridium difficile toxins A and B and their sigma factor TcdD is controlled by temperature. Infection and immunity. 2003;71(4):1784-93.

39. Aldape MJ, Packham AE, Nute DW, Bryant AE, Stevens DL. Effects of ciprofloxacin on the expression and production of exotoxins by Clostridium difficile. Journal of medical microbiology. 2013;62(Pt 5):741-7.

40. Chilton CH, Freeman J, Crowther GS, Todhunter SL, Nicholson S, Wilcox MH. Co-amoxiclav induces proliferation and cytotoxin production of Clostridium difficile ribotype 027 in a human gut model. The Journal of antimicrobial chemotherapy. 2012;67(4):951-4.

41. Freeman J, Baines SD, Saxton K, Wilcox MH. Effect of metronidazole on growth and toxin production by epidemic Clostridium difficile PCR ribotypes 001 and 027 in a human gut model. The Journal of antimicrobial chemotherapy. 2007;60(1):83-91.

42. Nakamura S, Mikawa M, Tanabe N, Yamakawa K, Nishida S. Effect of clindamycin on cytotoxin production by Clostridium difficile. Microbiology and immunology. 1982;26(11):985-92.

43. Karlsson S, Lindberg A, Norin E, Burman LG, Akerlund T. Toxins, butyric acid, and other short-chain fatty acids are coordinately expressed and down-regulated by cysteine in Clostridium difficile. Infection and immunity. 2000;68(10):5881-8.

44. Karasawa T, Maegawa T, Nojiri T, Yamakawa K, Nakamura S. Effect of arginine on toxin production by Clostridium difficile in defined medium. Microbiology and immunology. 1997;41(8):581-5.

45. Karlsson S, Burman LG, Akerlund T. Suppression of toxin production in Clostridium difficile VPI 10463 by amino acids. Microbiology (Reading, England). 1999;145 (Pt 7):1683-93.

46. Antunes A, Camiade E, Monot M, Courtois E, Barbut F, Sernova NV, et al. Global transcriptional control by glucose and carbon regulator CcpA in Clostridium difficile. Nucleic acids research. 2012;40(21):10701-18.

47. Dineen SS, Villapakkam AC, Nordman JT, Sonenshein AL. Repression of Clostridium difficile toxin gene expression by CodY. Molecular microbiology. 2007;66(1):206-19.

48. Aubry A, Hussack G, Chen W, KuoLee R, Twine SM, Fulton KM, et al. Modulation of toxin production by the flagellar regulon in Clostridium difficile. Infection and immunity. 2012;80(10):3521-32.

49. Edwards AN, Tamayo R, McBride SM. A novel regulator controls Clostridium difficile sporulation, motility and toxin production. Molecular microbiology. 2016;100(6):954-71.

50. El Meouche I, Peltier J, Monot M, Soutourina O, Pestel-Caron M, Dupuy B, et al. Characterization of the SigD regulon of C. difficile and its positive control of toxin production through the regulation of tcdR. PloS one. 2013;8(12):e83748.

51. Mackin KE, Carter GP, Howarth P, Rood JI, Lyras D. Spo0A differentially regulates toxin production in evolutionarily diverse strains of Clostridium difficile. PloS one. 2013;8(11):e79666.

52. Martin MJ, Clare S, Goulding D, Faulds-Pain A, Barquist L, Browne HP, et al. The agr locus regulates virulence and colonization genes in Clostridium difficile 027. Journal of bacteriology. 2013;195(16):3672-81.

53. McKee RW, Mangalea MR, Purcell EB, Borchardt EK, Tamayo R. The second messenger cyclic Di-GMP regulates Clostridium difficile toxin production by controlling expression of sigD. Journal of bacteriology. 2013;195(22):5174-85.

54. Saujet L, Monot M, Dupuy B, Soutourina O, Martin-Verstraete I. The key sigma factor of transition phase, SigH, controls sporulation, metabolism, and virulence factor expression in Clostridium difficile. Journal of bacteriology. 2011;193(13):3186-96.

55. Underwood S, Guan S, Vijayasubhash V, Baines SD, Graham L, Lewis RJ, et al. Characterization of the sporulation initiation pathway of Clostridium difficile and its role in toxin production. Journal of bacteriology. 2009;191(23):7296-305.

56. Lyerly DM, Lockwood DE, Richardson SH, Wilkins TD. Biological activities of toxins A and B of Clostridium difficile. Infection and immunity. 1982;35(3):1147-50.

57. Mitchell TJ, Ketley JM, Haslam SC, Stephen J, Burdon DW, Candy DC, et al. Effect of toxin A and B of Clostridium difficile on rabbit ileum and colon. Gut. 1986;27(1):78-85.

58. Lyerly DM, Saum KE, MacDonald DK, Wilkins TD. Effects of Clostridium difficile toxins given intragastrically to animals. Infection and immunity. 1985;47(2):349-52.

59. Babcock GJ, Broering TJ, Hernandez HJ, Mandell RB, Donahue K, Boatright N, et al. Human monoclonal antibodies directed against toxins A and B prevent Clostridium difficile-induced mortality in hamsters. Infection and immunity. 2006;74(11):6339-47.

60. Kim PH, Iaconis JP, Rolfe RD. Immunization of adult hamsters against Clostridium difficile-associated ileocecitis and transfer of protection to infant hamsters. Infection and immunity. 1987;55(12):2984-92.

61. Lyerly DM, Johnson JL, Frey SM, Wilkins TD. Vaccination against lethalClostridium difficile enterocolitis with a nontoxic recombinant peptide of toxin A. Current Microbiology. 1990;21(1):29-32.

62. Kyne L, Warny M, Qamar A, Kelly CP. Asymptomatic carriage of Clostridium difficile and serum levels of IgG antibody against toxin A. The New England journal of medicine. 2000;342(6):390-7.

63. Kyne L, Warny M, Qamar A, Kelly CP. Association between antibody response to toxin A and protection against recurrent Clostridium difficile diarrhoea. Lancet (London, England). 2001;357(9251):189-93.

64. Warny M, Vaerman JP, Avesani V, Delmee M. Human antibody response to Clostridium difficile toxin A in relation to clinical course of infection. Infection and immunity. 1994;62(2):384-9.

65. Drudy D, Fanning S, Kyne L. Toxin A-negative, toxin B-positive Clostridium difficile. International journal of infectious diseases : IJID : official publication of the International Society for Infectious Diseases. 2007;11(1):5-10.

66. King AM, Mackin KE, Lyras D. Emergence of toxin A-negative, toxin B-positive Clostridium difficile strains: epidemiological and clinical considerations. Future microbiology. 2015;10(1):1-4.

67. Chaves-Olarte E, Low P, Freer E, Norlin T, Weidmann M, von Eichel-Streiber C, et al. A novel cytotoxin from Clostridium difficile serogroup F is a functional hybrid between two other large clostridial cytotoxins. The Journal of biological chemistry. 1999;274(16):11046-52.

68. Chaves-Olarte E, Freer E, Parra A, Guzman-Verri C, Moreno E, Thelestam M. R-Ras glucosylation and transient RhoA activation determine the cytopathic effect produced by toxin B variants from toxin A-negative strains of Clostridium difficile. The Journal of biological chemistry. 2003;278(10):7956-63.

69. Riegler M, Sedivy R, Pothoulakis C, Hamilton G, Zacherl J, Bischof G, et al. Clostridium difficile toxin B is more potent than toxin A in damaging human colonic epithelium in vitro. The Journal of clinical investigation. 1995;95(5):2004-11.

70. Savidge TC, Pan WH, Newman P, O'Brien M, Anton PM, Pothoulakis C. Clostridium difficile toxin B is an inflammatory enterotoxin in human intestine. Gastroenterology. 2003;125(2):413-20.

71. Wilcox MH, Gerding DN, Poxton IR, Kelly C, Nathan R, Birch T, et al. Bezlotoxumab for Prevention of Recurrent Clostridium difficile Infection. The New England journal of medicine. 2017;376(4):305-17.

72. Lyras D, O'Connor JR, Howarth PM, Sambol SP, Carter GP, Phumoonna T, et al. Toxin B is essential for virulence of Clostridium difficile. Nature. 2009;458(7242):1176-9.

73. Kuehne SA, Cartman ST, Heap JT, Kelly ML, Cockayne A, Minton NP. The role of toxin A and toxin B in Clostridium difficile infection. Nature. 2010;467(7316):711-3.

74. Kuehne SA, Collery MM, Kelly ML, Cartman ST, Cockayne A, Minton NP. Importance of toxin A, toxin B, and CDT in virulence of an epidemic Clostridium difficile strain. The Journal of infectious diseases. 2014;209(1):83-6.

75. Carter GP, Chakravorty A, Pham Nguyen TA, Mileto S, Schreiber F, Li L, et al. Defining the Roles of TcdA and TcdB in Localized Gastrointestinal Disease, Systemic Organ Damage, and the Host Response during Clostridium difficile Infections. mBio. 2015;6(3):e00551.

76. Hamm EE, Voth DE, Ballard JD. Identification of Clostridium difficile toxin B cardiotoxicity using a zebrafish embryo model of intoxication. Proceedings of the National Academy of Sciences of the United States of America. 2006;103(38):14176-81.

77. Steele J, Mukherjee J, Parry N, Tzipori S. Antibody against TcdB, but not TcdA, prevents development of gastrointestinal and systemic Clostridium difficile disease. The Journal of infectious diseases. 2013;207(2):323-30.

78. von Eichel-Streiber C, Sauerborn M. Clostridium difficile toxin A carries a C-terminal repetitive structure homologous to the carbohydrate binding region of streptococcal glycosyltransferases. Gene. 1990;96(1):107-13.

79. von Eichel-Streiber C, Sauerborn M, Kuramitsu HK. Evidence for a modular structure of the homologous repetitive C-terminal carbohydrate-binding sites of Clostridium difficile toxins and Streptococcus mutans glucosyltransferases. Journal of bacteriology. 1992;174(20):6707-10.

80. Ho JG, Greco A, Rupnik M, Ng KK. Crystal structure of receptor-binding C-terminal repeats from Clostridium difficile toxin A. Proceedings of the National Academy of Sciences of the United States of America. 2005;102(51):18373-8.

81. Pruitt RN, Chambers MG, Ng KK, Ohi MD, Lacy DB. Structural organization of the functional domains of Clostridium difficile toxins A and B. Proceedings of the National Academy of Sciences of the United States of America. 2010;107(30):13467-72.

82. Dingle T, Wee S, Mulvey GL, Greco A, Kitova EN, Sun J, et al. Functional properties of the carboxy-terminal host cell-binding domains of the two toxins, TcdA and TcdB, expressed by Clostridium difficile. Glycobiology. 2008;18(9):698-706.

83. El-Hawiet A, Kitova EN, Kitov PI, Eugenio L, Ng KK, Mulvey GL, et al. Binding of Clostridium difficile toxins to human milk oligosaccharides. Glycobiology. 2011;21(9):1217-27.

84. Greco A, Ho JG, Lin SJ, Palcic MM, Rupnik M, Ng KK. Carbohydrate recognition by Clostridium difficile toxin A. Nature structural & molecular biology. 2006;13(5):460-1.

85. Krivan HC, Clark GF, Smith DF, Wilkins TD. Cell surface binding site for Clostridium difficile enterotoxin: evidence for a glycoconjugate containing the sequence Gal alpha 1-3Gal beta 1-4GlcNAc. Infection and immunity. 1986;53(3):573-81.

86. Pothoulakis C, Gilbert RJ, Cladaras C, Castagliuolo I, Semenza G, Hitti Y, et al. Rabbit sucrase-isomaltase contains a functional intestinal receptor for Clostridium difficile toxin A. The Journal of clinical investigation. 1996;98(3):641-9.

87. Teneberg S, Lonnroth I, Torres Lopez JF, Galili U, Halvarsson MO, Angstrom J, et al. Molecular mimicry in the recognition of glycosphingolipids by Gal alpha 3 Gal beta 4 GlcNAc beta-binding Clostridium difficile toxin A, human natural anti alpha-galactosyl IgG and the monoclonal antibody Gal-13: characterization of a binding-active human glycosphingolipid, non-identical with the animal receptor. Glycobiology. 1996;6(6):599-609.

88. Tucker KD, Wilkins TD. Toxin A of Clostridium difficile binds to the human carbohydrate antigens I, X, and Y. Infection and immunity. 1991;59(1):73-8.

89. Frisch C, Gerhard R, Aktories K, Hofmann F, Just I. The complete receptor-binding domain of Clostridium difficile toxin A is required for endocytosis. Biochemical and biophysical research communications. 2003;300(3):706-11.

90. Olling A, Goy S, Hoffmann F, Tatge H, Just I, Gerhard R. The repetitive oligopeptide sequences modulate cytopathic potency but are not crucial for cellular uptake of Clostridium difficile toxin A. PloS one. 2011;6(3):e17623.

91. Sauerborn M, Leukel P, von Eichel-Streiber C. The C-terminal ligand-binding domain of Clostridium difficile toxin A (TcdA) abrogates TcdA-specific binding to cells and prevents mouse lethality. FEMS microbiology letters. 1997;155(1):45-54.

92. Hernandez LD, Kroh HK, Hsieh E, Yang X, Beaumont M, Sheth PR, et al. Epitopes and Mechanism of Action of the Clostridium difficile Toxin A-Neutralizing Antibody Actoxumab. Journal of molecular biology. 2017.

93. Hussack G, Arbabi-Ghahroudi M, van Faassen H, Songer JG, Ng KK, MacKenzie R, et al. Neutralization of Clostridium difficile toxin A with single-domain antibodies targeting the cell receptor binding domain. The Journal of biological chemistry. 2011;286(11):8961-76.

94. Leuzzi R, Spencer J, Buckley A, Brettoni C, Martinelli M, Tulli L, et al. Protective efficacy induced by recombinant Clostridium difficile toxin fragments. Infection and immunity. 2013;81(8):2851-60.

95. Lyerly DM, Phelps CJ, Toth J, Wilkins TD. Characterization of toxins A and B of Clostridium difficile with monoclonal antibodies. Infection and immunity. 1986;54(1):70-6.

96. Na X, Kim H, Moyer MP, Pothoulakis C, LaMont JT. gp96 is a human colonocyte plasma membrane binding protein for Clostridium difficile toxin A. Infection and immunity. 2008;76(7):2862-71.

97. Liu B, Staron M, Hong F, Wu BX, Sun S, Morales C, et al. Essential roles of grp94 in gut homeostasis via chaperoning canonical Wnt pathway. Proceedings of the National Academy of Sciences of the United States of America. 2013;110(17):6877-82.

98. Staron M, Yang Y, Liu B, Li J, Shen Y, Zuniga-Pflucker JC, et al. gp96, an endoplasmic reticulum master chaperone for integrins and Toll-like receptors, selectively regulates early T and B lymphopoiesis. Blood. 2010;115(12):2380-90.

99. Yang Y, Liu B, Dai J, Srivastava PK, Zammit DJ, Lefrancois L, et al. Heat shock protein gp96 is a master chaperone for toll-like receptors and is important in the innate function of macrophages. Immunity. 2007;26(2):215-26.

100. Cabanes D, Sousa S, Cebria A, Lecuit M, Garcia-del Portillo F, Cossart P. Gp96 is a receptor for a novel Listeria monocytogenes virulence factor, Vip, a surface protein. The EMBO journal. 2005;24(15):2827-38.

101. Rechner C, Kuhlewein C, Muller A, Schild H, Rudel T. Host glycoprotein Gp96 and scavenger receptor SREC interact with PorB of disseminating Neisseria gonorrhoeae in an epithelial invasion pathway. Cell host & microbe. 2007;2(6):393-403.

102. Rolhion N, Barnich N, Bringer MA, Glasser AL, Ranc J, Hebuterne X, et al. Abnormally expressed ER stress response chaperone Gp96 in CD favours adherent-invasive Escherichia coli invasion. Gut. 2010;59(10):1355-62.

103. Orth P, Xiao L, Hernandez LD, Reichert P, Sheth PR, Beaumont M, et al. Mechanism of action and epitopes of Clostridium difficile toxin B-neutralizing antibody bezlotoxumab revealed by X-ray crystallography. The Journal of biological chemistry. 2014;289(26):18008-21.

104. Yuan P, Zhang H, Cai C, Zhu S, Zhou Y, Yang X, et al. Chondroitin sulfate proteoglycan 4 functions as the cellular receptor for Clostridium difficile toxin B. Cell research. 2015;25(2):157-68.

105. Tao L, Zhang J, Meraner P, Tovaglieri A, Wu X, Gerhard R, et al. Frizzled proteins are colonic epithelial receptors for C. difficile toxin B. Nature. 2016;538(7625):350-5.

106. Barroso LA, Moncrief JS, Lyerly DM, Wilkins TD. Mutagenesis of the Clostridium difficile toxin B gene and effect on cytotoxic activity. Microbial pathogenesis. 1994;16(4):297-303.

107. Genisyuerek S, Papatheodorou P, Guttenberg G, Schubert R, Benz R, Aktories K. Structural determinants for membrane insertion, pore formation and translocation of Clostridium difficile toxin B. Molecular microbiology. 2011;79(6):1643-54.

108. LaFrance ME, Farrow MA, Chandrasekaran R, Sheng J, Rubin DH, Lacy DB. Identification of an epithelial cell receptor responsible for Clostridium difficile TcdB-induced cytotoxicity. Proceedings of the National Academy of Sciences of the United States of America. 2015;112(22):7073-8.

109. Manse JS, Baldwin MR. Binding and entry of Clostridium difficile toxin B is mediated by multiple domains. FEBS letters. 2015;589(24 Pt B):3945-51.

110. Schorch B, Song S, van Diemen FR, Bock HH, May P, Herz J, et al. LRP1 is a receptor for Clostridium perfringens TpeL toxin indicating a two-receptor model of clostridial glycosylating toxins. Proceedings of the National Academy of Sciences of the United States of America. 2014;111(17):6431-6.

111. Lambert GS, Baldwin MR. Evidence for dual receptor-binding sites in Clostridium difficile toxin A. FEBS letters. 2016;590(24):4550-63.

112. Terada N, Ohno N, Murata S, Katoh R, Stallcup WB, Ohno S. Immunohistochemical study of NG2 chondroitin sulfate proteoglycan expression in the small and large intestines. Histochemistry and cell biology. 2006;126(4):483-90.

113. Gerhard R, Frenzel E, Goy S, Olling A. Cellular uptake of Clostridium difficile TcdA and truncated TcdA lacking the receptor binding domain. Journal of medical microbiology. 2013.

114. Papatheodorou P, Zamboglou C, Genisyuerek S, Guttenberg G, Aktories K. Clostridial glucosylating toxins enter cells via clathrin-mediated endocytosis. PloS one. 2010;5(5):e10673.

115. Florin I, Thelestam M. Internalization of Clostridium difficile cytotoxin into cultured human lung fibroblasts. Biochimica et biophysica acta. 1983;763(4):383-92.

116. Florin I, Thelestam M. Lysosomal involvement in cellular intoxication with Clostridium difficile toxin B. Microbial pathogenesis. 1986;1(4):373-85.

117. Henriques B, Florin I, Thelestam M. Cellular internalisation of Clostridium difficile toxin A. Microbial pathogenesis. 1987;2(6):455-63.

118. Qa'Dan M, Spyres LM, Ballard JD. pH-induced conformational changes in Clostridium difficile toxin B. Infection and immunity. 2000;68(5):2470-4.

119. Collier RJ, Young JA. Anthrax toxin. Annual review of cell and developmental biology. 2003;19:45-70.

120. Geny B, Popoff MR. Bacterial protein toxins and lipids: pore formation or toxin entry into cells. Biology of the cell. 2006;98(11):667-78.

121. Barth H, Pfeifer G, Hofmann F, Maier E, Benz R, Aktories K. Low pH-induced formation of ion channels by clostridium difficile toxin B in target cells. The Journal of biological chemistry. 2001;276(14):10670-6.

122. Giesemann T, Jank T, Gerhard R, Maier E, Just I, Benz R, et al. Cholesterol-dependent pore formation of Clostridium difficile toxin A. The Journal of biological chemistry. 2006;281(16):10808-15.

123. Chumbler NM, Rutherford SA, Zhang Z, Farrow MA, Lisher JP, Farquhar E, et al. Crystal structure of Clostridium difficile toxin A. Nature microbiology. 2016;1.

124. von Eichel-Streiber C, Laufenberg-Feldmann R, Sartingen S, Schulze J, Sauerborn M. Comparative sequence analysis of the Clostridium difficile toxins A and B. Molecular & general genetics : MGG. 1992;233(1-2):260-8.

125. Zhang Z, Park M, Tam J, Auger A, Beilhartz GL, Lacy DB, et al. Translocation domain mutations affecting cellular toxicity identify the Clostridium difficile toxin B pore. Proceedings of the National Academy of Sciences of the United States of America. 2014;111(10):3721-6.

126. Pfeifer G, Schirmer J, Leemhuis J, Busch C, Meyer DK, Aktories K, et al. Cellular uptake of Clostridium difficile toxin B. Translocation of the N-terminal catalytic domain into the cytosol of eukaryotic cells. The Journal of biological chemistry. 2003;278(45):44535-41.

127. Kreimeyer I, Euler F, Marckscheffel A, Tatge H, Pich A, Olling A, et al. Autoproteolytic cleavage mediates cytotoxicity of Clostridium difficile toxin A. Naunyn-Schmiedeberg's archives of pharmacology. 2011;383(3):253-62.

128. Rupnik M, Pabst S, Rupnik M, von Eichel-Streiber C, Urlaub H, Soling HD. Characterization of the cleavage site and function of resulting cleavage fragments after limited proteolysis of Clostridium difficile toxin B (TcdB) by host cells. Microbiology (Reading, England). 2005;151(Pt 1):199-208.

129. Reineke J, Tenzer S, Rupnik M, Koschinski A, Hasselmayer O, Schrattenholz A, et al. Autocatalytic cleavage of Clostridium difficile toxin B. Nature. 2007;446(7134):415-9.

130. Irvine RF, Schell MJ. Back in the water: the return of the inositol phosphates. Nature reviews Molecular cell biology. 2001;2(5):327-38.

131. Egerer M, Giesemann T, Jank T, Satchell KJ, Aktories K. Auto-catalytic cleavage of Clostridium difficile toxins A and B depends on cysteine protease activity. The Journal of biological chemistry. 2007;282(35):25314-21.

132. Pruitt RN, Chagot B, Cover M, Chazin WJ, Spiller B, Lacy DB. Structure-function analysis of inositol hexakisphosphate-induced autoprocessing in Clostridium difficile toxin A. The Journal of biological chemistry. 2009;284(33):21934-40.

133. Egerer M, Satchell KJ. Inositol hexakisphosphate-induced autoprocessing of large bacterial protein toxins. PLoS pathogens. 2010;6(7):e1000942.

134. Shen A. Allosteric regulation of protease activity by small molecules. Molecular bioSystems. 2010;6(8):1431-43.

135. Lupardus PJ, Shen A, Bogyo M, Garcia KC. Small molecule-induced allosteric activation of the Vibrio cholerae RTX cysteine protease domain. Science (New York, NY). 2008;322(5899):265-8.

136. Puri AW, Lupardus PJ, Deu E, Albrow VE, Garcia KC, Bogyo M, et al. Rational design of inhibitors and activity-based probes targeting Clostridium difficile virulence factor TcdB. Chemistry & biology. 2010;17(11):1201-11.

137. Shen A, Lupardus PJ, Gersch MM, Puri AW, Albrow VE, Garcia KC, et al. Defining an allosteric circuit in the cysteine protease domain of Clostridium difficile toxins. Nature structural & molecular biology. 2011;18(3):364-71.

138. Olling A, Huls C, Goy S, Muller M, Krooss S, Rudolf I, et al. The combined repetitive oligopeptides of clostridium difficile toxin A counteract premature cleavage of the glucosyl-transferase domain by stabilizing protein conformation. Toxins. 2014;6(7):2162-76.

139. Zhang Y, Hamza T, Gao S, Feng H. Masking autoprocessing of Clostridium difficile toxin A by the C-terminus combined repetitive oligo peptides. Biochemical and biophysical research communications. 2015;459(2):259-63.

140. Savidge TC, Urvil P, Oezguen N, Ali K, Choudhury A, Acharya V, et al. Host S-nitrosylation inhibits clostridial small molecule-activated glucosylating toxins. Nature medicine. 2011;17(9):1136-41.

141. Chumbler NM, Farrow MA, Lapierre LA, Franklin JL, Haslam DB, Goldenring JR, et al. Clostridium difficile Toxin B causes epithelial cell necrosis through an autoprocessing-independent mechanism. PLoS pathogens. 2012;8(12):e1003072.

142. Li S, Shi L, Yang Z, Feng H. Cytotoxicity of Clostridium difficile toxin B does not require cysteine protease-mediated autocleavage and release of the glucosyltransferase domain into the host cell cytosol. Pathogens and disease. 2013;67(1):11-8.

143. Li S, Shi L, Yang Z, Zhang Y, Perez-Cordon G, Huang T, et al. Critical roles of Clostridium difficile toxin B enzymatic activities in pathogenesis. Infection and immunity. 2015;83(2):502-13.

144. Craven R, Lacy DB. Clostridium sordellii Lethal-Toxin Autoprocessing and Membrane Localization Activities Drive GTPase Glucosylation Profiles in Endothelial Cells. mSphere. 2016;1(1).

145. Apolloni A, Prior IA, Lindsay M, Parton RG, Hancock JF. H-ras but not K-ras traffics to the plasma membrane through the exocytic pathway. Molecular and cellular biology. 2000;20(7):2475-87.

146. Palamidessi A, Frittoli E, Garre M, Faretta M, Mione M, Testa I, et al. Endocytic trafficking of Rac is required for the spatial restriction of signaling in cell migration. Cell. 2008;134(1):135-47.

147. Aktories K, Barbieri JT. Bacterial cytotoxins: targeting eukaryotic switches. Nature reviews Microbiology. 2005;3(5):397-410.

148. Jank T, Giesemann T, Aktories K. Rho-glucosylating Clostridium difficile toxins A and B: new insights into structure and function. Glycobiology. 2007;17(4):15r-22r.

149. Bishop AL, Hall A. Rho GTPases and their effector proteins. The Biochemical journal. 2000;348 Pt 2:241-55.

150. Etienne-Manneville S, Hall A. Rho GTPases in cell biology. Nature. 2002;420(6916):629-35.

151. Raaijmakers JH, Bos JL. Specificity in Ras and Rap signaling. The Journal of biological chemistry. 2009;284(17):10995-9.

152. Genth H, Aktories K, Just I. Monoglucosylation of RhoA at threonine 37 blocks cytosol-membrane cycling. The Journal of biological chemistry. 1999;274(41):29050-6.

153. Just I, Selzer J, Wilm M, von Eichel-Streiber C, Mann M, Aktories K. Glucosylation of Rho proteins by Clostridium difficile toxin B. Nature. 1995;375(6531):500-3.

154. Just I, Wilm M, Selzer J, Rex G, von Eichel-Streiber C, Mann M, et al. The enterotoxin from Clostridium difficile (ToxA) monoglucosylates the Rho proteins. The Journal of biological chemistry. 1995;270(23):13932-6.

155. Ihara K, Muraguchi S, Kato M, Shimizu T, Shirakawa M, Kuroda S, et al. Crystal structure of human RhoA in a dominantly active form complexed with a GTP analogue. The Journal of biological chemistry. 1998;273(16):9656-66.

156. Schaefer A, Reinhard NR, Hordijk PL. Toward understanding RhoGTPase specificity: structure, function and local activation. Small GTPases. 2014;5(2):6.

157. Herrmann C, Ahmadian MR, Hofmann F, Just I. Functional consequences of monoglucosylation of Ha-Ras at effector domain amino acid threonine 35. The Journal of biological chemistry. 1998;273(26):16134-9.

158. Sehr P, Joseph G, Genth H, Just I, Pick E, Aktories K. Glucosylation and ADP ribosylation of rho proteins: effects on nucleotide binding, GTPase activity, and effector coupling. Biochemistry. 1998;37(15):5296-304.

159. Geyer M, Wilde C, Selzer J, Aktories K, Kalbitzer HR. Glucosylation of Ras by Clostridium sordellii lethal toxin: consequences for effector loop conformations observed by NMR spectroscopy. Biochemistry. 2003;42(41):11951-9.

160. Genth H, Pauillac S, Schelle I, Bouvet P, Bouchier C, Varela-Chavez C, et al. Haemorrhagic toxin and lethal toxin from Clostridium sordellii strain vpi9048: molecular characterization and comparative analysis of substrate specificity of the large clostridial glucosylating toxins. Cellular microbiology. 2014;16(11):1706-21.

161. Just I, Selzer J, Hofmann F, Green GA, Aktories K. Inactivation of Ras by Clostridium sordellii lethal toxin-catalyzed glucosylation. The Journal of biological chemistry. 1996;271(17):10149-53.

162. Popoff MR, Chaves-Olarte E, Lemichez E, von Eichel-Streiber C, Thelestam M, Chardin P, et al. Ras, Rap, and Rac small GTP-binding proteins are targets for Clostridium sordellii lethal toxin glucosylation. The Journal of biological chemistry. 1996;271(17):10217-24.

163. Nagahama M, Ohkubo A, Oda M, Kobayashi K, Amimoto K, Miyamoto K, et al. Clostridium perfringens TpeL glycosylates the Rac and Ras subfamily proteins. Infection and immunity. 2011;79(2):905-10.

164. Selzer J, Hofmann F, Rex G, Wilm M, Mann M, Just I, et al. Clostridium novyi alpha-toxin-catalyzed incorporation of GlcNAc into Rho subfamily proteins. The Journal of biological chemistry. 1996;271(41):25173-7.

165. Jank T, Reinert DJ, Giesemann T, Schulz GE, Aktories K. Change of the donor substrate specificity of Clostridium difficile toxin B by site-directed mutagenesis. The Journal of biological chemistry. 2005;280(45):37833-8.

166. Alvin JW, Lacy DB. Clostridium difficile toxin glucosyltransferase domains in complex with a non-hydrolyzable UDP-glucose analogue. Journal of structural biology. 2017.

167. D'Urzo N, Malito E, Biancucci M, Bottomley MJ, Maione D, Scarselli M, et al. The structure of Clostridium difficile toxin A glucosyltransferase domain bound to Mn2+ and UDP provides insights into glucosyltransferase activity and product release. The FEBS journal. 2012;279(17):3085-97.

168. Pruitt RN, Chumbler NM, Rutherford SA, Farrow MA, Friedman DB, Spiller B, et al. Structural determinants of Clostridium difficile toxin A glucosyltransferase activity. The Journal of biological chemistry. 2012;287(11):8013-20.

169. Reinert DJ, Jank T, Aktories K, Schulz GE. Structural basis for the function of Clostridium difficile toxin B. Journal of molecular biology. 2005;351(5):973-81.

170. Ziegler MO, Jank T, Aktories K, Schulz GE. Conformational changes and reaction of clostridial glycosylating toxins. Journal of molecular biology. 2008;377(5):1346-56.

171. Unligil UM, Rini JM. Glycosyltransferase structure and mechanism. Current opinion in structural biology. 2000;10(5):510-7.

172. Busch C, Hofmann F, Selzer J, Munro S, Jeckel D, Aktories K. A common motif of eukaryotic glycosyltransferases is essential for the enzyme activity of large clostridial cytotoxins. The Journal of biological chemistry. 1998;273(31):19566-72.

173. Wiggins CA, Munro S. Activity of the yeast MNN1 alpha-1,3-mannosyltransferase requires a motif conserved in many other families of glycosyltransferases. Proceedings of the National Academy of Sciences of the United States of America. 1998;95(14):7945-50.

174. Chaves-Olarte E, Weidmann M, Eichel-Streiber C, Thelestam M. Toxins A and B from Clostridium difficile differ with respect to enzymatic potencies, cellular substrate specificities, and surface binding to cultured cells. The Journal of clinical investigation. 1997;100(7):1734-41.

175. Mehlig M, Moos M, Braun V, Kalt B, Mahony DE, von Eichel-Streiber C. Variant toxin B and a functional toxin A produced by Clostridium difficile C34. FEMS microbiology letters. 2001;198(2):171-6.

176. Muller S, von Eichel-Streiber C, Moos M. Impact of amino acids 22-27 of Rho-subfamily GTPases on glucosylation by the large clostridial cytotoxins TcsL-1522, TcdB-1470 and TcdB-8864. European journal of biochemistry / FEBS. 1999;266(3):1073-80.

177. Quesada-Gomez C, Lopez-Urena D, Chumbler N, Kroh HK, Castro-Pena C, Rodriguez C, et al. Analysis of TcdB Proteins within the Hypervirulent Clade 2 Reveals an Impact of RhoA

Glucosylation on Clostridium difficile Proinflammatory Activities. Infection and immunity. 2016;84(3):856-65.

178. Hofmann F, Rex G, Aktories K, Just I. The ras-related protein Ral is monoglucosylated by Clostridium sordellii lethal toxin. Biochemical and biophysical research communications. 1996;227(1):77-81.

179. Genth H, Hofmann F, Selzer J, Rex G, Aktories K, Just I. Difference in protein substrate specificity between hemorrhagic toxin and lethal toxin from Clostridium sordellii. Biochemical and biophysical research communications. 1996;229(2):370-4.

180. von Eichel-Streiber C, Zec-Pirnat I, Grabnar M, Rupnik M. A nonsense mutation abrogates production of a functional enterotoxin A in Clostridium difficile toxinotype VIII strains of serogroups F and X. FEMS microbiology letters. 1999;178(1):163-8.

181. Soehn F, Wagenknecht-Wiesner A, Leukel P, Kohl M, Weidmann M, von Eichel-Streiber C, et al. Genetic rearrangements in the pathogenicity locus of Clostridium difficile strain 8864--implications for transcription, expression and enzymatic activity of toxins A and B. Molecular & general genetics : MGG. 1998;258(3):222-32.

182. Busch C, Hofmann F, Gerhard R, Aktories K. Involvement of a conserved tryptophan residue in the UDP-glucose binding of large clostridial cytotoxin glycosyltransferases. The Journal of biological chemistry. 2000;275(18):13228-34.

183. Jank T, Giesemann T, Aktories K. Clostridium difficile glucosyltransferase toxin B-essential amino acids for substrate binding. The Journal of biological chemistry. 2007;282(48):35222-31.

184. Geissler B, Tungekar R, Satchell KJ. Identification of a conserved membrane localization domain within numerous large bacterial protein toxins. Proceedings of the National Academy of Sciences of the United States of America. 2010;107(12):5581-6.

185. Mesmin B, Robbe K, Geny B, Luton F, Brandolin G, Popoff MR, et al. A phosphatidylserine-binding site in the cytosolic fragment of Clostridium sordellii lethal toxin facilitates glucosylation of membrane-bound Rac and is required for cytotoxicity. The Journal of biological chemistry. 2004;279(48):49876-82.

186. Varela Chavez C, Hoos S, Haustant GM, Chenal A, England P, Blondel A, et al. The catalytic domains of Clostridium sordellii lethal toxin and related large clostridial glucosylating toxins specifically recognize the negatively charged phospholipids phosphatidylserine and phosphatidic acid. Cellular microbiology. 2015;17(10):1477-93.

187. Geissler B, Ahrens S, Satchell KJ. Plasma membrane association of three classes of bacterial toxins is mediated by a basic-hydrophobic motif. Cellular microbiology. 2012;14(2):286-98.

188. Varela Chavez C, Haustant GM, Baron B, England P, Chenal A, Pauillac S, et al. The Tip of the Four N-Terminal alpha-Helices of Clostridium sordellii Lethal Toxin Contains the Interaction Site with Membrane Phosphatidylserine Facilitating Small GTPases Glucosylation. Toxins. 2016;8(4):90.

189. Kelly CP, Kyne L. The host immune response to Clostridium difficile. Journal of medical microbiology. 2011;60(Pt 8):1070-9.

190. Voth DE, Ballard JD. Clostridium difficile toxins: mechanism of action and role in disease. Clinical microbiology reviews. 2005;18(2):247-63.

191. Feltis BA, Wiesner SM, Kim AS, Erlandsen SL, Lyerly DL, Wilkins TD, et al. Clostridium difficile toxins A and B can alter epithelial permeability and promote bacterial paracellular migration through HT-29 enterocytes. Shock (Augusta, Ga). 2000;14(6):629-34.

192. El Feghaly RE, Stauber JL, Deych E, Gonzalez C, Tarr PI, Haslam DB. Markers of intestinal inflammation, not bacterial burden, correlate with clinical outcomes in Clostridium difficile infection. Clinical infectious diseases : an official publication of the Infectious Diseases Society of America. 2013;56(12):1713-21.

193. Steiner TS, Flores CA, Pizarro TT, Guerrant RL. Fecal lactoferrin, interleukin-1beta, and interleukin-8 are elevated in patients with severe Clostridium difficile colitis. Clinical and diagnostic laboratory immunology. 1997;4(6):719-22.

194. Yu H, Chen K, Sun Y, Carter M, Garey KW, Savidge TC, et al. Cytokines are markers of the Clostridium difficile-induced inflammatory response and predict disease severity. Clinical and vaccine immunology : CVI. 2017.

195. Pothoulakis C, Lamont JT. Microbes and microbial toxins: paradigms for microbial-mucosal interactions II. The integrated response of the intestine to Clostridium difficile toxins. American Journal of Physiology - Gastrointestinal and Liver Physiology. 2001;280(2):G178-83.

196. Sun X, Hirota SA. The roles of host and pathogen factors and the innate immune response in the pathogenesis of Clostridium difficile infection. Molecular immunology. 2015;63(2):193-202.

197. Nobes CD, Hall A. Rho, rac, and cdc42 GTPases regulate the assembly of multimolecular focal complexes associated with actin stress fibers, lamellipodia, and filopodia. Cell. 1995;81(1):53-62.

198. Hecht G, Koutsouris A, Pothoulakis C, LaMont JT, Madara JL. Clostridium difficile toxin B disrupts the barrier function of T84 monolayers. Gastroenterology. 1992;102(2):416-23.

199. Hecht G, Pothoulakis C, LaMont JT, Madara JL. Clostridium difficile toxin A perturbs cytoskeletal structure and tight junction permeability of cultured human intestinal epithelial monolayers. The Journal of clinical investigation. 1988;82(5):1516-24.

200. May M, Wang T, Muller M, Genth H. Difference in F-actin depolymerization induced by toxin B from the Clostridium difficile strain VPI 10463 and toxin B from the variant Clostridium difficile serotype F strain 1470. Toxins. 2013;5(1):106-19.

201. Moore R, Pothoulakis C, LaMont JT, Carlson S, Madara JL. C. difficile toxin A increases intestinal permeability and induces Cl- secretion. The American journal of physiology. 1990;259(2 Pt 1):G165-72.

202. D'Auria KM, Donato GM, Gray MC, Kolling GL, Warren CA, Cave LM, et al. Systems analysis of the transcriptional response of human ileocecal epithelial cells to Clostridium difficile toxins and effects on cell cycle control. BMC systems biology. 2012;6:2.

203. Welsh CF, Roovers K, Villanueva J, Liu Y, Schwartz MA, Assoian RK. Timing of cyclin D1 expression within G1 phase is controlled by Rho. Nature cell biology. 2001;3(11):950-7.

204. Ando Y, Yasuda S, Oceguera-Yanez F, Narumiya S. Inactivation of Rho GTPases with Clostridium difficile toxin B impairs centrosomal activation of Aurora-A in G2/M transition of HeLa cells. Molecular biology of the cell. 2007;18(10):3752-63.

205. May M, Schelle I, Brakebusch C, Rottner K, Genth H. Rac1-dependent recruitment of PAK2 to G2 phase centrosomes and their roles in the regulation of mitotic entry. Cell cycle (Georgetown, Tex). 2014;13(14):2211-21.

206. Gerhard R, Nottrott S, Schoentaube J, Tatge H, Olling A, Just I. Glucosylation of Rho GTPases by Clostridium difficile toxin A triggers apoptosis in intestinal epithelial cells. Journal of medical microbiology. 2008;57(Pt 6):765-70.

207. Kim H, Kokkotou E, Na X, Rhee SH, Moyer MP, Pothoulakis C, et al. Clostridium difficile toxin A-induced colonocyte apoptosis involves p53-dependent p21(WAF1/CIP1) induction via p38 mitogen-activated protein kinase. Gastroenterology. 2005;129(6):1875-88.

208. Nottrott S, Schoentaube J, Genth H, Just I, Gerhard R. Clostridium difficile toxin A-induced apoptosis is p53-independent but depends on glucosylation of Rho GTPases. Apoptosis : an international journal on programmed cell death. 2007;12(8):1443-53.

209. Huelsenbeck SC, May M, Schmidt G, Genth H. Inhibition of cytokinesis by Clostridium difficile toxin B and cytotoxic necrotizing factors--reinforcing the critical role of RhoA in cytokinesis. Cell motility and the cytoskeleton. 2009;66(11):967-75.

210. Brito GA, Carneiro-Filho B, Oria RB, Destura RV, Lima AA, Guerrant RL. Clostridium difficile toxin A induces intestinal epithelial cell apoptosis and damage: role of Gln and Ala-Gln in toxin A effects. Digestive diseases and sciences. 2005;50(7):1271-8.

211. Brito GA, Fujji J, Carneiro-Filho BA, Lima AA, Obrig T, Guerrant RL. Mechanism of Clostridium difficile toxin A-induced apoptosis in T84 cells. The Journal of infectious diseases. 2002;186(10):1438-47.

212. Carneiro BA, Fujii J, Brito GA, Alcantara C, Oria RB, Lima AA, et al. Caspase and bid involvement in Clostridium difficile toxin A-induced apoptosis and modulation of toxin A effects by glutamine and alanyl-glutamine in vivo and in vitro. Infection and immunity. 2006;74(1):81-7.

213. Chumbler NM, Farrow MA, Lapierre LA, Franklin JL, Lacy DB. Clostridium difficile Toxins TcdA and TcdB Cause Colonic Tissue Damage by Distinct Mechanisms. Infection and immunity. 2016;84(10):2871-7.

214. Fiorentini C, Fabbri A, Falzano L, Fattorossi A, Matarrese P, Rivabene R, et al. Clostridium difficile toxin B induces apoptosis in intestinal cultured cells. Infection and immunity. 1998;66(6):2660-5.

215. Qa'Dan M, Ramsey M, Daniel J, Spyres LM, Safiejko-Mroczka B, Ortiz-Leduc W, et al. Clostridium difficile toxin B activates dual caspase-dependent and caspase-independent apoptosis in intoxicated cells. Cellular microbiology. 2002;4(7):425-34.

216. Broker LE, Kruyt FA, Giaccone G. Cell death independent of caspases: a review. Clinical cancer research : an official journal of the American Association for Cancer Research. 2005;11(9):3155-62.

217. Chipuk JE, Green DR. Dissecting p53-dependent apoptosis. Cell death and differentiation. 2006;13(6):994-1002.

218. Pradelli LA, Beneteau M, Ricci JE. Mitochondrial control of caspase-dependent and -independent cell death. Cellular and molecular life sciences : CMLS. 2010;67(10):1589-97.

219. Tait SW, Green DR. Mitochondria and cell death: outer membrane permeabilization and beyond. Nature reviews Molecular cell biology. 2010;11(9):621-32.

220. Matarrese P, Falzano L, Fabbri A, Gambardella L, Frank C, Geny B, et al. Clostridium difficile toxin B causes apoptosis in epithelial cells by thrilling mitochondria. Involvement of ATP-sensitive mitochondrial potassium channels. The Journal of biological chemistry. 2007;282(12):9029-41.

221. Matte I, Lane D, Cote E, Asselin AE, Fortier LC, Asselin C, et al. Antiapoptotic proteins Bcl-2 and Bcl-XL inhibit Clostridium difficile toxin A-induced cell death in human epithelial cells. Infection and immunity. 2009;77(12):5400-10.

222. Farrow MA, Chumbler NM, Lapierre LA, Franklin JL, Rutherford SA, Goldenring JR, et al. Clostridium difficile toxin B-induced necrosis is mediated by the host epithelial cell NADPH oxidase complex. Proceedings of the National Academy of Sciences of the United States of America. 2013;110(46):18674-9.

223. Wohlan K, Goy S, Olling A, Srivaratharajan S, Tatge H, Genth H, et al. Pyknotic cell death induced by Clostridium difficile TcdB: chromatin condensation and nuclear blister are induced independently of the glucosyltransferase activity. Cellular microbiology. 2014;16(11):1678-92.

224. Daiber A. Redox signaling (cross-talk) from and to mitochondria involves mitochondrial pores and reactive oxygen species. Biochimica et biophysica acta. 2010;1797(6-7):897-906.

225. Temple MD, Perrone GG, Dawes IW. Complex cellular responses to reactive oxygen species. Trends in cell biology. 2005;15(6):319-26.

226. Yu BP. Cellular defenses against damage from reactive oxygen species. Physiological reviews. 1994;74(1):139-62.

227. Doherty GJ, McMahon HT. Mechanisms of endocytosis. Annual review of biochemistry. 2009;78:857-902.

228. Mercer J, Schelhaas M, Helenius A. Virus entry by endocytosis. Annual review of biochemistry. 2010;79:803-33.

229. Boucrot E, Ferreira AP, Almeida-Souza L, Debard S, Vallis Y, Howard G, et al. Endophilin marks and controls a clathrin-independent endocytic pathway. Nature. 2015;517(7535):460-5.

230. Hansen CG, Howard G, Nichols BJ. Pacsin 2 is recruited to caveolae and functions in caveolar biogenesis. Journal of cell science. 2011;124(Pt 16):2777-85.

231. Senju Y, Itoh Y, Takano K, Hamada S, Suetsugu S. Essential role of PACSIN2/syndapin-II in caveolae membrane sculpting. Journal of cell science. 2011;124(Pt 12):2032-40.

232. Wang Q, Navarro MV, Peng G, Molinelli E, Goh SL, Judson BL, et al. Molecular mechanism of membrane constriction and tubulation mediated by the F-BAR protein Pacsin/Syndapin. Proceedings of the National Academy of Sciences of the United States of America. 2009;106(31):12700-5.

233. Qualmann B, Kelly RB. Syndapin isoforms participate in receptor-mediated endocytosis and actin organization. The Journal of cell biology. 2000;148(5):1047-62.

234. Kessels MM, Qualmann B. The syndapin protein family: linking membrane trafficking with the cytoskeleton. Journal of cell science. 2004;117(Pt 15):3077-86.

235. Hall AJ, Curns AT, McDonald LC, Parashar UD, Lopman BA. The roles of Clostridium difficile and norovirus among gastroenteritis-associated deaths in the United States, 1999-2007. Clinical infectious diseases : an official publication of the Infectious Diseases Society of America. 2012;55(2):216-23.

236. Kelly CP, LaMont JT. Clostridium difficile--more difficult than ever. The New England journal of medicine. 2008;359(18):1932-40.

237. McDonald LC, Killgore GE, Thompson A, Owens RC, Jr., Kazakova SV, Sambol SP, et al. An epidemic, toxin gene-variant strain of Clostridium difficile. The New England journal of medicine. 2005;353(23):2433-41.

238. Frey SM, Wilkins TD. Localization of two epitopes recognized by monoclonal antibody PCG-4 on Clostridium difficile toxin A. Infection and immunity. 1992;60(6):2488-92.

239. Mayor S, Pagano RE. Pathways of clathrin-independent endocytosis. Nature reviews Molecular cell biology. 2007;8(8):603-12.

240. Macia E, Ehrlich M, Massol R, Boucrot E, Brunner C, Kirchhausen T. Dynasore, a cell-permeable inhibitor of dynamin. Developmental cell. 2006;10(6):839-50.

241. Renard HF, Simunovic M, Lemiere J, Boucrot E, Garcia-Castillo MD, Arumugam S, et al. Endophilin-A2 functions in membrane scission in clathrin-independent endocytosis. Nature. 2015;517(7535):493-6.

242. Parton RG, Simons K. The multiple faces of caveolae. Nature reviews Molecular cell biology. 2007;8(3):185-94.

243. Field FJ, Born E, Murthy S, Mathur SN. Caveolin is present in intestinal cells: role in cholesterol trafficking? Journal of lipid research. 1998;39(10):1938-50.

244. Mirre C, Monlauzeur L, Garcia M, Delgrossi MH, Le Bivic A. Detergent-resistant membrane microdomains from Caco-2 cells do not contain caveolin. The American journal of physiology. 1996;271(3 Pt 1):C887-94.

245. Vogel U, Sandvig K, van Deurs B. Expression of caveolin-1 and polarized formation of invaginated caveolae in Caco-2 and MDCK II cells. Journal of cell science. 1998;111 (Pt 6):825-32.

246. Fujimoto T, Kogo H, Nomura R, Une T. Isoforms of caveolin-1 and caveolar structure. Journal of cell science. 2000;113 Pt 19:3509-17.

247. Drab M, Verkade P, Elger M, Kasper M, Lohn M, Lauterbach B, et al. Loss of caveolae, vascular dysfunction, and pulmonary defects in caveolin-1 gene-disrupted mice. Science (New York, NY). 2001;293(5539):2449-52.

248. Hill MM, Bastiani M, Luetterforst R, Kirkham M, Kirkham A, Nixon SJ, et al. PTRF-Cavin, a conserved cytoplasmic protein required for caveola formation and function. Cell. 2008;132(1):113-24.

249. Rothberg KG, Heuser JE, Donzell WC, Ying YS, Glenney JR, Anderson RG. Caveolin, a protein component of caveolae membrane coats. Cell. 1992;68(4):673-82.

250. de Kreuk BJ, Nethe M, Fernandez-Borja M, Anthony EC, Hensbergen PJ, Deelder AM, et al. The F-BAR domain protein PACSIN2 associates with Rac1 and regulates cell spreading and migration. Journal of cell science. 2011;124(Pt 14):2375-88.

251. Modi N, Gulati N, Solomon K, Monaghan T, Robins A, Sewell HF, et al. Differential binding and internalization of Clostridium difficile toxin A by human peripheral blood monocytes, neutrophils and lymphocytes. Scandinavian journal of immunology. 2011;74(3):264-71.

252. Schelhaas M, Shah B, Holzer M, Blattmann P, Kuhling L, Day PM, et al. Entry of human papillomavirus type 16 by actin-dependent, clathrin- and lipid raft-independent endocytosis. PLoS pathogens. 2012;8(4):e1002657.

253. Vercauteren D, Vandenbroucke RE, Jones AT, Rejman J, Demeester J, De Smedt SC, et al. The use of inhibitors to study endocytic pathways of gene carriers: optimization and pitfalls. Molecular therapy : the journal of the American Society of Gene Therapy. 2010;18(3):561-9.

254. Watanabe S, Hirose M, Miyazaki A, Tomono M, Takeuchi M, Kitamura T, et al. Calmodulin antagonists inhibit the phagocytic activity of cultured Kupffer cells. Laboratory investigation; a journal of technical methods and pathology. 1988;59(2):214-8.

255. Howes MT, Mayor S, Parton RG. Molecules, mechanisms, and cellular roles of clathrin-independent endocytosis. Current opinion in cell biology. 2010;22(4):519-27.

256. Sandvig K, Pust S, Skotland T, van Deurs B. Clathrin-independent endocytosis: mechanisms and function. Current opinion in cell biology. 2011;23(4):413-20.

257. Fra AM, Williamson E, Simons K, Parton RG. De novo formation of caveolae in lymphocytes by expression of VIP21-caveolin. Proceedings of the National Academy of Sciences of the United States of America. 1995;92(19):8655-9.

258. Chaudhary N, Gomez GA, Howes MT, Lo HP, McMahon KA, Rae JA, et al. Endocytic crosstalk: cavins, caveolins, and caveolae regulate clathrin-independent endocytosis. PLoS biology. 2014;12(4):e1001832.

259. Lajoie P, Kojic LD, Nim S, Li L, Dennis JW, Nabi IR. Caveolin-1 regulation of dynamin-dependent, raft-mediated endocytosis of cholera toxin-B sub-unit occurs independently of caveolae. Journal of cellular and molecular medicine. 2009;13(9b):3218-25.

260. Fielding PE, Fielding CJ. Plasma membrane caveolae mediate the efflux of cellular free cholesterol. Biochemistry. 1995;34(44):14288-92.

261. Frank PG, Cheung MW, Pavlides S, Llaverias G, Park DS, Lisanti MP. Caveolin-1 and regulation of cellular cholesterol homeostasis. American journal of physiology Heart and circulatory physiology. 2006;291(2):H677-86.

262. Murata M, Peranen J, Schreiner R, Wieland F, Kurzchalia TV, Simons K. VIP21/caveolin is a cholesterol-binding protein. Proceedings of the National Academy of Sciences of the United States of America. 1995;92(22):10339-43.

263. Itoh T, Erdmann KS, Roux A, Habermann B, Werner H, De Camilli P. Dynamin and the actin cytoskeleton cooperatively regulate plasma membrane invagination by BAR and F-BAR proteins. Developmental cell. 2005;9(6):791-804.

264. Kostan J, Salzer U, Orlova A, Toro I, Hodnik V, Senju Y, et al. Direct interaction of actin filaments with F-BAR protein pacsin2. EMBO reports. 2014;15(11):1154-62.

265. Modregger J, Ritter B, Witter B, Paulsson M, Plomann M. All three PACSIN isoforms bind to endocytic proteins and inhibit endocytosis. Journal of cell science. 2000;113 Pt 24:4511-21.

266. Qualmann B, Roos J, DiGregorio PJ, Kelly RB. Syndapin I, a synaptic dynamin-binding protein that associates with the neural Wiskott-Aldrich syndrome protein. Molecular biology of the cell. 1999;10(2):501-13.

267. Shimada A, Takano K, Shirouzu M, Hanawa-Suetsugu K, Terada T, Toyooka K, et al. Mapping of the basic amino-acid residues responsible for tubulation and cellular protrusion by the EFC/F-BAR domain of pacsin2/Syndapin II. FEBS letters. 2010;584(6):1111-8.

268. Plomann M, Lange R, Vopper G, Cremer H, Heinlein UA, Scheff S, et al. PACSIN, a brain protein that is upregulated upon differentiation into neuronal cells. European journal of biochemistry / FEBS. 1998;256(1):201-11.

269. Ritter B, Modregger J, Paulsson M, Plomann M. PACSIN 2, a novel member of the PACSIN family of cytoplasmic adapter proteins. FEBS letters. 1999;454(3):356-62.

270. Kessels MM, Qualmann B. Syndapin oligomers interconnect the machineries for endocytic vesicle formation and actin polymerization. The Journal of biological chemistry. 2006;281(19):13285-99.

271. de Kreuk BJ, Anthony EC, Geerts D, Hordijk PL. The F-BAR protein PACSIN2 regulates epidermal growth factor receptor internalization. The Journal of biological chemistry. 2012;287(52):43438-53.

272. Aktories K. Bacterial toxins that target Rho proteins. The Journal of clinical investigation. 1997;99(5):827-9.

273. Donta ST, Sullivan N, Wilkins TD. Differential effects of Clostridium difficile toxins on tissue-cultured cells. Journal of clinical microbiology. 1982;15(6):1157-8.

274. Meinecke M, Boucrot E, Camdere G, Hon WC, Mittal R, McMahon HT. Cooperative recruitment of dynamin and BIN/amphiphysin/Rvs (BAR) domain-containing proteins leads to GTP-dependent membrane scission. The Journal of biological chemistry. 2013;288(9):6651-61.

275. Kirchhausen T, Macia E, Pelish HE. Use of dynasore, the small molecule inhibitor of dynamin, in the regulation of endocytosis. Methods in enzymology. 2008;438:77-93.

276. Schindelin J, Arganda-Carreras I, Frise E, Kaynig V, Longair M, Pietzsch T, et al. Fiji: an open-source platform for biological-image analysis. Nature methods. 2012;9(7):676-82.

277. Papatheodorou P, Carette JE, Bell GW, Schwan C, Guttenberg G, Brummelkamp TR, et al. Lipolysis-stimulated lipoprotein receptor (LSR) is the host receptor for the binary toxin Clostridium difficile transferase (CDT). Proceedings of the National Academy of Sciences of the United States of America. 2011;108(39):16422-7.

278. Ivie SE, Fennessey CM, Sheng J, Rubin DH, McClain MS. Gene-trap mutagenesis identifies mammalian genes contributing to intoxication by Clostridium perfringens epsilon-toxin. PloS one. 2011;6(3):e17787.

279. Marzinke MA, Mavencamp T, Duratinsky J, Clagett-Dame M. 14-3-3epsilon and NAV2 interact to regulate neurite outgrowth and axon elongation. Archives of biochemistry and biophysics. 2013;540(1-2):94-100.

280. Muley PD, McNeill EM, Marzinke MA, Knobel KM, Barr MM, Clagett-Dame M. The atRA-responsive gene neuron navigator 2 functions in neurite outgrowth and axonal elongation. Developmental neurobiology. 2008;68(13):1441-53.

281. van Haren J, Draegestein K, Keijzer N, Abrahams JP, Grosveld F, Peeters PJ, et al. Mammalian Navigators are microtubule plus-end tracking proteins that can reorganize the cytoskeleton to induce neurite-like extensions. Cell motility and the cytoskeleton. 2009;66(10):824-38.

282. Vale RD. Aaa Proteins: Lords of the Ring. The Journal of cell biology. 2000;150(1):f13-20.

283. Stringham EG, Schmidt KL. Navigating the cell: UNC-53 and the navigators, a family of cytoskeletal regulators with multiple roles in cell migration, outgrowth and trafficking. Cell Adhesion & Migration. 2009;3(4):342-6.

284. Schmidt KL, Marcus-Gueret N, Adeleye A, Webber J, Baillie D, Stringham EG. The cell migration molecule UNC-53/NAV2 is linked to the ARP2/3 complex by ABI-1. Development (Cambridge, England). 2009;136(4):563-74.

285. Balklava Z, Pant S, Fares H, Grant BD. Genome-wide analysis identifies a general requirement for polarity proteins in endocytic traffic. Nature cell biology. 2007;9(9):1066-73.

286. Kadrmas JL, Beckerle MC. The LIM domain: from the cytoskeleton to the nucleus. Nature reviews Molecular cell biology. 2004;5(11):920-31.

287. Johannessen M, Moller S, Hansen T, Moens U, Van Ghelue M. The multifunctional roles of the four-and-a-half-LIM only protein FHL2. Cellular and molecular life sciences : CMLS. 2006;63(3):268-84.

288. Coghill ID, Brown S, Cottle DL, McGrath MJ, Robinson PA, Nandurkar HH, et al. FHL3 is an actin-binding protein that regulates alpha-actinin-mediated actin bundling: FHL3 localizes to actin stress fibers and enhances cell spreading and stress fiber disassembly. The Journal of biological chemistry. 2003;278(26):24139-52.

289. Gabriel B, Mildenberger S, Weisser CW, Metzger E, Gitsch G, Schule R, et al. Focal adhesion kinase interacts with the transcriptional coactivator FHL2 and both are overexpressed in epithelial ovarian cancer. Anticancer research. 2004;24(2b):921-7.

290. Samson T, Smyth N, Janetzky S, Wendler O, Muller JM, Schule R, et al. The LIM-only proteins FHL2 and FHL3 interact with alpha- and beta-subunits of the muscle alpha7beta1 integrin receptor. The Journal of biological chemistry. 2004;279(27):28641-52.

291. Wixler V, Geerts D, Laplantine E, Westhoff D, Smyth N, Aumailley M, et al. The LIM-only protein DRAL/FHL2 binds to the cytoplasmic domain of several alpha and beta integrin chains and is recruited to adhesion complexes. The Journal of biological chemistry. 2000;275(43):33669-78.

292. Park J, Will C, Martin B, Gullotti L, Friedrichs N, Buettner R, et al. Deficiency in the LIM-only protein FHL2 impairs assembly of extracellular matrix proteins. FASEB journal : official publication of the Federation of American Societies for Experimental Biology. 2008;22(7):2508-20.

293. Hynes RO. Integrins: bidirectional, allosteric signaling machines. Cell. 2002;110(6):673-87.

294. Cseke G, Maginnis MS, Cox RG, Tollefson SJ, Podsiad AB, Wright DW, et al. Integrin alphavbeta1 promotes infection by human metapneumovirus. Proceedings of the National Academy of Sciences of the United States of America. 2009;106(5):1566-71.

295. Feire AL, Koss H, Compton T. Cellular integrins function as entry receptors for human cytomegalovirus via a highly conserved disintegrin-like domain. Proceedings of the National Academy of Sciences of the United States of America. 2004;101(43):15470-5.

296. Guerrero CA, Mendez E, Zarate S, Isa P, Lopez S, Arias CF. Integrin alpha(v)beta(3) mediates rotavirus cell entry. Proceedings of the National Academy of Sciences of the United States of America. 2000;97(26):14644-9.

297. Maginnis MS, Forrest JC, Kopecky-Bromberg SA, Dickeson SK, Santoro SA, Zutter MM, et al. Beta1 integrin mediates internalization of mammalian reovirus. Journal of Virology. 2006;80(6):2760-70.

298. Kroh HK, Chandrasekaran R, Rosenthal K, Woods R, Jin X, Ohi MD, et al. Use of a neutralizing antibody helps identify structural features critical for binding of Clostridium difficile toxin TcdA to the host cell surface. The Journal of biological chemistry. 2017.

299. Murase T, Eugenio L, Schorr M, Hussack G, Tanha J, Kitova EN, et al. Structural basis for antibody recognition in the receptor-binding domains of toxins A and B from Clostridium difficile. The Journal of biological chemistry. 2014;289(4):2331-43.

300. Huang JH, Shen ZQ, Lien SP, Hsiao KN, Leng CH, Chen CC, et al. Biochemical and Immunological Characterization of Truncated Fragments of the Receptor-Binding Domains of C. difficile Toxin A. PloS one. 2015;10(8):e0135045.

301. Day CA, Baetz NW, Copeland CA, Kraft LJ, Han B, Tiwari A, et al. Microtubule motors power plasma membrane tubulation in clathrin-independent endocytosis. Traffic (Copenhagen, Denmark). 2015;16(6):572-90.